C.P. No. 755

MINISTRY OF AVIATION

AERONAUTICAL RESEARCH COUNCIL

CURRENT PAPERS

A Parameter Theory for the Compressible Flow through Variable-Area Turbo-Machines

By

Gordon S Beavers

LONDON: HER MAJESTY'S STATIONERY OFFICE

1965

Price £1 0s. 0d. net

C.P. No. 755

January, 1963

A Parameter Theory for the Compressible Flow through Variable-Area Turbo-machines

- by -

Gordon S. Beavers*

Summary

The single-parameter theory proposed by Whitehead and Beavers (1961) for the analysis of incompressible flows through constant-area turbo-machines has been extended in this paper to allow for the compressibility of the working fluid and for changes in the area of the turbo-machine. The assumption is made that at any axial position the density profile belongs to a fixed family of curves governed by a parameter μ, and the axial-velocity profile at the same point belongs to another family of profiles governed by μ and a second parameter λ.

The analysis is performed at a single radius, called the design radius, and from the values of λ and μ along this radius the full velocity and density variations may be found. The equations of motion are reduced to a second-order linear differential equation for λ, the solution of which is then used in conjunction with the assumption of isentropic flow to yield the value of μ.

The problem can only be solved using an electronic computer, and details are given of a programme which can be used on the EDSAC 2 computer of the Cambridge University Mathematical Laboratory to analyse the flow through any axial turbo-machine. Results obtained from this programme have been compared with existing theoretical and experimental results, and it is suggested that these comparisons establish that the theory is sufficiently accurate for design and performance calculations

---

Replaces A.R.C.25 029.

*Assistant Professor, Department of Aeronautics and Engineering Mechanics, University of Minnesota, Minneapolis, U.S.A.

List of Contents

1. Introduction

Many theories have been proposed for the design and performance predictions of axial-flow compressors and turbines. However, as stated by Howell (1963), most of these theories, although being mathematically accurate, are lengthy and complicated and are thus rarely referred to by practical turbo-machinery designers. A theoretical approach to the design of turbo-machines is required which is both suitably simple and easy to use, and at the same time possesses the accuracy required for design purposes. The criteria by which such a theory should be judged have been given in the paper by Whitehead and Beavers (1961), which presents an introduction to a method of predicting the flow through axial turbo-machines which it is thought will be of considerable value in design applications.

The development of a suitable theory is most readily accomplished in a sequential manner. First, the problem of predicting the flow through a given turbo-machine is attempted, the problem being reduced to the simplest possible form by considering the incompressible flow through a machine of constant annulus area. The theory is then improved as it is extended to allow for the important effects of compressibility and varying hub and tip radii, and then it is further refined as the effects of blade thickness, blade taper and radial blade forces are incorporated. Finally, having thus evolved a theory for the estimation of flows through existing machines, it can with confidence be transposed to a form suitable for design purposes. This paper is concerned with the second stage in the development of the single-parameter theory proposed by Whitehead and Beavers, namely the introduction into the analysis of compressibility of the working fluid and taper of the hub and tip radii.

Existing theories in various stages of development have been summarized in the paper by Whitehead and Beavers and by Horlock (1962). The most accurate solution for compressible flow through machines with tapered walls is the numerical solution of the full equations of motion, derived by Wu (1952.a). The theory presented in this paper has been compared with Wu's calculations for both incompressible and compressible flows through a single-stage constant-area compressor (Wu, 1953) and through a single-stage constant-area turbine (Wu,1952.b), and also for the compressible flow through a seven-stage compressor with a tapering hub radius (Wu, 1953).

The method of solution in which it is assumed that the streamlines in a plane containing the axis of the machine vary periodically with a wavelength equal to the axial length of a stage has been used by Wu and Wolfenstein (1950) and Schnittger (1954) for compressible flow through turbo-machines with tapered walls. This oscillatory motion of the streamlines in multi-stage machines has been observed by Whitehead and Beavers for the restricted case of incompressible flow through a constant-area compressor, and by Bammert (1961) for the more general flow problem. This last author obtained solutions for the axial velocities in the gaps just behind all the blade rows by dropping the derivatives in the axial direction from the Euler equation of motion expressed for the radial direction.

The actuator-disc method of solution, which involves replacing each blade row by an infinitesimally thin disc across which there is a sudden change in the tangential velocity and static pressure, has been extensively studied for incompressible flows in constant-area turbo-machines, and a selection of papers is included in the Bibliography. Lewis (1960) has extended the theory for flow through conical turbo-machines and Horlock (1958) and Hawthorne and Ringrose (1962)

have/

have applied actuator-disc theory to the compressible flow through constant-area turbo-machines. As yet the theory cannot be applied to solve the problem of compressible flow through a general multi-stage turbo-machine.

Approximate methods of solution in which the equations of motion are satisfied exactly at one radius only and are reduced to a single differential equation in terms of a dimensionless parameter have been proposed by Whitehead and Beavers (1961), Howell (1963) and Mellor (1962). All three of these papers consider the problem of incompressible flow through a constant-area turbo-machine, and in each case the parameter involved is a non-dimensional slope of the axial-velocity profile at any cross-section. Whitehead and Beavers assumed that the axial-velocity profile at any axial position belongs to a family of profiles governed by the single parameter λ, and the equations of motion were satisfied exactly at a design radius defined as the root mean square of the hub and tip radii. At the same time Mellor, working independently, also assumed that the axial-velocity profiles belong to a family of curves and he derived a differential equation at a design radius which was so chosen that the equation could be solved analytically. Howell also made a similar assumption about the axial-velocity profiles and used as the design radius the mean of the hub and tip radii. Both Mellor and Howell made assumptions which enabled the differential equations to be solved exactly, whereas Whitehead and Beavers obtained a more general solution in the form of a programme for use on a high-speed digital computer.

The original single-parameter theory has been greatly modified in this paper to allow for variations in density of the working medium and variations in annulus area of the turbo-machine. The inclusion of the density as a variable necessitates a modification to the definition of the parameter λ, plus the introduction of a second parameter μ defined as the dimensionless slope of the density profile at the design radius, where the assumption has been made that the density profile belongs to a single-parameter family of curves. The result of these modifications is that the assumed variation of axial velocity with radius belongs to a family of curves governed by the two parameters λ and μ, thus considerably increasing the range of allowed profiles. The equations of motion are again satisfied exactly at a single design radius, defined as the root mean square of the hub and tip radii at any axial position. Isentropic flow is assumed and all blade losses are neglected. The problem is reduced to a single second-order linear differential equation for λ, which can only be solved by means of an electronic computer. Details are given in Section 8 of a programme which exists for use on the EDSAC 2 computer of the Cambridge University Mathematical Laboratory, and which can be used to analyse the flow through any variable-area turbo-machine. Examples of the way in which this programme may be used are given in Sections 9 to 15, which also serve as comparisons of the parameter-theory results with existing experimental and theoretical results. The assumptions made, and the method of solution employed, require that the flow within a machine be always subsonic. Consequently it has not been possible to compare parameter-theory calculations with the compressible actuator-disc calculations of Hawthorne and Ringrose (1962), in which the flow is in part supersonic.

2. Notation

The notation used is illustrated in Figures 1, 2, 3 and 4.

Co-ordinate/

Co-ordinate system and velocities

r - radial co-ordinate

x - axial co-ordinate

θ - tangential co-ordinate

U - radial component of velocity

V - axial component of velocity

W - tangential component of velocity

General Notation

a - axial chord of blade or axial length of gap

A - constant defined by equation (59)

b - scaling factor defined by equation (86)

B - constant defined by equation (55) expressed at inlet to a gap

C - constant defined in equation (31)

C_p - specific heat at constant pressure

g - static-pressure gradient

G - radial gradient of relative stagnation temperature

h - hub radius

k_o - constant defined by equation (67)

K - gas constant

m - mass-flow rate

M - Mach number relative to a blade row

M_x - axial component of Mach number

p - static pressure

p_s - stagnation pressure

R - design radius $= \left[\frac{t^2 + h^2}{2}\right]^{\frac{1}{2}}$

t - tip radius

T - static temperature

T_s - stagnation temperature relative to a blade row

α - gas angle relative to a blade row

β - = Tan α

γ - ratio of specific heats

η - variable defined as $\frac{(t^2 - h^2)\lambda}{32R^2}$

slope of/

λ - slope of (ρ V) profile at the design radius $= \dfrac{R}{\rho_R V_R}\left[\dfrac{\partial}{\partial r}(\rho V)\right]_{r=R}$

μ - slope of density profile at the design radius $= \dfrac{R}{\rho_R}\left[\dfrac{\partial \rho}{\partial r}\right]_{r=R}$

ρ - density

ψ - stream function defined by equations (10) and (11)

Ω - angular velocity of rotor

Suffices

R - conditions at design radius

S - stagnation conditions

o - conditions at entry to the turbo-machine

1 - conditions at entry to a rotor row

2 - conditions at exit from a rotor row

3 - conditions at entry to a stator row

4 - conditions at exit from a stator row

Primed numbers refer to conditions in the gaps at the points corresponding to the above numbers.

3. Approximations

Most of the approximations made in this paper will be introduced in the relevant sections. However, it is thought to be convenient to present, at this point, a complete list of the approximations which will be made.

(a) The flow is assumed to be rotationally symmetric and non-turbulent, and the gas is assumed to be inviscid. This neglects all blade grid effects such as wakes and secondary flows, and also all boundary-layer effects so that the streamlines at the hub and tip radii follow exactly the shape of the turbo-machine at those radii.

(b) It is assumed that each blade row can be replaced by a large number of infinitely thin blades having the same axial chord as the actual blades. The outlet angle of these blades is the gas outlet angle, but the inlet angle is the gas inlet angle determined by the conditions at exit from the previous blade row.

(c) It is assumed that the radial displacement of the streamlines from the position they would have under uniform flow conditions is small.

(d) The variation of density with radius is assumed to be of the form of a one-dimensional parameter family of curves. Likewise the radial variation of the product (ρ V) is assumed to be of the form of a one-dimensional parameter family of curves. Hence the radial variation of axial velocity is governed by a family of curves which depend on two parameters.

(e)/

(e) The equations of motion will be satisfied exactly at one radius only, called the design radius. Away from the design radius the equations of motion will not be satisfied exactly. However, since the axial-velocity profile and its radial derivative are correctly determined at the design radius, as are the density profile and its associated radial derivative, it is possible to draw the complete axial-velocity and density profiles with little error.

(f) It is assumed that the blades exert no radial force on the gas.

(g) It is assumed that the gas flows through each row of blades on a path such that the tangent of the relative air angle varies linearly from the leading to the trailing edge of the blades. This assumption is exact for a row of infinitely thin untwisted blades designed on a parabolic centre-line working at zero incidence.

It is not essential to the theory that this last assumption be made in the given form. The theory can readily be modified to allow for any given variation in the tangent of the relative air angle through a blade passage. However the linear variation has been chosen because it combines simplicity with a good approximation to the actual variation through the centre of a blade passage.

(h) Within an axial gap it will be assumed that the circulation along the design-radius streamline is constant.

(i) Within a blade passage or gap it will be assumed that the hub and tip radii vary linearly from the inlet to the outlet of the section. This means that the flare in compressors and turbines is achieved by having discontinuities in the slopes of the hub and tip radii at the leading and trailing edges of the blade rows.

(j) Within a blade row it is assumed that the stagnation temperature relative to that blade row is constant along a streamline.

(k) It is assumed that the flow is isentropic throughout the turbo-machine. This neglects any change in the enthalpy caused by blade losses.

(l) It is assumed that the radial component of velocity at the design radius is small compared with the axial and tangential components.

4. Basic Theory

4.1 Assumed Profiles

In the single-parameter theory for the flow of an incompressible fluid through a constant area turbo-machine (Whitehead and Beavers 1961) the

fundamental/

fundamental approximation was made that the distribution of axial velocity with radius could be represented by the family of profiles

$$V = V_R\left[1 + \frac{\lambda}{2}\left(\frac{r^2}{R^2} - 1\right)\right]. \qquad \cdots (1)$$

The introduction of compressibility into the analysis necessitates a modification to the profiles defined by equation (1) in order to allow for the radial variation of density. This is achieved by assuming that the radial distribution of the axial mass-flow rate per unit area belongs to a family of profiles of the type defined by equation (1). Hence the fundamental approximation now becomes

$$\rho V = \rho_R V_R\left[1 + \frac{\lambda}{2}\left(\frac{r^2}{R^2} - 1\right)\right] \qquad \cdots (2)$$

and the differentiation of this equation in the radial direction yields the definition of λ, which is

$$\lambda = \frac{R}{\rho_R V_R}\left[\frac{\partial}{\partial r}(\rho V)\right]_{r=R}. \qquad \cdots (3)$$

In order to solve the equations of motion it will be found necessary to know how the density at any axial point varies with radius, and it is convenient at this juncture to specify this variation. Consequently a second fundamental approximation has to be made, which involves the introduction into the analysis of a second dimensionless parameter. It will be assumed that at any axial position within the turbo-machine the radial variation of density is governed by the family of profiles.

$$\rho = \rho_R\left[1 + \frac{\mu}{2}\left(\frac{r^2}{R^2} - 1\right)\right], \qquad \cdots (4)$$

where μ is proportional to the radial density gradient at the radius R, and is defined by

$$\mu = \frac{R}{\rho_R}\left[\frac{\partial \rho}{\partial r}\right]_{r=R}. \qquad \cdots (5)$$

The assumed density profiles are shown in Figure 5.

Equations (3) and (5) can be combined to give the slope of the axial-velocity profile at the radius R, and this is

$$\frac{R}{V_R}\left[\frac{\partial V}{\partial r}\right]_{r=R} = \lambda - \mu. \qquad \cdots (6)$$

Equations/

Equations (2) and (4) show that the assumed axial-velocity profiles belong to a family of curves governed by the two parameters λ and μ, and expressed by the equation

$$V = V_R \frac{\left[1 + \frac{\lambda}{2}\left(\frac{r^2}{R^2} - 1\right)\right]}{\left[1 + \frac{\mu}{2}\left(\frac{r^2}{R^2} - 1\right)\right]} .$$

The assumed axial-velocity profiles for various values of λ and μ are shown in Figure 6. Equations (2) and (4) are not the only profiles which can be used. They have been chosen to maintain algebraic simplicity and because they give profiles close to those normally obtained in practice.

Since restricted ranges of both axial-velocity and density profiles have been chosen, it will be possible to satisfy the equations of motion exactly at one radius only. This radius will be termed the design radius and denoted by R, and it is defined as the root mean square of the hub and tip radii, so that

$$R^2 = \frac{t^2 + h^2}{2} . \qquad \ldots (7)$$

The mass-flow rate through the machine is given by

$$m = \int_h^t 2\pi r V \rho . dr ,$$

and using equation (2) this can be expressed as

$$m = 2\pi\rho_R V_R \int_h^t \left[r + \frac{\lambda}{2}\left(\frac{r^3}{R^2} - r\right)\right] dr ,$$

which can be reduced to

$$m = \pi\rho_R V_R (t^2 - h^2) \qquad \ldots (8)$$

by application of equation (7).

Equation (8) gives the important result that the expression for the mass-flow rate is independent of λ and μ. The assumed axial-velocity and density profiles, and the definition of the design radius, have been chosen to this end.

4.2/

4.2 The Continuity Equation

For axisymmetric flow, the continuity equation is

$$\frac{\partial}{\partial r}(\rho r U) + \frac{\partial}{\partial x}(\rho r V) = 0 \quad . \qquad \ldots (9)$$

Thus, a stream function ψ can be defined so that

$$\frac{\partial \psi}{\partial r} = -\rho r V \qquad \ldots (10)$$

$$\frac{\partial \psi}{\partial x} = \rho r U \quad . \qquad \ldots (11)$$

If the assumed profile for ρV given by equation (2) is now substituted into equation (10), there results

$$\frac{\partial \psi}{\partial r} = -\rho_R V_R r \left[1 + \frac{\lambda}{2}\left(\frac{r^2}{R^2} - 1\right)\right] \quad .$$

This equation can now be integrated in the radial direction between the hub radius and a radius r to give

$$\psi_r - \psi_h = -\rho_R V_R \left[\frac{r^2 - h^2}{2} + \frac{\lambda}{2}\left(\frac{r^4 - h^4}{4R^2} - \frac{r^2 - h^2}{2}\right)\right] \quad . \qquad \ldots (12)$$

If equation (12) is now differentiated with respect to x, and the expression for $\partial\psi/\partial x$ given by equation (11) substituted into the result, an equation for the radial velocity at any radius r is obtained in the form

$$\rho r U = \frac{\partial \psi_h}{\partial x} - \frac{\partial}{\partial x}\left[\rho_R V_R \left(\frac{r^2 - h^2}{2}\right)\right] - \frac{\partial}{\partial x}\left[\frac{\rho_R V_R \lambda}{2}\left(\frac{r^4 - h^4}{4R^2} - \frac{r^2 - h^2}{2}\right)\right] \qquad \ldots (13)$$

To obtain an expression for $\partial\psi_h/\partial x$, it is noted that

$$\frac{\partial \psi_h}{\partial x} = \left(\frac{\partial \psi}{\partial x}\right)_h + \left(\frac{\partial \psi}{\partial r}\right)_h \cdot \frac{\partial h}{\partial x} \quad , \qquad \ldots (14)$$

and by substituting equations (10) and (11) into this equation there follows at once the result

$$\frac{\partial \psi_h}{\partial x} = \rho_h U_h h - \rho_h V_h h \frac{\partial h}{\partial x} \quad . \qquad \ldots (15)$$

However, at the hub radius, since the flow must be parallel to the surface,

$$\frac{\partial h}{\partial x} = \frac{U_h}{V_h}$$

so/

so that equation (15) becomes

$$\frac{\partial \psi_h}{\partial x} = 0 \qquad \ldots (16)$$

This result may be obtained at once from the assumption that the streamline at the hub radius remains on the hub at all times.

Using this result, equation (13) can be written in the form

$$\rho r U = -\frac{r^2}{2}\cdot\frac{\partial}{\partial x}(\rho_R V_R) + \frac{\partial}{\partial x}\left(\frac{\rho_R V_R h^2}{2}\right) - r^4\frac{\partial}{\partial x}\left(\frac{\rho_R V_R \lambda}{8R^2}\right) + r^2\frac{\partial}{\partial x}\left(\frac{\rho_R V_R \lambda}{4}\right) + \frac{\partial}{\partial x}\left[\frac{\rho_R V_R \lambda}{2}\left(\frac{h^4}{4R^2} - \frac{h^2}{2}\right)\right] \quad \ldots (17)$$

If this equation is now differentiated with respect to x and the result expressed at the design radius, the following equation is obtained after simplification

$$R\left[\frac{\partial}{\partial x}(\rho U)\right]_R = \left[\frac{\partial^2}{\partial x^2}\left[\frac{(t^2-h^2)^2 \rho_R V_R \lambda}{32.R^2}\right] + 2\frac{\partial}{\partial x}(\rho_R V_R) R\frac{\partial R}{\partial x} + V_R \rho_R \frac{\partial}{\partial x}\left(R\frac{\partial R}{\partial x}\right) - \frac{\lambda \rho_R V_R}{R^2}\left(R\frac{\partial R}{\partial x}\right)^2\right]_{r=R} \quad \ldots (18)$$

Using equation (8), this can be written as

$$R\left[\frac{\partial(\rho U)}{\partial x}\right] = \frac{m}{\pi}\left[\frac{\partial^2}{\partial x^2}\left[\frac{(t^2-h^2)\lambda}{32.R^2}\right] + 2\frac{\partial}{\partial x}\left(\frac{1}{t^2-h^2}\right) R\frac{\partial R}{\partial x} + \frac{1}{(t^2-h^2)}\frac{\partial}{\partial x}\left(R\frac{\partial R}{\partial x}\right) - \frac{\lambda}{(t^2-h^2)R^2}\left(R\frac{\partial R}{\partial x}\right)^2\right]_{r=R} \quad \ldots (19)$$

Equation (19) expresses $[\partial(\rho U)/\partial x]$ at the design radius as a function of λ and the known geometry of the compressor or turbine, and is thus in a suitable form for use with the equation of motion in the radial direction, which will also be expressed in terms of the same variables.

4.3 The Basic Differential Equation for λ.

Neglecting any radial force exerted by or on the blades, the equation of motion in the radial direction for axi-symmetric flow is

$$U\frac{\partial U}{\partial r} + V\frac{\partial U}{\partial x} - \frac{W^2}{r} = -\frac{1}{\rho}\frac{\partial p}{\partial r} \,. \qquad \ldots (20)$$

Since both the density and velocity variations have been limited to fixed sets of profiles, equation (20) will only be exactly true at the design radius as defined by equation (7). Thus at the design radius, this equation becomes

$$\frac{R}{V_R}\left(\frac{\partial U}{\partial x}\right)_R - \left(\frac{W}{V}\right)_R^2 = -\frac{R}{V_R^2}\left[\frac{1}{\rho_R}\left(\frac{\partial p}{\partial r}\right)_R + U_R\left(\frac{\partial U}{\partial r}\right)_R\right] \,. \qquad \ldots (21)$$

Since $$R\left[\frac{\partial(\rho U)}{\partial x}\right]_R = R\left[\rho_R\left(\frac{\partial U}{\partial x}\right)_R + U_R\left(\frac{\partial \rho}{\partial x}\right)_R\right] \qquad \ldots (22)$$

equation (21) can be written in the form

$$\frac{R}{\rho_R V_R}\left[\frac{\partial}{\partial x}(\rho U)\right]_R - \frac{R U_R}{\rho_R V_R}\left[\frac{\partial \rho}{\partial x}\right]_R - \left(\frac{W}{V}\right)_R^2 = -g \,, \qquad \ldots (23)$$

where $$g = \frac{R}{V_R^2}\left[\frac{1}{\rho_R}\left(\frac{\partial p}{\partial r}\right)_R + U_R\left(\frac{\partial U}{\partial r}\right)_R\right] \,, \qquad \ldots (24)$$

In/

In general the radial velocity at the design radius will be small so that the term $U_R(\partial U/\partial r)_R$ can be neglected, and then g can be thought of as a dimensionless radial static-pressure gradient at the design radius.

Now equation (17) expressed at the design radius can be written as

$$R\rho_R U_R = \frac{\partial}{\partial x}\left[\frac{(R^2 - h^2)^2 \rho_R V_R \lambda}{8R^2}\right] + \rho_R V_R R\frac{\partial R}{\partial x} .$$

Using equations (7) and (8), an expression for U_R, the radial component of velocity, can be obtained in the form

$$U_R = \frac{m}{\pi\rho_R R}\left[\frac{\partial}{\partial x}\left[\frac{(t^2 - h^2)\lambda}{32\,R^2}\right] + \frac{R\frac{\partial R}{\partial x}}{t^2 - h^2}\right]_R . \qquad \ldots (25)$$

Substituting equation (25) into equation (23) gives

$$R\left[\frac{\partial}{\partial x}(\rho U)\right]_R = \frac{m}{\pi(t^2-h^2)}\left[\left(\frac{W}{V}\right)_R^2 - g\right] + \frac{m}{\pi}\left(\frac{1}{\rho}\frac{\partial \rho}{\partial x}\right)_R \left\{\frac{\partial}{\partial x}\left[\frac{(t^2-h^2)\lambda}{32\,R^2}\right] + \frac{R\frac{\partial R}{\partial x}}{t^2-h^2}\right\}_R . \qquad \ldots (26)$$

Then the elimination of $R[\partial(\rho U)/\partial x]_R$ from equations (19) and (26) yields the equation

$$\left\{\frac{\partial^2}{\partial x^2}\left[\frac{(t^2-h^2)\lambda}{32\,R^2}\right] - \frac{1}{\rho}\frac{\partial \rho}{\partial x}\cdot\frac{\partial}{\partial x}\left[\frac{(t^2-h^2)\lambda}{32\,R^2}\right] - \frac{\lambda}{(t^2-h^2)R^2}\left(R\frac{\partial R}{\partial x}\right)^2\right\}_R \qquad \ldots (27)$$

$$= \left\{\frac{1}{(t^2-h^2)}\left[\left(\frac{W}{V}\right)^2 - g - \frac{\partial}{\partial x}\left(R\frac{\partial R}{\partial x}\right)\right] - 2\frac{\partial}{\partial x}\left[\frac{1}{t^2-h^2}\right]R\frac{\partial R}{\partial x} + \frac{1}{\rho}\frac{\partial \rho}{\partial x}\left[\frac{R\frac{\partial R}{\partial x}}{t^2-h^2}\right]\right\}_R .$$

Now, define a variable η such that

$$\eta = \frac{(t^2 - h^2)\lambda}{32\,R^2} . \qquad \ldots (28)$$

Substituting this definition into equation (2) gives

$$\frac{\rho V}{\rho_R V_R} = 1 + 16\eta\frac{r^2 - R^2}{t^2 - h^2} .$$

Thus, at the tip radius, $\rho V/\rho_R V_R = 1 + 8\eta$

and at the hub radius, $\rho V/\rho_R V_R = 1 - 8\eta$

so that separation occurs at the hub or tip radius when $\eta = \pm\frac{1}{8}$

Returning/

Returning to the main analysis, since equation (27) has been derived for a fixed radius, it is dependent on x only, and hence the partial derivatives may be replaced by total derivatives. Introducing the variable η, equation (27) then becomes

$$\frac{d^2\eta}{dx^2} - \left(\frac{1}{\rho}\frac{\partial\rho}{\partial x}\right)_R \frac{d\eta}{dx} - \frac{32\left(R\frac{dR}{dx}\right)^2}{(t^2-h^2)^2}\eta = \frac{1}{(t^2-h^2)}\left[\left(\frac{W}{V}\right)_R^2 - g - \frac{d}{dx}\left(R\frac{dR}{dx}\right)\right]$$

$$- 2\frac{d}{dx}\left(\frac{1}{t^2-h^2}\right)R\frac{dR}{dx} + \left(\frac{1}{\rho}\frac{\partial\rho}{\partial x}\right)_R\left[\frac{R\frac{dR}{dx}}{t^2-h^2}\right] . \qquad \ldots (29)$$

This is the basic differential equation to be solved. However, before a solution can be obtained it is necessary to know how the various quantities appearing in this equation vary with the co-ordinate distance x. The hub, tip and design radius at any point will all be known from the geometry of the turbo-machine under analysis, and the quantity $(W/V)_R$ will also be known as this depends upon the blade geometry. It therefore remains to obtain expressions for the variations with x of $\rho_R(1/\rho.\partial\rho/\partial x)_R$ and g. This will be done in section 4.5, but preceding this the assumed variations of hub and tip radii will be discussed.

4.4 Hub and Casing Profiles

To simplify the arithmetic it will be assumed that both the hub and tip radii change in a linear fashion within any blade row or duct. This assumption will, usually, be exact, as the mechanical difficulties encountered in the manufacture of the individual blades are such that only rarely are compressor or turbine blades made with hub and tip variations which are other than linear. This means that the hub and casing profiles of a turbo-machine each consist of a series of straight lines which may or may not have discontinuities in slope at the leading and trailing edges of the blade rows. Typical hub and casing shapes can be seen in Figures 1, 14, 28(a), 28(b), 47 and 52.

Since the hub and tip radii vary linearly within any blade row, dh/dx and dt/dx are both constant within that row. Then from equation (7)

$$R\frac{dR}{dx} = \frac{1}{2}\left[t\frac{dt}{dx} + h\frac{dh}{dx}\right] \qquad \ldots (30)$$

and

$$\frac{d}{dx}\left(R\frac{dR}{dx}\right) = \frac{1}{2}\left[\left(\frac{dt}{dx}\right)^2 + \left(\frac{dh}{dx}\right)^2\right]$$

Thus it can be seen that at any point within a blade row or gap the term $R.dR/dx$ depends upon the values of the hub and tip radii at that point, whereas the term $d(RdR/dx)/dx$ is the same at all points within the given section.

4.5 The Density Variation

In order to find how the density, and hence $(1/\rho.d\rho/dx)_R$ and g, varies with axial distance through a blade row or gap, it is necessary

to/

to make further assumptions about the nature of the flow. Consequently, it will be assumed that,

(i) the stagnation temperature relative to a blade row is constant along a streamline; and

(ii) the flow is isentropic.

The second of these assumptions implies that the flow obeys the law

$$T = C\rho^{\gamma-1}, \qquad \cdots (31)$$

where C is a constant for any given blade row or gap between adjacent blade rows, and has the same value for all blade rows and gaps. This follows since across any interface between a blade row and gap both the static temperature and the density must be continuous, so that C must also be continuous.

Now, relative to the blade row under consideration, the energy equation for a perfect gas expressed at the design radius may be written as

$$C_p T_s = C_p T + \frac{1}{2} V_R^2 (1 + \beta_R^2) , \qquad \cdots (32)$$

where T_s is the stagnation temperature relative to the blade row and β is the tangent of the relative gas angle α at any point. Combining equations (8), (31) and (32) there results

$$\rho_R^{\gamma+1} - \frac{T_s}{C} \cdot \rho_R^2 + \frac{m^2 (1 + \beta_R^2)}{2C_p C \pi^2 (t^2 - h^2)^2} = 0 , \qquad \cdots (33)$$

which is the equation governing the variation of ρ_R within any blade passage or duct. Since the values of all the quantities appearing in equation (33) except ρ_R will be known at any axial position, this equation can be solved numerically to give the value of the density at the design radius for that chosen axial position. Some notes on the method used for solving equation (33) are given in the Appendix. For the purposes of calculating the variation in density within a blade passage or gap it will be assumed that the relative stagnation temperature is constant along the design radius. This will have an insignificant effect on the solution of equation (33) since the radial displacement of the design-radius streamline is very small.

To calculate $(1/\rho . \partial\rho/\partial x)_R$, equation (33) is differentiated with respect to x. Since T_s, m and C are constants, this gives

$$\left[C(\gamma + 1)\rho_R^{\gamma+1} - 2T_s\rho_R^2 \right] \left(\frac{1}{\rho} \frac{\partial \rho}{\partial x} \right)_R = \frac{m^2 (1 + \beta_R^2)}{C_p \pi^2 (t^2 - h^2)^2} \left[\frac{2\left(t\frac{dt}{dx} - h\frac{dh}{dx} \right)}{(t^2 - h^2)} - \frac{\beta_R \frac{d\beta_R}{dx}}{(1+\beta_R^2)} \right] . \qquad \cdots (34)$$

Using/

Using equations (7), (31) and (32), this equation can be written in the form

$$\left[1 - \frac{V_R^2(1+\beta_R^2)}{(\gamma-1)C_pT}\right]\left(\frac{1}{\rho}\frac{\partial\rho}{\partial x}\right)_R = \frac{V_R^2(1+\beta_R^2)}{(\gamma-1)C_pT}\left[\frac{2\left(t\frac{dt}{dx} - h\frac{dh}{dx}\right)}{(t^2-h^2)} - \frac{\beta_R\frac{d\beta_R}{dx}}{(1+\beta_R^2)}\right] \quad \ldots (35)$$

Now, let the axial Mach number at the design radius be denoted by M_x, and the Mach number relative to the blade row at the design radius be **M**. Then

$$M_x^2 = \frac{V_R^2}{(\gamma-1)C_pt} \quad \ldots (36)$$

and

$$M^2 = M_x^2(1+\beta_R^2) \quad . \quad \ldots (37)$$

Using these definitions, equation (35) becomes

$$\left(\frac{1}{\rho}\cdot\frac{\partial\rho}{\partial x}\right)_R = \frac{M^2}{1-M^2}\left[\frac{2\left(t\frac{dt}{dx} - h\frac{dh}{dx}\right)}{(t^2-h^2)} - \frac{\beta_R\frac{d\beta_R}{dx}}{(1+\beta_R^2)}\right] . \quad \ldots (38)$$

This equation gives the required variation of $(1/\rho\ \partial\rho/\partial x)_R$ in terms of the relative Mach number and quantities which are functions of the geometry of the turbo-machine being analysed. The relative Mach number can be obtained by combining equations (7), (31) (36) and (37) to give

$$M^2 = \frac{m^2(1+\beta_R^2)}{\pi^2(t^2-h^2)^2(\gamma-1)C_pC\rho_R^{\gamma+1}} . \quad \ldots (39)$$

The final quantity required to make the solving of equation (29) possible is the value of the static-pressure gradient, g, along the axial direction. However, as the static-pressure gradient will vary along the machine in a manner that cannot readily be evaluated, it is convenient to express it in terms of the radial gradient of the relative stagnation temperature, the variation of which can be calculated. Before this is done the relationship between μ and g will be derived.

The equation of state for a perfect gas is

$$p = K\rho T \quad , \quad \ldots (40)$$

where K is the gas constant for the particular gas being used. By eliminating the static temperature, T, from equations (31) and (40), and differentiating along the radial direction, there results

$$\frac{1}{p}\frac{\partial p}{\partial r} = \frac{\gamma}{\rho}\frac{\partial\rho}{\partial r} .$$

$$\therefore \quad \mu = \frac{1}{\gamma}\left(\frac{R}{p}\frac{\partial p}{\partial r}\right)_R \quad \ldots (41)$$

Hence,/

Hence, since
$$\mu = \frac{R}{\rho_R}\left(\frac{\partial \rho}{\partial r}\right)_R \qquad \ldots (41)$$

and
$$g = \frac{M}{\rho_R V_R^2}\left(\frac{\partial p}{\partial r}\right)_R ,$$

(neglecting the UdU/dr term in equation (24)) equation (41) can be expressed as

$$\mu = g M_x^2 \qquad \ldots (42)$$

To relate g to the radial gradient of relative stagnation temperature, equation (32) is specified at a general point in the co-ordinate system, differentiated in the radial direction and the result then expressed at the design radius. If these steps are performed the following equation is obtained:

$$C_p\left(\frac{\partial T_s}{\partial r}\right)_R = C_p\left(\frac{\partial T}{\partial r}\right)_R + \left(V\frac{\partial V}{\partial r}\right)_R(1+\beta_R^2) + \left(\beta\frac{\partial \beta}{\partial r}\right)_R V_R^2 . \qquad \ldots (43)$$

Equations (31) and (40) can be differentiated and combined to give

$$C_p\left(\frac{\partial T}{\partial r}\right)_R = \left(\frac{1}{\rho}\frac{\partial p}{\partial r}\right)_R ,$$

and this can then be substituted, together with equation (6), into equation (43) to produce the equation

$$\frac{R.C_p}{V_R^2}\left(\frac{\partial T_s}{\partial r}\right)_R = g + (\lambda - \mu)(1+\beta_R^2) + R\beta_R\left(\frac{\partial \beta}{\partial r}\right)_R . \qquad \ldots (44)$$

Hence, using the expression for μ given in equation (42) this equation becomes

$$g = \frac{G - \lambda(1+\beta_R^2) - R\beta_R\left(\frac{\partial \beta}{\partial r}\right)_R}{1 - M^2} \qquad \ldots (45)$$

where
$$G = \frac{RC_p}{V_R^2}\left(\frac{\partial T_s}{\partial r}\right)_R \qquad \ldots (46)$$

This expression for the static-pressure gradient can now be substituted into equation (29) to produce the general equation governing the flow in a blade passage or in the gaps between the blade rows. The resultant general equation is

$$\frac{d^2\eta}{dx^2} - \left[\frac{1}{\rho}\frac{\partial \rho}{\partial x}\right]_R \frac{d\eta}{dx} - \frac{32\eta}{(t^2-h^2)^2}\left[\left(R\frac{dR}{dx}\right)^2 + \frac{R^2(1+\beta_R^2)}{1-M^2}\right]$$
$$= \frac{R\beta_R\left(\frac{\partial \beta}{\partial r}\right)_R - G}{(1-M^2)(t^2-h^2)} + \frac{1}{(t^2-h^2)}\left[\left(\frac{W}{V}\right)_R^2 - \frac{d}{dx}\left(R\frac{dR}{dx}\right) + R\frac{dR}{dx}\left(\frac{1}{\rho}\frac{\partial \rho}{\partial x}\right)_R + \ldots \right.$$
$$\left. + \frac{4R\frac{dR}{dx}\left(t\frac{dt}{dx} - h\frac{dh}{dx}\right)}{(t^2-h^2)}\right] . \qquad \ldots (47)$$

It only remains now to find how the gradient of relative stagnation temperature varies through a blade row or gap and equation (47) can be solved. To derive the required variation consider two planes, an axial distance Δx apart, within any one blade row or gap, as shown in Figure 4. Consider now the neighbouring streamlines, AB and CD, which are always close to the design radius, and which intersect the two planes in points A and C, B and D respectively, where A and D lie on the design radius. The points A and C are at radii R_1 and $R_1 - \delta R_1$ respectively, and like-wise the points B and D are at radii $R_2 + \delta R_2$ and R_2. Then since there can be no flow across these streamlines,

$$\pi V_{R_1} \rho_{R_1} \left[R_1^2 - (R_1 - \delta R_1)^2 \right] = \pi V_{R_2} \rho_{R_2} \left[(R_2 + \delta R_2)^2 - R_2^2 \right] .$$

$$V_{R_1} \rho_{R_1} R_1 \delta R_1 = V_{R_2} \rho_{R_2} R_2 \delta R_2$$

At the design radius,

$$V_R \rho_R R \delta R = \text{constant} \qquad \cdots (48)$$

Hence, since T_s has been assumed constant along a streamline,

$$\left(\frac{\partial T_S}{\partial r} \right)_R \propto V_R \rho_R R .$$

$\therefore$ From the definition of G given by equation (46)

$$G \propto \frac{RC_p}{V_R^2} V_R \rho_R R .$$

Thus, using equation (8),

$$G \propto \rho_R^2 R^2 (t^2 - h^2) . \qquad \cdots (49)$$

Hence, if the value of G is known at inlet to a blade row or duct, the value at any other axial station within that same blade row or duct can be found from equation (49).

All the information necessary for solving equation (47) has now been derived. In Sections 5, 6 and 7 details of the methods employed for obtaining solutions in annular ducts, isolated blade rows and multi-stage machines will be presented. However, before considering these particular solutions of equation (47) it will be shown how the value of η at any axial position within a turbo-machine can be used to predict the radial displacement of the design-radius streamline at that position.

4.6 The Displacement of the 'Design-Radius' Streamline

Referring to Figure 4, the stream function ψ at the point A is given by equation (12) as

$$\psi_A - \psi_{h_1} = - \frac{V_{R_1} \rho_{R_1}}{2} \left[R_1^2 - h_1^2 + \lambda \left(\frac{R_1^4 - h_1^4}{4R_1^2} - \frac{R_1^2 - h_1^2}{2} \right) \right] ,$$

where the subscript 1 refers to plane 1.

By/

By making use of equations (7), (8) and (28) this equation can be written as

$$\psi_A - \psi_{h_1} = -\frac{m}{\pi}\left(\frac{1}{4} - \eta_1\right) . \qquad \ldots (50)$$

Similarly, at the point D

$$\psi_o - \psi_{h_2} = -\frac{m}{\pi}\left(\frac{1}{4} - \eta_2\right) . \qquad \ldots (51)$$

Subtracting equation (50) from equation (51) gives

$$\psi_o - \psi_A = \frac{m}{\pi}(\eta_2 - \eta_1) + \psi_{h_2} - \psi_{h_1} .$$

Now, the streamline at the hub radius will always remain at the hub radius since all boundary-layer effects have been neglected. Hence $\psi_{h_1} = \psi_{h_2}$. This result could also have been deduced from the equation

$$(\partial\psi)_h = \left(\frac{\partial\psi}{\partial x}\right)_h \delta x + \left(\frac{\partial\psi}{\partial r}\right)_h \delta r ,$$

together with equation (14) written in the form

$$\left(\frac{\partial\psi}{\partial x}\right)_h = -\left(\frac{\partial\psi}{\partial r}\right)_h \cdot \frac{\partial h}{\partial x} ,$$

since $\partial\psi_h/\partial x = 0$ from equation (16).

Consequently, $$\psi_o - \psi_A = \frac{m}{\pi}(\eta_2 - \eta_1) . \qquad \ldots (52)$$

However, at the plane 2, equation (10) can be written as

$$\psi_B - \psi_D = -V_{R_2}\rho_{R_2} \cdot R_2 \cdot \delta R_2 , \qquad \ldots (53)$$

and since A and B lie on the same streamline, $\psi_A = \psi_B$, so that equation (53) becomes

$$\psi_o - \psi_A = V_{R_2}\rho_{R_2} \cdot R_2 \cdot \delta R_2 .$$

Equating this equation to equation (52) and using equation (8), gives

$$\delta R_2 = \frac{(t_2^2 - h_2^2)}{R_2} \cdot (\eta_2 - \eta_1) ,$$

where δR_2 is the radial displacement from the design radius at plane 2 of the streamline which was coincident with the design radius at plane 1. Thus, if the plane 1 is taken well upstream of the turbo-machine where the flow is uniform and

there/

there is no radial displacement of the streamlines, the value of η at this point being denoted by η_∞, then at any axial point in the turbo-machine the radial displacement from the design radius of the streamline which originally coincided with the design radius is given by

$$\delta R = \frac{(t^2 - h^2)}{R} \cdot (\eta - \eta_\infty) \quad . \qquad \ldots (54)$$

5. Flow in an Annular Duct

The first part of this section will be concerned with the solution of equation (47) in a general variable-area duct. This will therefore include the method of solving this equation in the annular gaps between adjacent rows of blades in a multi-stage turbo-machine. In the second part of this section the solutions of equation (47) in the annular ducts which form the inlet and exit of a compressor or turbine will be considered, and it will be shown how the solutions in these two components can be used as boundary conditions for the complete solution of equation (47) in a multi-stage compressor or turbine.

5.1 General Variable-Area Duct

For flow in an annular duct the criterion which must be satisfied is that the circulation along a streamline is constant. Hence, along a streamline,

$$\begin{aligned} Wr &= \text{constant} \\ \text{or} \qquad \beta Vr &= \text{constant} \end{aligned} \qquad \ldots (55)$$

Now, whereas in a blade row the variation of $(\partial\beta/\partial r)_R$ in the axial direction is specified, in a duct the variation cannot be so specified and the terms involving $(\partial\beta/\partial r)_R$ must be eliminated from equation (47) before a solution can be obtained.

Referring to Figure 4, which shows an elementary section of duct, 1 and 2 are two radial planes distance Δx apart. The design radius cuts plane 1 in A and plane 2 in D, and the streamline through point A cuts the plane 2 in B. Likewise the streamline through D cuts plane 1 in the point C. $CA = \delta R_1$ and $DB = \delta R_2$. Then at the plane 2,

$$(Wr)_B = (Wr)_D + \frac{\partial}{\partial r}(Wr)_D \cdot \delta R_2 \quad , \qquad \ldots (56)$$

and at the plane 1

$$(Wr)_C = (Wr)_A - \frac{\partial}{\partial r}(Wr)_A \cdot \delta R_1 \quad . \qquad \ldots (57)$$

Since A and B lie on the same streamline, from equation (55),

$$(Wr)_A = (Wr)_B \quad .$$

Similarly C and D also lie on the same streamline, and so

$$(Wr)_C = (Wr)_D \quad .$$

Hence,/

Hence, using these results, equations (56) and (57) can be combined to give for any two adjacent streamlines

$$\frac{\partial}{\partial r}(Wr)_D \delta R_2 = \frac{\partial}{\partial r}(Wr)_A \delta R_1 \quad . \qquad \ldots (58)$$

But, from equation (48),

$$V_{R1} \rho_{R1} R_1 \delta R_1 = V_{R2} \rho_{R2} R_2 \delta R_2$$

so that, by combining this equation with equation (58),

$$\frac{1}{R\rho_R V_R}\left[\frac{\partial}{\partial r}(Wr)\right]_R = \text{CONSTANT} = A \quad . \qquad \ldots (59)$$

Expanding equation (59), and inserting the expression for $(1/V_R)(\partial V/\partial r)_R$ given by equation (6), leads to the result

$$\frac{\beta_R}{\rho_R R}\left[\lambda - \mu + 1 + \frac{R}{\beta_R}\left(\frac{\partial \beta}{\partial r}\right)_R\right] = A \quad .$$

Using the expression given by equation (42) for μ , this equation becomes

$$R\beta_R\left(\frac{\partial \beta}{\partial r}\right)_R = A\rho_R R\beta_R - \beta_R^2 - (\lambda + 1 - gM_x^2) \quad ,$$

and this can now be substituted into equation (45) to give

$$g = \frac{G - \lambda(1 + \beta_R^2) - A\rho_R R\beta_R + \beta_R^2(\lambda + 1 - gM_x^2)}{1 - M^2} \quad .$$

Therefore

$$g = \frac{G - \lambda - A\rho_R R\beta_R + \beta_R^2}{1 - M_x^2} \quad . \qquad \ldots (60)$$

Noting that $\left(\frac{W}{V}\right)_R = \beta_R$ for the flow in a duct, and substituting equation (60) into equation (29), the general equation governing the flow in a duct can be obtained in the form

$$\frac{d^2\eta}{dx^2} - \left(\frac{1}{\rho}\frac{\partial \rho}{\partial x}\right)_R \frac{d\eta}{dx} - \frac{32\eta}{(t^2 - h^2)^2}\left[\left(R\frac{dR}{dx}\right)^2 + \frac{R^2}{1 - M_x^2}\right]$$

$$= \frac{1}{(t^2 - h^2)}\left[\frac{A\rho_R R\beta_R - G - \beta_R^2 M_x^2}{1 - M_x^2} - \frac{d}{dx}\left(R\frac{dR}{dx}\right) + \left(\frac{1}{\rho}\frac{\partial \rho}{\partial x}\right)_R R\frac{dR}{dx} + \frac{4(t\frac{dt}{dx} - h\frac{dh}{dx})}{(t^2 - h^2)} R\frac{dR}{dx}\right] \qquad \ldots (61)$$

The equations governing the variation of density, equations (33) and (38), have also to be modified for flow in a duct, since they both contain β_R explicitly. In a duct β_R is not a simple function of axial distance, as it is in a blade passage, but because of the condition of constant circulation along a streamline β_R at any axial position depends upon the value of ρ_R at that position.

Equation (33)/

Equation (33) is

$$\rho_R^{\gamma+1} - \frac{T_s}{C}\rho_R^2 + \frac{m^2(1+\beta_R^2)}{2C_pC\pi^2(t^2-h^2)^2} = 0 \ .$$

In order to keep the equation for the density at the design radius as simple as possible, an approximation will be made at this point concerning the streamline displacement. It will be assumed for the purpose of calculating the value of the density at the design radius that the radial displacement of the design-radius streamline is small so that equation (55) may be assumed to hold at the design radius.

From equation (55), $\beta_R V_R R = \text{constant} = B$.

Substituting this into equation (33) gives the equation for the variation of the density at the design radius within an annular duct:

$$\rho_R^{\gamma+1} - \rho_R^2\left[\frac{T_s}{C} - \frac{B^2}{2C_pCR^2}\right] + \frac{m^2}{2C_pC\pi^2(t^2-h^2)^2} = 0 \ . \qquad \cdots (62)$$

By differentiating this equation in the axial direction, and using equations (8) and (36), there results

$$\left(\frac{1}{\rho}\frac{\partial\rho}{\partial x}\right)_R = \frac{M_x^2}{1-M_x^2}\left[\frac{2\left(t\frac{dt}{dx} - h\frac{dh}{dx}\right)}{(t^2-h^2)} + \frac{\beta_R^2}{R^2}R\frac{dR}{dx}\right] . \qquad \cdots (63)$$

Having obtained ρ_R from equation (62), β_R can be found from equations (8) and (55), and this can then be used in equation (63) to calculate the value of $(1/\rho.\partial\rho/\partial x)_R$.

Equations (61), (62) and (63) are the relevant equations for flow in an annular duct. At any point on the design radius the value of the density is calculated from equation (62), and this value is then used in equation (63) to give $(1/\rho.\partial\rho/\partial x)_R$ at that point. Finally equation (61) can be solved using these two results and the known geometry of the duct.

For the special case of flow in a duct having constant hub and tip radii, equations (62) and (63) show that ρ_R is constant and $(1/\rho\cdot\partial\rho/\partial x)_R = 0$. Hence the problem is reduced to solving the differential equation

$$\frac{d^2\eta}{dx^2} - \frac{32.R^2.\eta}{(t^2-h^2)^2(1-M_x^2)} - \frac{A\rho_R R\beta_R - G - \beta_R^2 M_x^2}{(t^2-h^2)(1-M_x^2)} = 0 \ . \qquad \cdots (64)$$

5.2 Flow at Inlet to a Compressor or Turbine

It will be assumed that the flow at inlet to a turbo-machine displays the characteristics of flow in a constant-area duct. This is equivalent to placing directly upstream of the first blade row a section of duct which has constant hub and tip radii equal to the values at the leading edge of this blade row, as shown in Figures 1 and 52.

Denoting/

Denoting the values of all quantities at the leading edge of the first blade row by the subscript o, η_o is the solution of the general equation (47) written as

$$\frac{d^2\eta}{dx^2} - \frac{32 R_o^2(1 + \beta_R^2)\eta}{(t_o^2 - h_o^2)^2(1 - M_o^2)} + \frac{G_o - R\beta_R\left(\frac{\partial\beta}{\partial r}\right)_R - \beta_R^2(1 - M_o^2)}{(1 - M_o^2)(t_o^2 - h_o^2)} = 0 \quad , \qquad \ldots (65)$$

where β_R in this equation is the tangent of the air angle relative to space at inlet to the first blade row, i.e., β_R is the tangent of the absolute air angle into the first blade row: $(\partial\beta/\partial r)_R$ is the corresponding radial gradient of β at the design radius. Except in some special cases both β_R and $(\partial\beta/\partial r)_R$ at inlet to the first blade row will be zero.

Introducing now constants k_o and $\eta_{\infty u}$ equation (65) can be expressed in the form

$$k_o^2\frac{d^2\eta}{dx^2} - \eta = -\eta_{\infty u} \quad , \qquad \ldots (66)$$

where

$$k_o^2 = \frac{(t_o^2 - h_o^2)^2(1 - M_o^2)}{32 R_o^2(1 + \beta_r^2)} \qquad \ldots (67)$$

and

$$\eta_{\infty u} = \frac{(t_o^2 - h_o^2)\left[G_o - R\beta_R\left(\frac{\partial\beta}{\partial r}\right)_R - \beta_R^2(1 - M_o^2)\right]}{32 R_o^2(1 + \beta_R^2)} \quad . \qquad \ldots (68)$$

The solution of equation (66) is

$$(\eta - \eta_{\infty u}) = (\eta_o - \eta_{\infty u})e^{x/k_o} \quad ,$$

and it is seen that $\eta_{\infty u}$ is the value of η far upstream of the first blade row.

It is convenient to express the solution of equation (66) in the form

$$\left(\frac{d\eta}{dx}\right)_o = \frac{1}{k_o}(\eta_o - \eta_{\infty u}) \quad , \qquad (69)$$

since this result can be used as a boundary condition at entry to the first blade row for the solution in a multi-stage turbo-machine. By writing equation (69) in the form shown, the boundary condition at entry to a turbo-machine has been transferred from a boundary condition expressed far upstream of the machine to one at the leading edge of the first blade row, which is more suitable for the numerical method used to solve the general flow equation.

Before/

Before $\eta_{\infty u}$ and k_Q can be evaluated, and before the solution for a multistage machine can proceed, it is necessary to know the values of ρ, V, p, T and M_x at inlet to the machine (station o). Let the ambient stagnation pressure and temperature be denoted by p_{so} and T_{so} respectively. Then, at the design radius, for isentropic flow

$$T_{SRo} = T_{Ro} + \frac{V_{Ro}^2(1 + \beta_{Ro}^2)}{2C_p}$$

$$m = \pi V_{Ro}\rho_{Ro}(t_o^2 - h_o^2)$$

$$M_{xo}^2 = \frac{V_{Ro}^2}{(\gamma - 1)C_p T_{Ro}}, \qquad p_{Ro} = K\rho_{Ro}T_{Ro},$$

where the subscript o again refers to conditions at entry to the turbo-machine. These equations can be re-arranged to give the following expressions:

$$\frac{m\sqrt{C_p T_{sRo}}}{\pi p_{sRo}(t_o^2 - h_o^2)} = \frac{\gamma M_{xo}}{\sqrt{\gamma - 1}}\left[1 + \frac{\gamma-1}{2} M_{xo}^2(1 + \beta_{Ro}^2)\right]^{-\frac{1}{2}\frac{\gamma+1}{\gamma-1}}, \qquad \ldots (70)$$

$$\frac{V_{Ro}}{\sqrt{C_p T_{sRo}}} = \frac{\sqrt{M_{xo}^2(\gamma - 1)}}{\left[1 + \frac{\gamma-1}{2} M_{xo}^2(1 + \beta_{Ro}^2)\right]^{\frac{1}{2}}}, \qquad \ldots (71)$$

$$\frac{T_{Ro}}{T_{sRo}} = \frac{1}{\left[1 + \frac{\gamma-1}{2} M_{xo}^2(1 + \beta_{Ro}^2)\right]}, \qquad \ldots (72)$$

$$\frac{p_{Ro}}{p_{sRo}} = \frac{1}{\left[1 + \frac{\gamma-1}{2} M_{xo}^2(1 + \beta_{Ro}^2)\right]^{\gamma/\gamma-1}} \qquad \ldots (73)$$

Hence M_{xo} can be found from equation (70) and substituted into equations (71), (72) and (73) to give the velocity, static temperature and static pressure at the station o, the density following from the perfect gas law.

5.3 Flow at Exit from a Compressor or Turbine

Corresponding to the assumption made at inlet to a turbo-machine that the flow behaves like the flow in a constant-area duct, at exit it will also be assumed that the flow behaves in this manner. Consequently it will be imagined that the hub and tip radii are constant after the trailing edge of the final blade row. It is not essential that the hub and tip radii should remain constant immediately after the final blade row; it is only necessary that the turbo-machine should eventually be terminated with a duct of constant hub and tip radii.

Since/

Since ρ_R is constant in a duct of constant area, V_R, β_R and M_x^2 will also be constant, so that equation (64) can be written as

$$k_e^2 \frac{d^2\eta}{dx^2} - \eta = -\eta_{\infty u} \qquad \ldots (74)$$

where

$$k_e^2 = \frac{(t_e^2 - h_e^2)^2 (1 - M_{xe}^2)}{32\, R_e^2}$$

and

$$\eta_{\infty d} = \frac{(G_e + \beta_e^2 M_{xe}^2 - A\rho_{Re} R_e \beta_{Re})(t_e^2 - h_e^2)}{32\, R_e^2}$$

The subscript e denotes conditions at the exit plane, i.e., the plane where the turbo-machine joins the hypothetical constant-area exit duct.

The solution of equation (74) is

$$(\eta - \eta_{\infty d}) = (\eta_e - \eta_{\infty d})_e^{-x/k_e}$$

Thus $\eta_{\infty d}$ is the value η would have far downstream of the final blade row of the turbo-machine. This equation can be written as

$$\left(\frac{d\eta}{dx}\right)_e = \frac{1}{k_e}(\eta_e - \eta_{\infty d}) \quad , \qquad \ldots (75)$$

and this represents the boundary condition at the exit plane for the solution in a multi-stage turbine or compressor. The method of using the boundary conditions expressed by equation (69) and (75) will be indicated in Section 8.

The results obtained in this section may be compared with the solutions of Hawthorne and Ringrose (1962) for the compressible flow in constant-area ducts. These solutions have exponential decays of the types given by equations (69) and (75), consisting of a series of terms each having a different value of k. Hawthorne and Ringrose show that the k's are given by the equation

$$\frac{J_{p+1}\left(\frac{h}{k}\right)}{Y_{p+1}\left(\frac{h}{k}\right)} = \frac{J_{p+1}\left(\frac{t}{k}\right)}{Y_{p+1}\left(\frac{t}{k}\right)} \quad .$$

Comparing these solutions with those obtained by Bragg and Hawthorne (1950) for incompressible flows in annular ducts it will be observed that the value of k for incompressible flow is multiplied by the factor $\sqrt{1 - M_x^2}$ on the introduction of compressibility effects. This effect will also be observed by comparing the expressions for k given in this section with the expressions derived for k by Whitehead and Beavers (1961) for incompressible flow in constant-area turbo-machines.

6./

6. Flow in a Blade Passage

The equation governing the flow through a row of blades is equation (47), which has been derived without considering any specific type of blade row, and is therefore true for both stator and rotor rows. The only term in this equation which depends upon the type of blade row under consideration is $(W/V)_R^2$. Referring to Figure 3,

$$\text{for a rotor row} \qquad \left(\frac{W}{V}\right)_R^2 = \left(\frac{\Omega R}{V_R} - \beta_R\right)^2 \qquad \ldots (76a)$$

$$\text{and for a stator row} \qquad \left(\frac{W}{V}\right)_R^2 = \beta_R^2 \ , \qquad \ldots (76b)$$

where Ω is the angular velocity of the rotor. Thus any analysis applied to equation (47) for the blade passage of a rotor row will also apply for the blade passage of a stator row if Ω is put equal to zero. The remainder of this section will therefore be devoted to the flow through a single row of rotor blades.

In order to solve equation (47) at any point within a blade row the value of β_R and of $(\partial\beta/\partial r)_R$ at that point must be known. Within an annular duct these quantities were determined from the condition that the circulation along a streamline must be constant. However, within a blade passage this condition no longer applies since the variation of β_R through the passage is fixed by the blade profile geometry. The value of β_R at any point could be obtained from an analysis of the pressure distribution round the cascade blade, but this is not practicable and so an assumption about the variation of β_R through a blade row has to be made. In this analysis it has been assumed that β at the design radius varies linearly with x from the leading to the trailing edge of the blade. Consequently, β_R and $(\partial\beta/\partial r)_R$ are given by

$$\left.\begin{aligned} \beta_R &= \beta_{R1} + (\beta_{R2} - \beta_{R1})\frac{x}{a} \\ \text{and} \qquad \left(\frac{\partial\beta}{\partial r}\right)_R &= \left(\frac{\partial\beta}{\partial r}\right)_{R1} + \left[\left(\frac{\partial\beta}{\partial r}\right)_{R2} - \left(\frac{\partial\beta}{\partial r}\right)_{R1}\right]\frac{x}{a} \end{aligned}\right\} \qquad \ldots (77)$$

This assumption is very close for the central streamlines in a blade passage, and is exact for a row of infinitely thin blades working at zero incidence and having a parabolic centre-line at the design radius.

All the information necessary for obtaining the value of η at any axial position within a blade row has now been set up. The solution is performed by first deriving the value of the density from equation (33), and then this result, together with equations (30), (38), (76) and (77), can be substituted into equation (47), to yield a differential equation of the type

$$\frac{d^2\eta}{dx^2} - f_1(x)\frac{d\eta}{dx} - f_2(x).\eta = f_3(x) \qquad (78)$$

where $f_1(x)$, $f_2(x)$ and $f_3(x)$ are functions of x only. Equation (78) requires two boundary conditions. For a single isolated blade row these boundary conditions are furnished by equations (69) and (75), whereas for a multi-stage

turbo-machine/

turbo-machine the boundary conditions at the leading and trailing edges of any one blade row depend upon the flow conditions in the two adjacent gaps or blade rows. In this case equations (69) and (75) provide the boundary conditions which must be satisfied at inlet to and exit from the turbo-machine. The method used for solving equation (47) in a multi-stage turbo-machine will be discussed in sections 7 and 8.

7. Flow in a Multi-stage Turbo-machine

In sections 5 and 6 it has been shown how equation (47) may be solved in annular ducts and in individual blade rows. Since a compressor or turbine consists of alternate rows of stator blades and rotor blades separated by small axial gaps, the solution for η in such a machine consists of solving equation (47) in each of the blade rows and gaps in turn. In order to show how the solution is continued through the successive blade rows and gaps of a turbo-machine, consider a small section of a compressor consisting of a rotor row followed by a gap which is followed then by a stator row, as shown in Figure 3. In this figure the primed (') numbers represent conditions on the gap side of an interface between a gap and a blade row, and the unprimed numbers represent conditions on the blade row side of the same interface.

On passing from a blade row into a gap, or from a gap into a blade row, the hub and tip radii must be continuous, and hence the design radius will be continuous, although there need not necessarily be continuity of $\frac{dh}{dx}$, $\frac{dt}{dx}$ and $\frac{dR}{dx}$. Also, at an interface the density, static temperature and static-pressure gradient (g) must be the same in both the gap and the blade row, and hence it follows from the first of these conditions that μ must be continuous at the interface. In addition the axial and tangential components of velocity will be continuous across an interface, so that the values of λ and μ at inlet to any section are equal to the corresponding values of these quantities at exit from the preceding section. Finally, since there will, in general, be discontinuities in the gradients of the hub and tip radii at the interfaces, there will be corresponding discontinuities in the gradients of the streamlines at these radii. Across an interface where the hub and tip radii change it will only be possible to have one streamline with a continuous gradient, and it will be assumed that this is the design-radius streamline.

At any axial position, the design-radius streamline will have been displaced radially through a small distance δR, so that it is at a radius $R + \delta R$, where δR is given by equation (54). Thus, from equation (17) the radial velocity on this streamline is given by

$$(R + \delta R)\rho_{R+\delta R}U_{R+\delta R} = -\frac{(R + \delta R)^2}{2} \cdot \frac{\partial}{\partial x}\left(\rho_R V_R\right) + \frac{\partial}{\partial x}\left(\frac{\rho_R V_R h^2}{2}\right) - (R + \delta R)^4 \frac{\partial}{\partial x}\left(\frac{\rho_R V_R \lambda}{8R^2}\right)$$

$$+ (R + \delta R)^2 \frac{\partial}{\partial x}\left(\frac{\rho_R V_R \lambda}{4}\right) + \frac{\partial}{\partial x}\left[\frac{\rho_R V_R \lambda}{2}\left(\frac{h^4}{4R^2} - \frac{h^2}{2}\right)\right] .$$

Using/

Using equation (8), and neglecting all second-order terms in δR and above, this equation can be simplified to

$$\rho_{R+\delta R} U_{R+\delta R} = \frac{m}{\pi R}\left(1 - \frac{\delta R}{R}\right)\left\{\frac{\partial}{\partial x}\left[\frac{(t^2 - h^2)\lambda}{32\,R^2}\right] + \frac{R\,\frac{dR}{dx}}{t^2 - h^2} - R^2\,\frac{\partial}{\partial x}\left(\frac{1}{t^2 - h^2}\right)\right\}$$

or

$$\rho_{R+\delta R} U_{R+\delta R} = \frac{m}{\pi R}\left\{\frac{d\eta}{dx} + \frac{R\,\frac{dR}{dx}}{t^2 - h^2} - \frac{\delta R}{R}\left[R^2\frac{\partial}{\partial x}\left(\frac{1}{t^2 - h^2}\right) + \frac{R\frac{dR}{dx}}{t^2 - h^2}\right]\right\} .$$

This can be written as

$$\rho_{R+\delta R} U_{R+\delta R} = \frac{m}{\pi R}\left\{\frac{d\eta}{dx} + \frac{R\frac{dR}{dx}}{t^2 - h^2} + \frac{R^2\,\delta R}{(t^2 - h^2)^2}\,\frac{\partial}{\partial x}\left(\frac{t^2 - h^2}{R}\right)\right\} . \qquad \ldots (79)$$

Thus equation (79) implies that, across an interface between a gap and a blade row,

$$\frac{d\eta}{dx} + \frac{R\,\frac{dR}{dx}}{t^2 - h^2} + \frac{R^2\,\delta R}{(t^2 - h^2)^2}\cdot\frac{\partial}{\partial x}\left(\frac{t^2 - h^2}{R}\right) = \text{CONTINUOUS} . \qquad \ldots (80)$$

This result could also have been obtained from the condition that the slope of the design-radius streamline is everywhere continuous, for this implies that

$$\frac{\partial}{\partial x}\left(R + \delta R\right) \text{ is continuous.}$$

Hence using equation (54)

$$\frac{\partial}{\partial x}\left[R + \frac{(t^2 - h^2)(\eta - \eta_\infty)}{R}\right] \text{ is continuous.}$$

Thus $\left[\frac{dR}{dx} + \frac{t^2 - h^2}{R}\cdot\frac{d\eta}{dx} + \frac{R\delta R}{(t^2 - h^2)}\cdot\frac{\partial}{\partial x}\left(\frac{t^2 - h^2}{R}\right)\right]$ is continuous,

which is the same condition as equation (80) because h, t and R are everywhere continuous. The final term in equation (80) will normally be very small, so that by comparing this equation with the expression for U_R given by equation (25) it is seen that U_R will be very nearly continuous across an interface.

The two conditions, namely the continuity of η and equation (80), enable η and $d\eta/dx$ at inlet to any blade row or gap to be found from the values of these quantities at exit from the preceding gap or blade row. These inlet values provide the two boundary conditions necessary for a unique solution of equation (47) to be determined. It therefore follows that if the values of η and $d\eta/dx$ are known at inlet to a turbo-machine their values at every other point on the design radius can be found.

It should be noted here that although η and λ are continuous from one component of a variable-area turbo-machine to the next, $d\eta/dx$ and $d\lambda/dx$ are not, so that curves of η and λ will have discontinuities in gradient at

the/

the various interfaces. This is a result of the assumed geometry for the turbo-machine, in which the hub and tip radii are allowed to have changes in slope at each interface. η and λ will only have continuous gradients when the gradients of the hub and tip radii are the same on both sides of an interface. However, in general, for small changes in the slopes of the turbo-machine walls there will only be small changes in the gradients of η and λ .

Having shown how η and $d\eta/dx$ are determined at inlet to any section of a turbo-machine it now remains to show how the various quantities which form the coefficients in equation (47) are determined at inlet to that section. In this context a section is any blade row or gap in the machine.

Consider first the terms β_R and $(\partial\beta/\partial r)_R$. The values of these quantities at inlet to a section are calculated from the values of the corresponding terms at exit from the previous section by applying the condition of continuity of tangential velocity. Since β is the tangent of the relative gas angle at any point, it follows that at any radius r the whirl velocity W is given by

$$W = \Omega r - \beta V \quad \text{for a rotor row} \qquad \ldots (81)$$

$$W = \beta V \quad \text{for a stator row or gap.} \qquad \ldots (82)$$

Hence, referring to Figure 3, equations (80) and (81) can be used to yield the following expressions for the values of β_R at inlet to the various sections.

For the gap-rotor row interface (interface 1)

$$\beta_{R1} = -\beta_{R1}' + \frac{\Omega R_1}{V_1} \qquad \ldots (83a)$$

and for the rotor row-gap interface (interface 2)

$$\beta_{R2}' = -\beta_{R2} + \frac{\Omega R_2}{V_2} \ . \qquad \ldots (83b)$$

Likewise, for the stator row-gap interfaces,

$$\beta_{R3} = \beta_{R3}' \ , \qquad \beta_{R4} = \beta_{R4}' \ . \qquad \ldots (83c)$$

Expressions for the values of $(\partial\beta/\partial r)_R$ at inlet can be obtained by differentiating the above relationships in the radial direction. For example, at an interface between a gap and a rotor row, the value of $(\partial\beta/\partial r)_R$ at inlet to the rotor row is given by

$$\left(\frac{\partial\beta}{\partial r}\right)_{R1} = -\left(\frac{\partial\beta}{\partial r}\right)_{R1}' + \frac{\Omega}{V_1}\left(1 + \mu_1 - \lambda_1\right) \ .$$

Also/

Also, across a stator row-gap interface it follows from the expressions for β_R that the value of $(\partial\beta/\partial r)_R$ is constant. Consequently the required values of β_R and $(\partial\beta/\partial r)_R$ can be found at inlet to any blade row or gap.

Consider next the change in the relative stagnation temperature T_s across an interface. On passing from a gap into a stator row, or vice-versa, there will be no change in the value of the relative stagnation temperature. However, for any interface involving a rotor row there will be a sudden change in this quantity, but this change can readily be calculated.

Equation (32) at the interface 1 of Figure 3 gives

$$T_{s1'} = T_{1'} + \frac{V_{1'}^2}{2C_p}\left(1 + \beta_{R1'}^2\right) \quad \text{for the gap}$$

$$T_{s1} = T_1 + \frac{V_1^2}{2C_p}\left(1 + \beta_{R1}^2\right) \quad \text{for the rotor row.}$$

As the static temperature is continuous across an interface these two equations can be combined to give

$$T_{s1} = T_{s1'} + \frac{V_1^2}{2C_p}\left(\beta_{R1}^2 - \beta_{R1'}^2\right) . \qquad \ldots (84)$$

Equation (84) expresses the relative stagnation temperature in a rotor row in terms of the relative stagnation temperature in the gap preceding the rotor row and the known relative gas angles at the interface between the gap and the rotor row. A similar equation can be found for the interface 2 of Figure 3. This is

$$T_{s2'} = T_{s2} + \frac{V_2^2}{2C_p}\left(\beta_{R2'}^2 - \beta_{R2}^2\right) .$$

Returning to equation (47) it is seen that the only quantity which remains to be determined across an interface is the radial gradient of the relative stagnation temperature, denoted by G. Across an interface composed of a gap and a stator row G will be constant, but across any interface having a rotor row as one of the components there will be a sudden change in the value of G. This change in G can be found by applying the condition of constant radial static-pressure gradient at the interface. Thus at the interface 1 of Figure 3, equation (45) gives for the two constituents

$$g = \frac{G_{1'} - \lambda_1\left(1 + \beta_{R1'}^2\right) - R_1\beta_{R1'}\left(\frac{\partial\beta}{\partial r}\right)_{R1'}}{1 - M_{1'}^2} \quad \text{for the gap}$$

and

$$g = \frac{G_1 - \lambda_1\left(1 + \beta_{R1}^2\right) - R_1\beta_{R1}\left(\frac{\partial\beta}{\partial r}\right)_{R1}}{1 - M_1^2} \quad \text{for the rotor row.}$$

Hence/

Hence G at inlet to the rotor row is given in terms of G at exit from the gap by the equation

$$G_1 = \frac{1 - M_1^2}{1 - M_1'^2}\left[G_1' - \lambda_1(1 + \beta_{R1}^2) - R_1\beta_{R_1'}\left(\frac{\partial\beta}{\partial r}\right)_{R_1'}\right] + \lambda_1(1+\beta_{R_1}^2) + R\beta_{R_1}\left(\frac{\partial\beta}{\partial r}\right)_{R_1} \quad \ldots (85)$$

A similar equation exists for the interface formed by the trailing edge of a rotor row and the following gap.

The above results thus show how the form of equation (47) in any section of a turbo-machine is related to the form of the equation in the preceding section. Hence, once a solution for η has been found at inlet to the machine, it is possible to obtain a solution at every other point along the design radius. The numerical method of solving equation (47) will be described in Section 8.

In the foregoing analysis it has been assumed that the individual blade rows are always separated by axial gaps. This condition is not essential to the analysis, which will still hold if the gaps are omitted. This follows because across an interface involving a gap and a stator row G, T_s, β_R and $(\partial\beta/\partial r)_R$ are all continuous, so that the conditions derived for the transference of the solution across a rotor row-gap interface are unchanged when the gap is replaced by a stator row. Consequently, if so desired, the gap between the blade rows may be omitted and the turbo-machine analysed as a succession of rotor and stator rows. This solution will differ slightly from that obtained by including the gaps, the magnitude of the difference depending upon the relative axial lengths of the blade rows and the neglected gaps.

8. The Numerical Method of Solution

In general it is not possible to derive an exact analytical solution of equation (47) in either a blade row or a gap. Consequently a numerical method of solving this equation must be employed, and this can only be conveniently done using an electronic computer. For any turbo-machine equation (47) has to be solved in the individual blade rows and gaps in turn, and the complete solutions have to satisfy given boundary conditions at the two ends of the machine. The easiest method of obtaining the solution which satisfies these two boundary conditions depends upon the linearity condition of equation (47). This equation is a linear differential equation in η for both blade rows and gaps. Thus, if η_1 is any solution of the equation and η_2 is any other solution, then $b\eta_1 + (1-b)\eta_2$ is also a solution, where b is any constant. Hence, if two individual solutions which satisfy the boundary condition at inlet are continued through the machine these solutions may be scaled at exit so that the resultant solution satisfies the boundary condition at that point. This will yield the value of the constant b, which can then be used to obtain the true solution at every point within the turbo-machine. This is the method used in the programme written for the EDSAC 2 computer of the Cambridge University Mathematical Laboratory. A short description of the techniques used in this programme will now be given.

Two initial guesses are made for the value of η at inlet to the turbo-machine, and from these initial guesses two entirely separate solutions

are/

are obtained simultaneously in each succeeding blade row and gap. For any blade row or gap the inlet conditions are first derived from the exit conditions of the previous component, as described in Section 7. The component under consideration is then divided into a large number of small axial elements, and a Runge-Kutta-Gill numerical method is used to advance the solution from one element to the next. However, before this Runge-Kutta-Gill process can be used at any point, the values at this point of t, h, R, β_R, $(\partial\beta/\partial r)_R$, G, ρ_R, V_R, M and $(1/\rho\cdot\partial\rho/\partial x)_R$ must all be known. The first six of these quantities can readily be obtained by the methods described in the foregoing sections. V_R, M, and $(1/\rho\cdot\partial\rho/\partial x)_R$ all depend upon ρ_R at that point, which itself is obtained by solving equation (33).

On reaching the exit from the turbo-machine neither of the two solutions will, in general, satisfy the boundary condition at that point, which is given by equation (75) as

$$\left(\frac{d\eta}{dx}\right)_e = -\frac{1}{k_e}(\eta_e - \eta_{\infty d}) \quad . \qquad \ldots (75)(\text{bis})$$

However the two solutions can now be scaled so that the resultant solution does satisfy equation (75). The scaling factor b is obtained in the following manner. Denoting the two solutions by the subscripts 1 and 2, it follows from equation (75) that

$$b\left(\frac{d\eta}{dx}\right)_{e_1} + (1-b)\left(\frac{d\eta}{dx}\right)_{e_2} = -\frac{1}{k_e}\left[b\eta_{e_1} + (1-b)\eta_{e_2} - b\eta_{\infty d_1} - (1-b)\eta_{\infty d_2}\right]$$

Hence, this equation gives

$$b = \frac{1}{1 - \dfrac{(\eta_{\infty d_1} - \eta_{e_1}) - k_e\left(\dfrac{d\eta}{dx}\right)_{e_1}}{(\eta_{\infty d_2} - \eta_{e_2}) - k_e\left(\dfrac{d\eta}{dx}\right)_{e_2}}} \quad . \qquad \ldots (86)$$

This scaling factor b can then be used to scale the two original solutions at every point within the machine to yield the true solution of equation (47).

It is a property of equation (47) that any solution which is not the exact solution will diverge very rapidly, so that after a few stages of a multi-stage machine the numerical value of η becomes exceedingly large and even on a computer accuracy begins to be lost. Hence a method has been incorporated in the computer programme which prevents the two individual solutions from becoming large and at the same time makes them both tend towards the true solution. This is achieved by testing the values of λ_1 and λ_2 at the exit from each blade row and gap, and if either of these two values is numerically greater than ten, the solutions are stopped. Both solutions up to that point are then scaled in the manner described above in such a way that the values of λ_1 and λ_2 at the point where the solutions were stopped are +1 and -1 respectively, and the solutions are then restarted. This repeated scaling of the solutions in a multi-stage machine has the result that in the earlier stages both solutions approach more and more closely the final exact

solution/

solution. This is what would be expected, since the boundary condition governing the flow at exit from the machine has a decreasing influence on going forward towards the middle of the machine, and likewise, the boundary condition governing the flow at inlet has a decreasing influence on going from the inlet towards the middle of the machine. Consequently as the solutions approach the last few stages of a machine their values in the first few stages have both become close to the true solution in that region.

To enable the solution to proceed it is necessary to provide the computer with certain information about the compressor or turbine under analysis. This information is provided in blocks, arranged so that there is first a block of general information about the machine, followed by small blocks of data for each individual blade row and gap, these blocks of data being arranged in the order the blade rows and gaps appear in the machine. The general information block must provide the following quantities:

Mass flow rate (m)

Inlet stagnation pressure (p_{so})

Inlet stagnation temperature (T_{so})

Inlet hub radius (h_o)

Inlet tip radius (t_o)

Inlet stagnation-temperature gradient (G_o)

Ratio of specific heats (γ)

Gas constant (K)

Speed of rotor in R.P.M. (N)

Two initial guesses for λ

The number of steps per section to be used in the Runge-Kutta-Gill process, and how often values are to be printed out.

β_R and $(\partial\beta/\partial r)_R$ at inlet.

Each individual data block must then provide the following information:

The axial length of the section.

The inlet and outlet hub and tip radii.

The outlet values of β_R and $(\partial\beta/\partial r)_R$.

The output from the machine occurs in blocks corresponding to the blocks of data provided. Each block of output is in the form of a table of results, these results being given at various axial positions within the section for which the block applies. Output values are provided under the following headings:

Axial distance of the position from the front of the section.

The design radius.

The radial position of the design-radius streamline.

The density at the design radius.

The axial velocity at the design radius.

μ .
λ .

In/

In addition the axial component of the Mach number is given at every interface between adjacent sections, i.e., between every block of output.

The computer programme has been written so that it can be used for any axial-flow turbo-machine, which can either include or neglect the gaps between the blade rows. It can also be used for the flow in converging and diverging ducts and nozzles, if these are regarded as sets of small axial gaps following one another. An example of the use of the programme to analyse the flow in a converging-diverging nozzle is given in Section 14.

The remaining sections of this paper will now be devoted to comparisons of results obtained using the EDSAC 2 computer programme with existing theoretical and experimental results.

9. Flow through a Single-stage Compressor - Comparison with Wu

The parameter theory has been used to calculate the flow through a single-stage compressor of constant hub and tip radii, and the derived results have been compared with the theoretical results of Wu (1953) for the same compressor operating under the same conditions. The products of these investigations are shown in Figures 7 to 13. The compressor analysed is shown in Figure 7 and consisted of a row of inlet guide vanes, a row of rotor blades and a stator blade row, each blade row having a hub-to-tip ratio of 0.6 and an aspect ratio, based on the axial length, of 2.67. The axial length of the gaps separating the blade rows was equal to one-third the axial chord of a blade. The value of r/t at the design radius was 0.82462. Both incompressible and compressible flows through this compressor have been studied and the results compared with Wu's calculations. For all calculations the ratio of inlet velocity to rotor tip speed was taken to be 0.7378, and for the compressible calculations the ratio of inlet density to inlet stagnation density was made equal to 0.8578, with an inlet Mach number of 0.567.

In order to obtain solutions Wu had first to specify the axial rate of change of the quantity Wr on the mean stream surface, and from this he obtained solutions for the axial velocity at all points within the compressor. The gas angles obtained by Wu have been used in the parameter-theory calculations for both the incompressible and compressible flows. The variations of λ and μ for both types of flow are shown in Figures 8 and 9, and the graph of the slope of the axial-velocity profile at the design radius is given in Figure 10. It will be seen for the compressible flow calculations that whereas the plot of λ has a continuous gradient at all interfaces, the graph of the slope of the axial-velocity profile has discontinuities in gradient at the interfaces, even though the machine has constant hub and tip radii. These discontinuities are caused by the discontinuities in the gradient of μ at the interfaces.

The values of the axial velocities determined by means of the parameter theory have been compared with Wu's calculations at r/t ratios of 0.6, 0.8 and 1.0, and these comparisons are shown in Figure 11 for the incompressible flow and Figure 12 for the compressible flow. Figure 13 compares the density variations obtained by the two methods at the same three radius ratios. In all these figures it will be observed that the parameter-theory calculations agree very closely with those of Wu. This would be expected in the neighbourhood of the design radius, where the parameter theory is made to satisfy the equations of motion exactly. The close agreement at both the hub radius ($r/t = 0.6$) and the tip radius ($r/t = 1.0$)

would/

would indicate that the assumed form of the chosen profiles is acceptable over a much greater proportion of the blade length than merely within the immediate vicinity of the design radius.

The displacement of the design-radius streamline in compressible flow is shown in Figure 7, which also shows the streamline pattern calculated by Wu. The two streamline patterns agree very closely, and this close agreement combined with the very close agreement of the axial-velocity and density variations at the design radius justifies the assumption that the tangent of the relative gas angle varies in a linear manner through a blade passage. Finally, by comparing Figures 11 and 12, it will be observed that the introduction of compressibility into the calculations has a very marked effect upon the axial velocity, as would be expected. However, Figure 8 shows that both graphs of λ have the same form, only differing appreciably in the final blade row.

10. Flow through a Seven-stage Compressor

In order to demonstrate some of the ways in which the computer programme may be used to investigate the flow through a multistage turbo-machine under different conditions, and at the same time to obtain solutions which could be compared with existing results, calculations were performed on the flow through a seven-stage compressor previously analysed by Wu (1953). The compressor used for the analysis is shown in Figure 14, having a constant tip radius and a variable hub radius. The curvature of the hub radius is obtained by discontinuities in the slope of this bounding wall at the majority of the interfaces between the blade rows and the gaps. The design mass-flow rate was 94.56 pounds per second for a rotor tip speed of 815 feet per second. The design ratio of inlet velocity to rotor tip speed was 0.74433 and the inlet Mach number was arranged to be 0.56.

Four calculations were performed. The first was under 'as-designed' conditions; the second was for the same conditions but with a dimensionless relative stagnation-temperature gradient, G, at inlet of +1, compared with 0 for the 'as-designed' calculation; the third was the same as the second with G changed to -1; and the final calculation was for a mass-flow rate of 80.00 pounds per second and a dimensionless relative stagnation-temperature gradient at inlet of 0. Plots of λ through the machine for each of these four calculations are given in Figure 15. It will be seen that all the curves have discontinuities in slope at the interfaces where there are discontinuities in the slope of the hub radius. Whitehead and Beavers (1961) found that for flow in constant-area turbo-machines the plots of λ through the machine were, in general, smooth oscillating curves. For this compressor having a variable hub radius it will be observed that the oscillatory nature of the flow is retained, although it is less obvious than before because of the sudden changes in slope. Normally it is found that the graphs of λ are fairly sensitive to changes in the slope of the walls of the turbo-machine, the effects becoming more apparent as the Mach number increases. This is demonstrated in Figure 15, where it will be seen that all the curves have a slight depression on going through the fifth-stage rotor row. This is caused by the shape of the hub in this region. On going through the compressor the slope of the hub always decreases or remains constant at an interface. However at the trailing edge of the fifth-stage rotor row there is a slight increase in the slope in the following gap, thus causing a 'kink' in the hub profile and the resulting 'kink' in the plot of λ .

It/

It will be observed from Figure 15 that the effect of the radial gradient of relative stagnation temperature at inlet gradually decreases through the machine, becoming very small in the final stage but not actually becoming zero. Decreasing the mass-flow rate has negligible effect on λ at inlet to the machine, but in the later stages causes a large increase in the magnitude of the variation of λ through any blade row, thus having a corresponding effect on the path of the design-radius streamline. The paths of the design-radius streamlines for mass-flow rates of 80 and 94.56 pounds per second and values of G of zero at inlet are shown on Figure 14. Both paths have an oscillating pattern, although this cannot be seen clearly on the figure, since the amplitudes of the oscillations are very small compared with the design radius. These oscillations are such that, relative to the design radius, their displacements are increasing through a stator row and decreasing through a rotor row. This is the same effect as that observed by Whitehead and Beavers (1961) for the flow of an incompressible fluid through a ten-stage constant-area compressor.

Figure 16 gives the variation of μ through the machine for the two mass-flow rates. The introduction of a radial gradient of stagnation temperature at inlet has the same effect on μ as on λ, although in this case the magnitude of the difference is much smaller. A point of interest in Figure 16 is the large change in μ through the sixth-stage stator and the seventh-stage rotor and stator rows for the lower mass-flow rate. This implies that there are large changes in the radial gradient of static pressure through these blade rows. This is probably caused by the machine changing from variable area to constant area at the trailing edge of the seventh-stage rotor row, with the result that the design-radius streamline is displaced radially inwards in the vicinity of this point in order to 'cut off' the corner. Likewise all the other streamlines will be displaced radially inwards, so that a large gradient of static pressure will be established.

The axial velocities and densities along the design radius for the two mass-flow rates are given in Figures 17 and 18 respectively. The inlet gradient of relative stagnation temperature has no effect on the density and axial velocity at inlet, since these values depend only on the mass-flow rate, the ambient conditions and the angle at which the flow enters the compressor. It will be observed that under design conditions the axial velocity increases through the machine, but that most of this increase arises from the increase in velocity in the gaps between the blade rows and not in the blade rows themselves. This increase in the gaps would be anticipated from the theory for subsonic flow in a converging passage.

Finally, for the design flow rate the axial Mach number changed from 0.567 at inlet to 0.579 at entry to the first rotor row, and dropped to 0.501 at exit from this blade row. It then increased steadily to 0.605 after the fifth stage, and finally more rapidly to 0.799 at the leading edge of the final blade row, falling to 0.690 at exit from the machine. For the reduced mass flow the axial Mach number was 0.447 at inlet and changed from 0.453 to 0.391 through the first rotor row. Through the remainder of the compressor it varied between 0.35 and 0.39, falling to 0.323 at exit.

Few results were given by Wu, but the design-radius streamline path predicted by the parameter theory for the design mass-flow rate was compared with Wu's predicted streamline pattern and agreement was very close. For the sake of clarity, Wu's results have not been included on Figure 14.

11./

11. Flow through a Single-stage Turbine - Comparison with Wu

Corresponding to the comparisons made with Wu's calculations for the flow through a single-stage compressor given in Section 9, the flow through a single-stage turbine has been analysed and the calculations compared with Wu's (1952b) calculations for the same turbine, these comparisons being shown in Figures 19 to 24. The turbine used for the analysis is given in Figure 19, and consisted of a stator row followed by a rotor row, the blade rows being separated by a gap of axial length equal to one-third the axial chord of the blade rows. The turbine had a constant hub-to-tip ratio of 0.6, and both blade rows had aspect ratios of 2.67. As for the single-stage compressor, solutions for both compressible and incompressible flows were derived. In all calculations the ratio of inlet velocity to rotor tip speed was made equal to 0.650, and for the compressible flow the inlet Mach number was arranged to be 0.308. The ambient conditions were chosen such that the ratio of inlet density to inlet stagnation density was 0.95033, and the ratio of the inlet stagnation enthalpy to the square of the rotor tip speed was 12.546.

Wu obtained solutions by specifying the variation of the angular momentum per unit mass of gas, Wr, through the blade rows. A linear variation with axial distance was termed uniform loading, and a non-linear variation with axial distance was termed non-uniform loading. Wu performed two sets of calculations for incompressible flow, one for uniform loading and the other for non-uniform loading. The gas angles obtained by Wu have been used in the parameter theory, and the resultant axial-velocity variations at $^{r}/_{t}$ ratios of 0.6, 0.7, 0.8, 0.9 and 1.0 are compared with Wu's results in Figure 22. It will be observed that the agreement between the parameter-theory results and Wu's results is not as good as for the compressor calculations shown in Figure 11. However the methods give reasonably good agreement near the design radius, but towards the boundaries of the machine, and especially at the hub, the agreement is rather poor. Nevertheless the agreement is close enough to justify the use of the parameter theory for axial velocities in the neighbourhood of the design radius.

For the compressible-flow analysis, the gas angles obtained from Wu's results were again used in the parameter theory and the resulting solutions were compared with Wu's calculations for three different non-uniform loadings, denoted in Figures 23 and 24 by cases C, D and E. These two figures show respectively the axial-velocity and density variations at the same five ratios of $^{r}/_{t}$ as used in the incompressible-flow analysis. It will be seen that the densities agree closely at the leading and trailing edges of the blades, but differ in the form of their variations within the blade passages. This can be expected, since the density variation within a blade passage in the parameter theory is governed by the assumed variation of the relative gas angle through that passage. Consequently if Wu's assumed variation for the tangential velocity within a blade passage yields a relative gas angle variation which differs appreciably from that assumed in the parameter theory, discrepancies in the densities within the blade passages would be anticipated.

Figures 20 and 21 show the plots of λ and μ through the turbine, and from the latter it can be seen that the radial gradient of static pressure at exit from the turbine is almost zero. This agrees closely with the free-vortex design, since the rotor blade was designed to yield a tangential component of velocity at exit of zero.

12./

12. Flow through Conical Ducts - Comparison with Lewis

The parameter theory has been used to predict the flow through converging and diverging conical ducts, and the results compared with the experimental and theoretical results obtained by Lewis (1960). Five comparisons have been made, and these are denoted by Tests Numbers 1 to 5 in Figures 25 to 46. These tests show how the parameter theory may be used to predict the flow through annular ducts in which the hub radius has the value of zero and the flow is symmetric about the axis. In all five tests the mean axial velocities were very low so that Lewis assumed the flow to be incompressible and made his theoretical predictions accordingly. The parameter-theory calculations were performed twice for each test, once assuming the flow to be incompressible and the second time assuming it to be compressible. These calculations showed that for every test the assumption of incompressibility was justified, the total variation in density being no greater than one per cent of the inlet stagnation density, with corresponding velocity differences of one foot per second or less. In making the comparison the incompressible calculations have been used, so that the value of μ is always zero and λ represents the dimensionless slope of the axial-velocity profile.

The duct used for the first test is shown in Figure 25. It consisted of a conical contraction from 14 inches diameter to 10.76 inches diameter, with a total angle of 20°24', and bounded at both ends by sections of cylindrical duct. λ for this duct is given in Figure 26, and the path of the design-radius streamline is shown on Figure 25, where it will be noticed that the streamline 'rounds-off' the corners formed by the sudden changes in the slope of the actual design radius. In Figure 27 the axial-velocity profiles predicted by the parameter theory at stations 1 and 2 are compared with the experimental curves of Lewis at these stations, the agreement being very close with a maximum error of about 2 per cent in the region outside the wall boundary layer. Also shown on this figure are the parameter-theory predictions for the axial-velocity profiles at stations 1A and 2A where the slope of the casing suddenly changes. Since all the streamlines have the same pattern as the design-radius streamline, it would be expected that at station 1A the axial velocity would increase towards the outer casing and at station 2A the axial velocity would decrease towards this casing. These effects are predicted in Figure 27.

Test Numbers 2 and 3 were conducted on a converging conical duct with a row of free-vortex nozzle guide vanes positioned mid-way along the duct. Test Numbers 4 and 5 were carried out with the same blade row and the duct arranged as a diverging passage. The duct configurations are shown in Figures 28 (a) and 28 (b). The outer casing included angle was 20°24' with a maximum diameter of 14 inches, while the inner casing included angle was 9°36' with a maximum diameter of 6.58 inches. The axial length of the conical section was 9 inches, thus giving an area ratio of 1.69, and the blade row occupied the middle 1.2 inches of the duct. For each duct configuration calculations were performed for a uniform inlet stagnation pressure (Test Numbers 2 and 4) and for a non-uniform inlet stagnation pressure (Test Numbers 3 and 5).

Plots of λ for the two converging duct tests are shown in Figure 29, where it will be seen that the effects of the inlet stagnation-pressure gradient becomes small about one blade chord downstream of the blades. Figures 30 to 33 apply to Test Number 2, and compare the axial-velocity profiles predicted by the

parameter/

parameter theory with Lewis's experimental and theoretical results at stations 1, 2, 3 and 4 of Figure 28(a). Similarly Figures 34 to 37 compare axial-velocity profiles at the same four stations for Test Number 3. All the comparisons show good agreement of the parameter-theory predictions with the experimental traverses, the predictions being at least as good as those obtained using the actuator-disc theory.

Calculations corresponding to Figures 29 to 37 have been made for the flow through the diverging conical duct. Figure 38 shows the variations in λ for the uniform and non-uniform inlet stagnation pressures. It will be noticed in this case that, unlike the converging duct, the effect of the non-uniform stagnation pressure is maintained through the whole duct. Axial-velocity profiles have been compared at stations 1, 2, 3 and 4 of Figure 28(b), and these are shown in Figures 39 to 42 for Test Number 4 and Figures 43 to 46 for Test Number 5. For these diverging duct tests the parameter-theory predictions do not agree as closely with the experimental results as they do in the converging duct tests. This discrepancy is most marked at station 4, where the experimental results show a very large boundary layer on the hub wall. The parameter theory is unable to allow for this effect. As before, the parameter theory appears to give solutions which are at least as good as the actuator-disc predictions.

13. Flow through a Three-stage Turbine - Comparison with Johnston and Sansome

Johnston and Sansome (1961) performed an experimental investigation on the flow through a three-stage turbine, shown diagrammatically in Figure 47. The axial-velocity profiles they obtained were very irregular, and as such made comparisons with profiles calculated by the parameter theory of very little significance. Nevertheless these theoretical predictions and comparisons with the experimental curves are included in this paper, for they help to demonstrate fairly closely some of the limitations by which the parameter theory is controlled.

The turbine had a constant hub diameter of 12.5 inches and a tip diameter varying from 15.34 inches at inlet to 17.6156 inches at exit. The gaps between all blade rows was 0.6 inches, and the blades were designed to conform to free-vortex flow and constant axial velocity through the machine. All gas angles were taken from the report by Johnston and Sansome, and the machine was assumed to be operating with inlet stagnation conditions of 225°F and 39.8 pounds per square inch. Solutions were derived for mass-flow rates of 19.48 pounds per second and 20.06 pounds per second, the former corresponding to a pressure ratio of approximately 0.37 based on the observed performance, and the latter corresponding to the same pressure ratio based on the estimated performance. The rotor speed was taken to be 6825 to correspond to the value of $N/\sqrt{T}$ used by Johnston and Sansome.

Graphs of λ and μ for the two mass-flow rates are given in Figures 48 and 49 respectively. At the trailing edges of the second and third rotor rows both λ and μ are very small for the mass-flow rate of 20.06 pounds per second, thus implying that the axial velocities at these points must be very nearly constant. This can be seen in Figure 51, which compares the axial velocities at the trailing edges of the blade rows as predicted by the parameter theory with the axial velocities observed by Johnston and Sansome at these positions. As would be anticipated there is no agreement between the experimental and theoretical curves.

The parameter theory does not even predict constant axial velocity at the design radius through the machine, but yields instead a steadily decreasing value, as shown in Figure 50. However it will be observed from this figure that except for the first row of nozzle guide vanes most of the change in axial velocity takes place within the gaps and not within the blade rows themselves. Nevertheless if the gaps were made much smaller so that they could be neglected the same overall decrease in the axial velocity would be observed. This follows from equation (33) because for any given machine operating under given flow conditions the density, and hence the axial velocity, at the trailing edge of a blade is determined by the prescribed gas angle at that point. Consequently if the gaps were omitted from this machine and the machine were then run under the same conditions the densities and axial velocities at the blade trailing edges at the design radius would be the same as those obtained in the present investigations.

One reason why the predicted axial-velocity variation does not agree with experimental variation is that the parameter theory assumes an expansion efficiency of 100 per cent, whereas the turbine was designed assuming an expansion efficiency of 90 per cent. Thus the parameter theory neglects any losses that occur during the expansion process, and it is clear that in order to obtain accurate solutions in diverging flows some means of allowing for such losses must be incorporated in the theory. However in defence of the parameter theory it must be remembered that the solutions have been compared with results from a turbine having excessive losses in the rotor blade rows and hence a very poor efficiency.

14. Analysis of a Rolls-Royce Two-Stage Low-Pressure Turbine

In order to demonstrate how the computer programme may be used to investigate the effects of various changes in the flow conditions of a turbine a Rolls-Royce two-stage low-pressure turbine has been studied. A diagrammatic representation of the turbine is given in Figure 52. Both nozzle guide vane rows had constant axial-chord lengths, but the rotor rows did not, and it will be seen in the figure that the shapes of the rotor rows have been approximated by blades of constant axial chord in order to apply the parameter theory. The gradients of the hub and tip radii were constant from the leading edge of the first nozzle guide vanes to the trailing edge of the second rotor row.

The effect of varying the mass-flow rate was first investigated, and calculations for six different mass-flow rates were performed. The inlet stagnation conditions for all six mass-flow rates were 1516.4°F and 98.05 pounds per square inch, and the gas was assumed to have a mean specific heat of 0.2802 and a ratio of specific heats of 1.4. The rotor speed was 6710 revs. per minute, and all gas angles were taken from a Rolls-Royce internal report (1959). The design mass-flow rate was 237.4 pounds per second, and in addition to this, mass-flow rates of 200, 220, 230, 236 and 238 pounds per second have been used. Graphs of λ and μ for the different mass flows are shown in Figures 53 and 54 respectively, and Figure 55 shows the displacement of the design-radius streamline for three of the flow rates.

It will be observed that for all the mass-flow rates the graphs of λ have an oscillatory form so that the usual oscillating motions of the design-radius streamlines are produced. An interesting feature about Figure 53 is the inter-section near the trailing edge of the first rotor row of all the curves. The distribution of the curves in this figure suggests that as the mass-flow rate is decreased the flow through the second of the two stages is such that it moves radially outwards towards the tip, the outward radial movement being increased as the mass-flow rate is decreased. This is verified by the displacement of the design-radius streamlines shown in Figure 55, where it can be seen that for the design mass-flow rate the displacement of the streamline is reduced in the second stage whereas for the lower mass flow the streamline displacement is considerably increased within the second stage. In addition it will be observed that the oscillatory motion of the streamlines is more pronounced for the design mass flow than for the lower mass flows.

Since the radial gradient of static pressure is proportional to μ , it will be seen from Figure 54 that as the mass-flow rate is increased the static-pressure gradient at the trailing edges of the blade rows is also increased, except for the first-stage rotor row. At the trailing edge of this blade row an increase in the mass-flow rate causes a decrease in the static-pressure gradient, and for the higher mass flows the static-pressure gradient falls very rapidly at the trailing edge and assumes a negative value. This negative value of μ at the rotor trailing edge implies that there is a decrease of static pressure from hub to tip at this point, and this inversion of the static-pressure gradient has been observed on traversing behind this blade row (Rolls-Royce internal report, 1961). The very sudden change in the value of μ in the neighbourhood of the trailing edge is caused by the relative Mach number reaching a value of almost unity, so that the flow is very nearly choked at this point.

Using the same flow conditions as above two calculations were performed, one having a uniform axial flow at inlet and the other with a swirling flow at inlet. These two calculations were then repeated with the value of the ratio of the specific heats (γ) changed from 1.4 to 1.333. Figure 56 shows the four variations of λ , and it will be observed that the swirl at inlet has negligible effect on λ after the first row of nozzle guide vanes. Also, by comparing Figures 53 and 56, it will be noticed that keeping the mass-flow rate fixed and changing the value of γ is almost equivalent in this case to keeping the value of γ fixed and adjusting the mass-flow rate. This can also be seen by inspection of the appropriate curves in Figures 57 and 58, which show the variations of the axial velocities and densities at the design radius for several of the different flow rates and conditions.

15. Flow through a Converging-Diverging Nozzle

As a further example of the flexibility of the parameter-theory programme it was used to investigate the flow of air through a converging-diverging nozzle of circular cross-section. It was assumed that the converging and diverging sections were identical, with a maximum diameter of 28 inches and a minimum diameter at the throat of 12 inches. To produce the necessary curvature of the walls the nozzle was divided into seventeen sections each of 4 inches axial length, and it was assumed that each section had a linear variation of the outer wall. Thus in effect the nozzle consisted of seventeen consecutive sections of conical duct. The inlet stagnation conditions were taken to be 14.7 pounds per square inch and 60°F, and a mass-flow rate of 38.44 pounds per second was assumed.

This/

This gave an axial Mach number at inlet of 0.106 and a maximum axial Mach number at the throat of 0.897.

A plan of the nozzle is given in Figure 59(a) together with the predicted displacement of the design-radius streamline. Figure 59(b) shows the variations of λ and μ through the nozzle, and from these graphs it can be deduced that the magnitudes of the radial gradients of static pressure and velocity are greatly increased at the discontinuities in the slope of the wall. The mid-points of the first nine sections of the nozzle were denoted by the station numbers 1 to 9, and axial-velocity profiles for these nine stations are given in Figure 60. Since the nozzle is symmetrical, axial-velocity profiles for the last eight sections correspond to those for the first eight sections. If it is assumed that the effects of the discontinuities in the wall shape have negligible effect on the flow at the stations 1 to 9 it can be seen that the curvature of the axial-velocity profile changes sign as the curvature of the wall changes sign. This influences the streamline pattern, such that the streamlines are displaced towards the axis of the nozzle through that part of the converging section where the rate of change of cross-sectional area is increasing, and are displaced towards the wall of the nozzle where the rate of change of area is decreasing. This effect can be seen in Figure 59(a).

For real nozzles in which the cross-sectional area changes smoothly and continuously, the graphs of λ and μ would also be smooth, continuous curves. This can be achieved using the parameter-theory programme by dividing the nozzle into a very large number of sections such that the changes in slope of the wall across the interfaces are very small. By considering then the solutions at the mid-points only of all the individual sections, smooth plots of λ and μ may be derived which would be close approximations to the actual curves.

16. Conclusions

The versatility of the original single-parameter theory proposed by Whitehead and Beavers (1961) has been greatly increased by the allowances made for compressibility and variable-area effects, but this has been accompanied by a corresponding increase in the complexity of the analysis. The single-parameter theory was first envisaged for the incompressible flow through constant-area turbo-machines because it presented a method of solution which was conceptually simple, easy to programme for an electronic computer, and yet sufficiently accurate for design purposes. In extending the theory to include these two extra effects it has been attempted to adhere to the same criteria as closely as possible, the object of the analysis being to obtain a general solution of the flow in the form of a computer programme which could be used to analyse any axial-flow turbo-machine. This programme now exists for use on the EDSAC 2 computer of the Cambridge University Mathematical Laboratory, and some of the applications to which the programme may be put have been demonstrated in sections 9 to 15 of this paper.

Comparisons with the theoretical results of Wu show good agreement for both compressible and incompressible flows. The agreement is particularly good over the whole annulus area for the single-stage compressor, but for the single-stage turbine slight discrepancies in axial velocity and density occur at the hub and tip radii. The variations of axial velocity and density within a blade passage do not correspond exactly, even at the design radius, but this would be expected since these variations depend upon the assumed variation for the gas

angle/

angle through the blade passage. At the trailing edges of the blade rows, where the gas angles are the same for both methods, the axial velocities and densities are identical in the neighbourhood of the design radius.

The parameter-theory calculations for the flow of air through converging and diverging ducts agree closely with the experimental results of Lewis (1961) and indicate that the theory can be used to give accurate predictions of this type of flow when boundary-layer effects are not significant. It has been shown that large boundary-layer effects seriously reduce the accuracy of both actuator-disc and parameter-theory predictions, so that the inaccuracies caused by neglecting the presence of boundary layers are much greater than the inherent errors resulting from the limitation that the axial velocity and density belong to definite families of profiles. This suggests that greater accuracy of the theory is not warranted unless a suitable method of allowing for the boundary layers is introduced.

Some limitations of the parameter theory are demonstrated in the comparisons of the predictions for the flow in a three-stage turbine with the experimental results of Johnston and Sansome (1961). These would indicate that greater accuracy could be obtained by including in the theory a means of allowing for blade losses and the introduction of some form of expansion efficiency for diverging flows. However, the experimental axial-velocity profiles obtained by Johnston and Sansome are such that any theoretical prediction would be, at the very best, a poor approximation.

The calculations for the seven-stage compressor show how the oscillatory form for the variation of λ, observed by Whitehead and Beavers (1961) for the flow through a model ten-stage compressor, is still maintained although the definition of λ has been slightly modified. Likewise, the periodic form of the design-radius streamline observed in that paper and assumed by several authors has been shown to exist in compressible flow through a turbo-machine of non-constant area. These results have also been demonstrated for the flow through a two-stage turbine, which has been included to show how the computer programme may be used to investigate the effects produced by varying various operating conditions and parameters.

Further extensions now being made to the theory include a method of allowing for the thickness of the blades. Existing turbo-machines have blades which occupy a substantial proportion of the annulus area, so that appreciable errors in the density and axial velocity within a blade passage could be caused by neglecting this area occupied by the blades. By including an allowance for blade thickness the assumption that a blade row consists of an infinite number of blades of zero thickness can be omitted and machines with a finite number of real blades may be analysed. Finally it is proposed to write a computer programme for the modified theory in such a way that it can readily be translated for use on other high-speed digital computers.

17. Acknowledgements

The author gratefully acknowledges the invaluable help and advice given to him by Dr. D. S. Whitehead of the Cambridge University Engineering Laboratory.

The author is indebted to Messrs. Rolls-Royce Ltd. for permission to use the data for the turbine discussed in section 14, and to Dr. M. V. Wilkes, who made the computing facilities at the Cambridge University Mathematical Laboratory available to him.

Bibliography/

Bibliography

Author(s)	Title, etc.
BAMMERT, K.	Die Strömung durch vielstufige Axialturbinen mit geraden Shaufeln. (The flow in multi-stage axial turbines with straight blades.) Atomkernenergie 1961. Vol. 6, No. 68, pp.291-300. 1961.
BRAGG, S.L. and HAWTHORNE, W.R.	Some Exact Solutions of the Flow through Annular Cascade Actuator Discs. J.Ae.Sci., Vol.17, No.4, p.243. 1950.
HAWTHORNE, W.R. and HORLOCK, J.H.	Actuator disc theory of the incompressible flow in axial compressors. Proc. I. Mech. E., Vol.176, No.30. 1962.
HAWTHORNE, W.R. and RINGROSE, J.	Actuator Disc Theory of the compressible flow in free-vortex turbomachinery. A.R.C.22 341. September, 1962.
HOLMQUIST, C.O. and RANNIE, W.D.	Approximate method of calculating three-dimensional compressible flow in axial turbo-machines. J. Ae. Sci., Vol.23, p.543. 1956.
HORLOCK, J.H.	The compressible flow through cascade actuator discs. Aeronautical Quarterly. Vol.9. p.110. 1958.
HORLOCK, J.H.	Three-dimensional design of compressors and turbines. A review of the present position. A.R.C.24 124. October, 1962.
HOWELL, W.T.	Approximate three dimensional flow theory for axial turbo-machines. Aeronautical Quarterly, Vol.XIV, Part 2. May, 1963.
JOHNSTON, I.H. and SANSOME, G.E.	Tests on an experimental three-stage turbine fitted with low reaction blading of unconventional form. A.R.C. R. & M.3220. January, 1958.
LEWIS, R.I.	Flow through non-cylindrical axial turbo-machines. Ph.D. Thesis. Cambridge University. 1960.
MARBLE, F.E. and MICHELSON, I.	Analytical investigation of some three-dimensional flow problems in turbo-machines. N.A.C.A. Tech. Note 2614. March, 1952.
MELLOR, G.L.	Reconsideration of the annulus flow problem in axial turbo-machinery. A.S.M.E. Paper No. 61-WA-186. 1962.

Schnittger/

SCHNITTGER, J.R. — Vortex flow in axial turbo-machines. Trans. Royal Inst. of Technology. Stockholm. No. 74. 1954.

SMITH, L.H., TRAUGOTT, S.C. and WISLICENUS, G.F. — A practical solution of a three-dimensional flow problem of axial-flow turbo-machinery. Trans. ASME. Vol.75 p.789. 1953.

WHITEHEAD, D.S. and BEAVERS, G.S. — A single-parameter theory of vortex flow in turbo-machines. A.R.C. R. & M.3335. August, 1961.

WU, C.H., and WOLFENSTEIN, L. — Application of radial-equilibrium condition to axial-flow compressor and turbine design. N.A.C.A. Report 955. 1950.

WU, C.H. — A general theory of three-dimensional flow in subsonic and supersonic turbo-machines of axial-, radial- and mixed-flow types. N.A.C.A. Tech. Note 2604. January, 1952(a).

WU, C.H. — Matrix and relaxation solutions that determine subsonic through flow in an axial-flow gas turbine. N.A.C.A. Tech. Note 2750. July, 1952(b).

WU, C.H. — Subsonic flow of air through a single-stage and a seven-stage compressor. N.A.C.A. Tech. Note 2961. June, 1953.

ROLLS-ROYCE LTD. — Technical Report. SFS/DWS. 2/SH. 11 June, 1959.

ROLLS-ROYCE LTD. — Technical Report. SFS/KG. 4/DJS. 9 June, 1961.

APPENDIX/

APPENDIX

The Solution of the Density Equation

The density at any axial point within a blade row or gap is a solution of the equation

$$\rho_R^{\gamma+1} - \frac{T_s}{C}\rho_R^2 + \frac{m^2(1+\beta_R^2)}{2C.C_p\pi^2(t^2-h^2)^2} = 0 \quad . \qquad \ldots \quad (33)$$

This equation may be written as

$$f(\rho_R) \equiv \rho_R^{\gamma+1} - A\rho_R^2 + B = 0 \quad , \qquad \ldots \quad (33.1)$$

where A and B are given by

$$\left.\begin{aligned} A &= \frac{T_s}{C} \\ B &= \frac{m^2(+\beta_R^2)}{2C.C_p\pi^2(t^2-h^2)^2} \end{aligned}\right\} \qquad \ldots \quad (33.2)$$

Since T_s is constant within a blade row or gap, A is a constant, but B depends upon the values of β_R, t and h at any point.

The function $f(\rho_R)$ has a maximum point at $\rho_R = 0$, a minimum point at $\rho_R = \left[2A/\gamma+1\right]^{1/\gamma-1}$ and a point of inflexion at $\rho_R = \left[2A/\gamma(\gamma+1)\right]^{1/\gamma-1}$

Its form is shown in Figure 61, and it is seen that there are two positive real roots.

At the minimum point,

$$\rho_R^{\gamma-1} = \frac{2A}{\gamma+1} = \frac{2T_s}{C(\gamma+1)}$$

$$\therefore \quad \frac{T_s}{T} = \frac{\gamma+1}{2} \quad .$$

But

$$\frac{T_s}{T} = 1 + \frac{\gamma-1}{2}M^2 \quad ,$$

so that $M^2 = 1$.

Consider/

Consider now the greater of the roots. (2 in Figure 60). Then, since ρ_R is less than unity and $\gamma - 1$ is less than unity,

$$\rho_{R_2}^{\gamma-1} > \frac{2A}{\gamma + 1}$$

$$\therefore \quad \rho_{R_2}^{\gamma-1} > \frac{2T_s}{C(\gamma + 1)}$$

$$\therefore \quad \frac{T}{T_s} > \frac{2}{\gamma + 1}$$

$$\therefore \quad \frac{\gamma + 1}{2} > 1 + \frac{\gamma - 1}{2} M^2$$

$$\therefore \quad M^2 < 1$$

The root at 2 corresponds to subsonic flow.
Similarly, it can be shown that the root at 1 corresponds to supersonic flow.

Now since B changes but A remains constant on passing through a blade row or gap, this is equivalent to displacing the whole curve vertically. It can thus be seen that a critical case occurs when the curve is such that minimum point falls on the ρ_R - axis. At this point the flow will change from subsonic to supersonic, or vice-versa, and B will have its maximum possible value for that blade-row or gap.

A Newton-Ralphson process has been used to solve equation (33). For this particular problem this process can be expressed by the following statement:- if ρ_{Ri} is any approximation to the true value of ρ_R at any point, a better approximation $\rho_{R(i+1)}$ is given by

$$\rho_{R(i+1)} = \frac{\gamma\rho_{Ri}^{\gamma+1} - A\rho_{Ri}^2 - B}{(\gamma+1)\rho_{Ri}^{\gamma} - 2A\rho_{Ri}}$$

This method will break down when the denominator of the above expression becomes zero. This occurs when $\rho_R^{\gamma-1} = 2A/\gamma + 1$ which is the condition for unity Mach number.

This method of solution, coupled with the assumptions made about the machine and blade geometry, imposes a limitation upon the uses of the existing computer programme. It has been assumed that within a blade row or gap, dh/dx, dt/dx and $\partial\beta/\partial x$ always have constant signs. Consequently the function B in equation (33.1) always increases or decreases continuously from the beginning to the end of any section, with the result that the Mach number at the design radius can never be greater than unity. Thus the computer programme can only be used for flows which are subsonic throughout at the design radius.

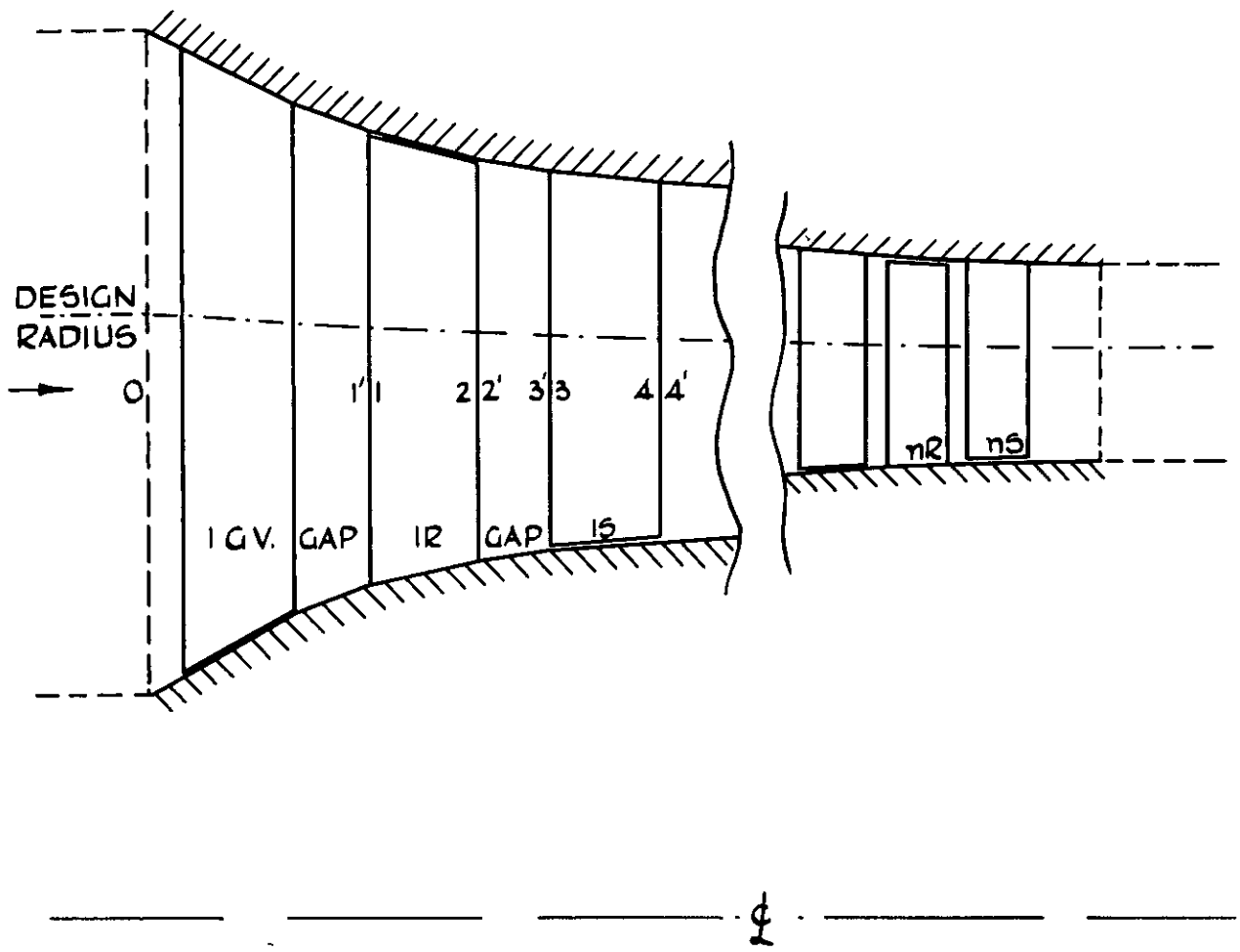

FIG. 1. TYPICAL SYSTEM UNDER ANALYSIS

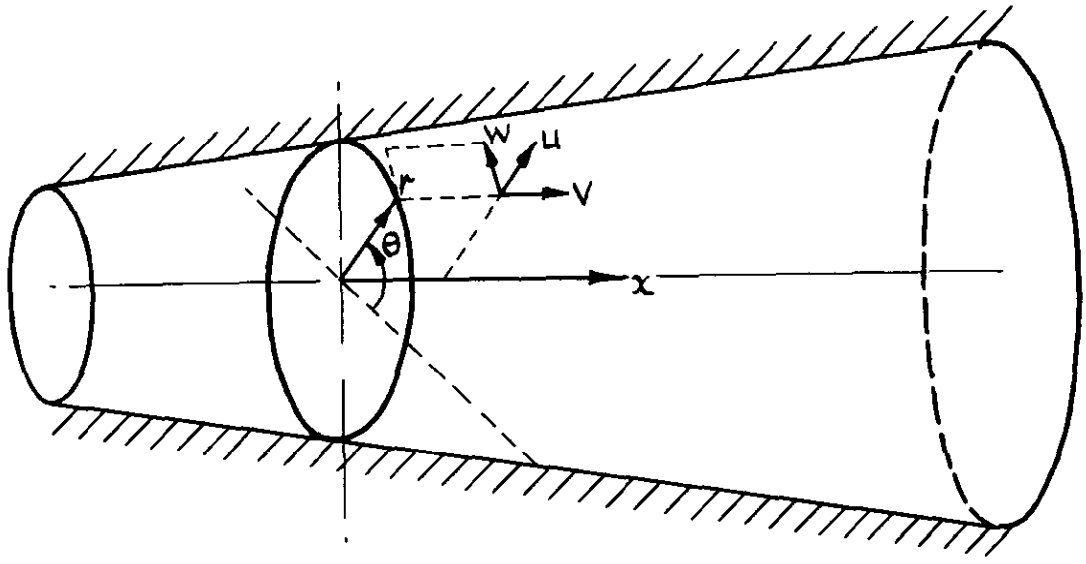

FIG 2. THE CO-ORDINATE SYSTEM

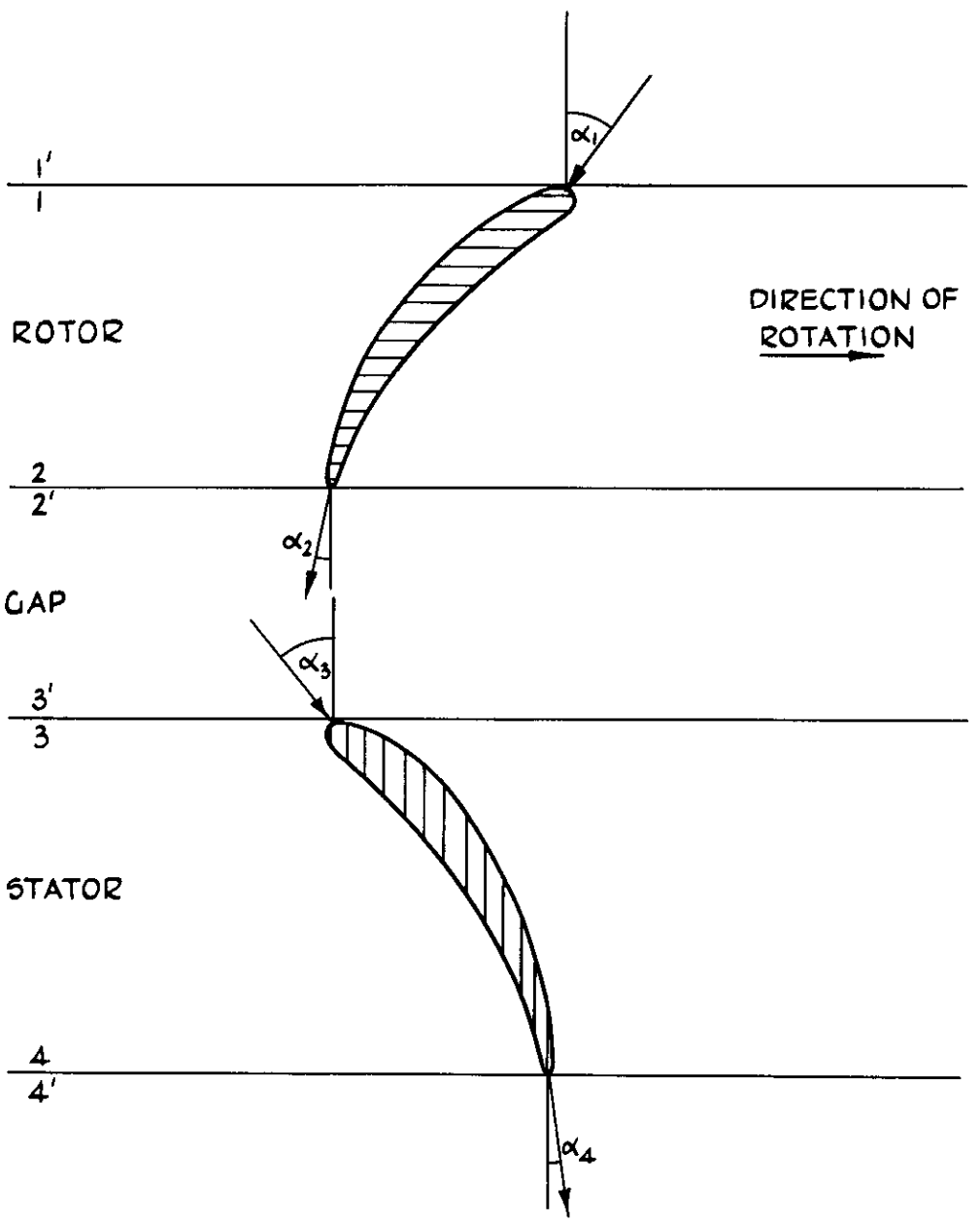

α - GAS ANGLE RELATIVE TO BLADE
ALL ANGLES SHOWN POSITIVE

FIG 3. NOTATION FOR GAS ANGLES

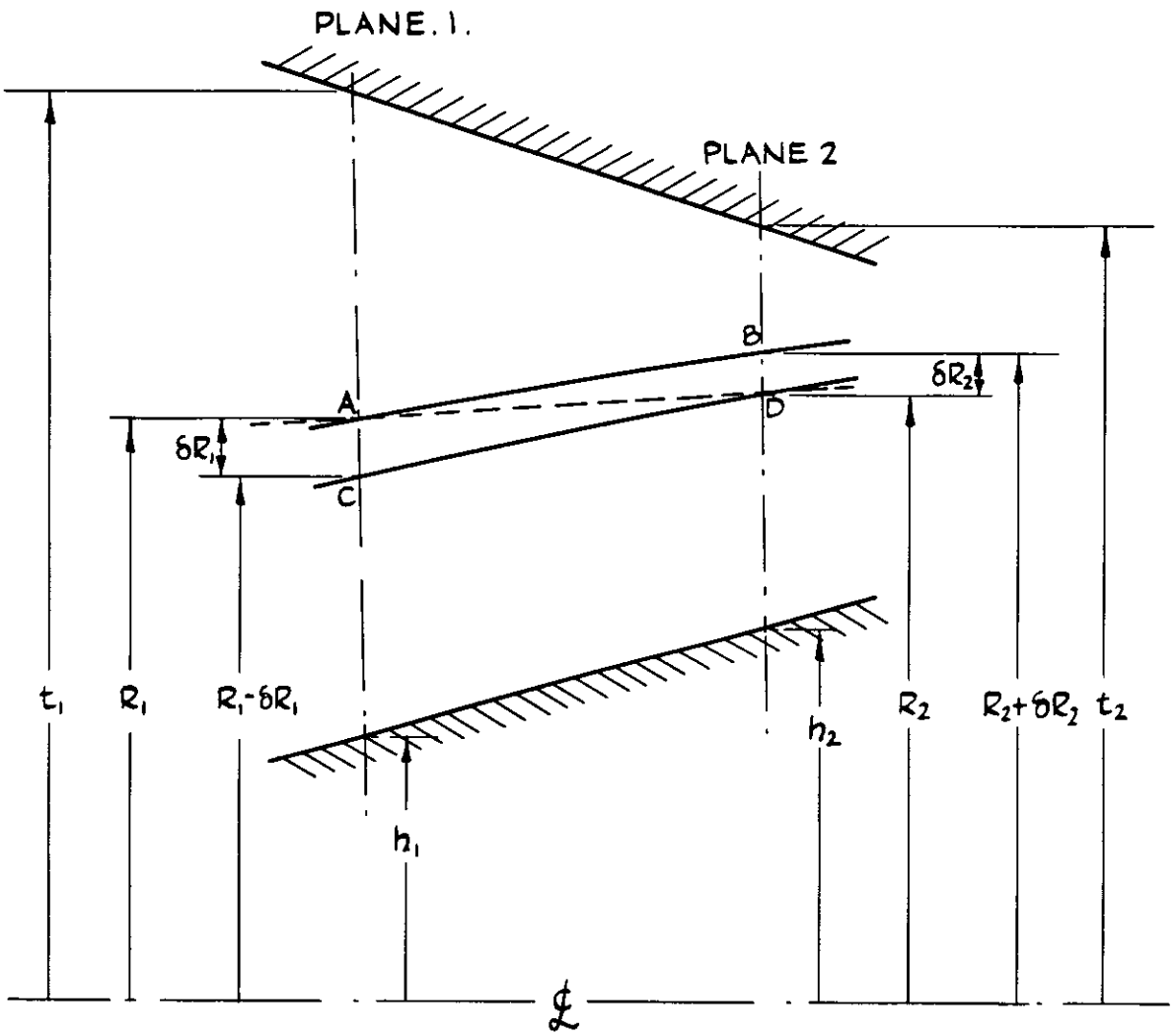

FIG.4. DISPLACEMENT OF STREAMLINES NEAR THE DESIGN RADIUS

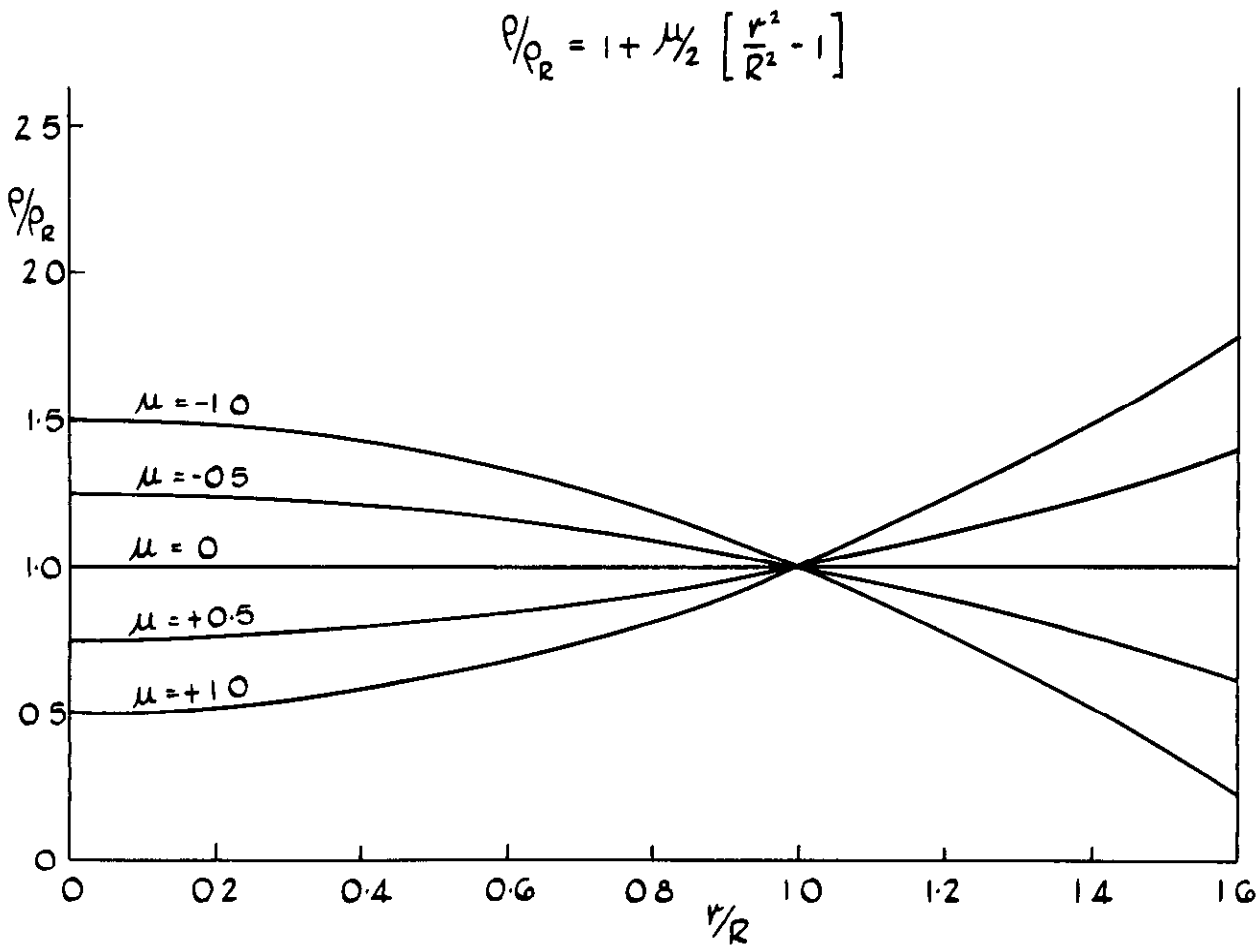

FIG.5 ASSUMED DENSITY PROFILES

$$\frac{V}{V_R} = \frac{1 + \lambda/2\left[\frac{r^2}{R^2} - 1\right]}{1 + \mu/2\left[\frac{r^2}{R^2} - 1\right]}$$

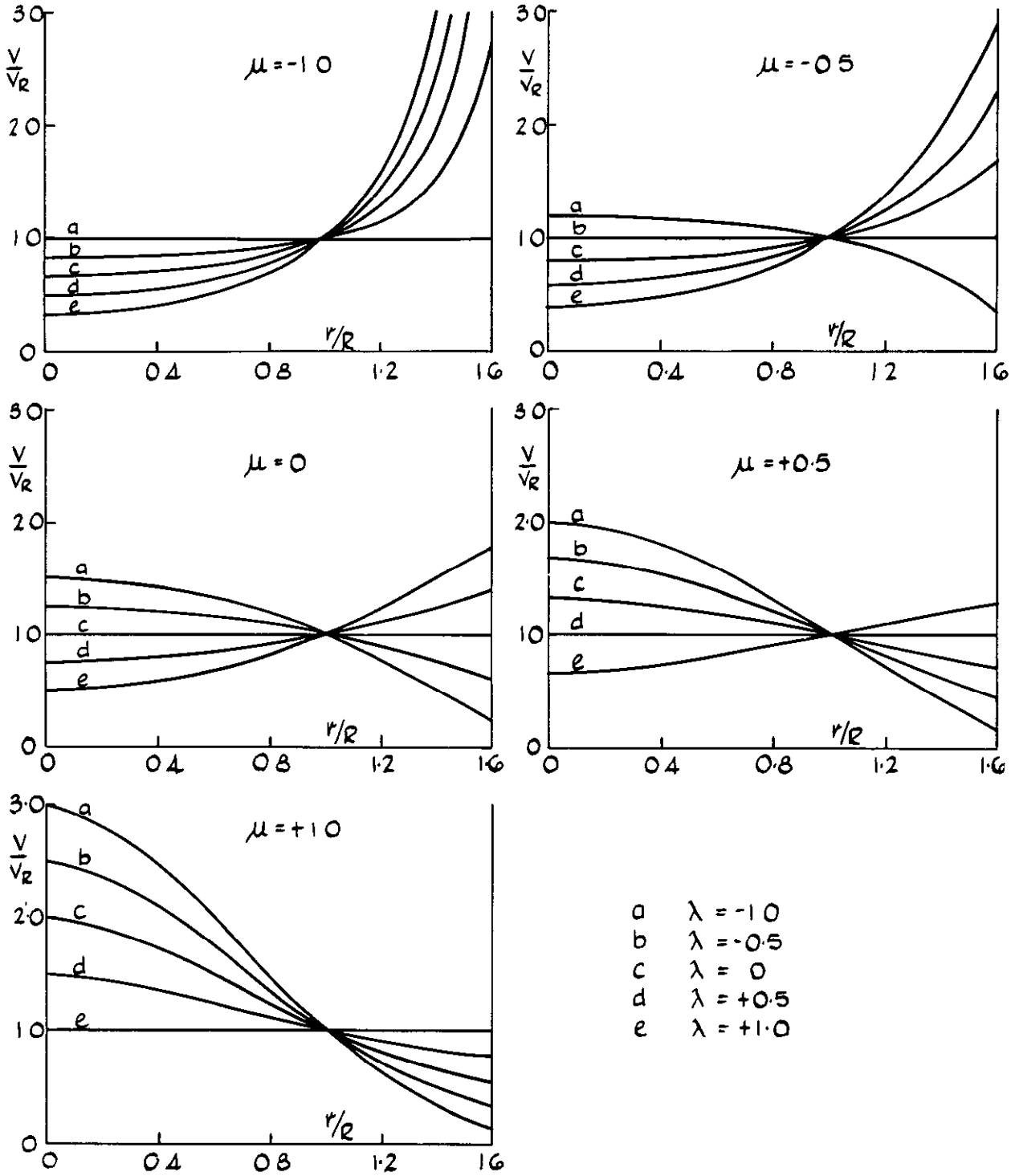

FIG. 6 ASSUMED AXIAL-VELOCITY PROFILES

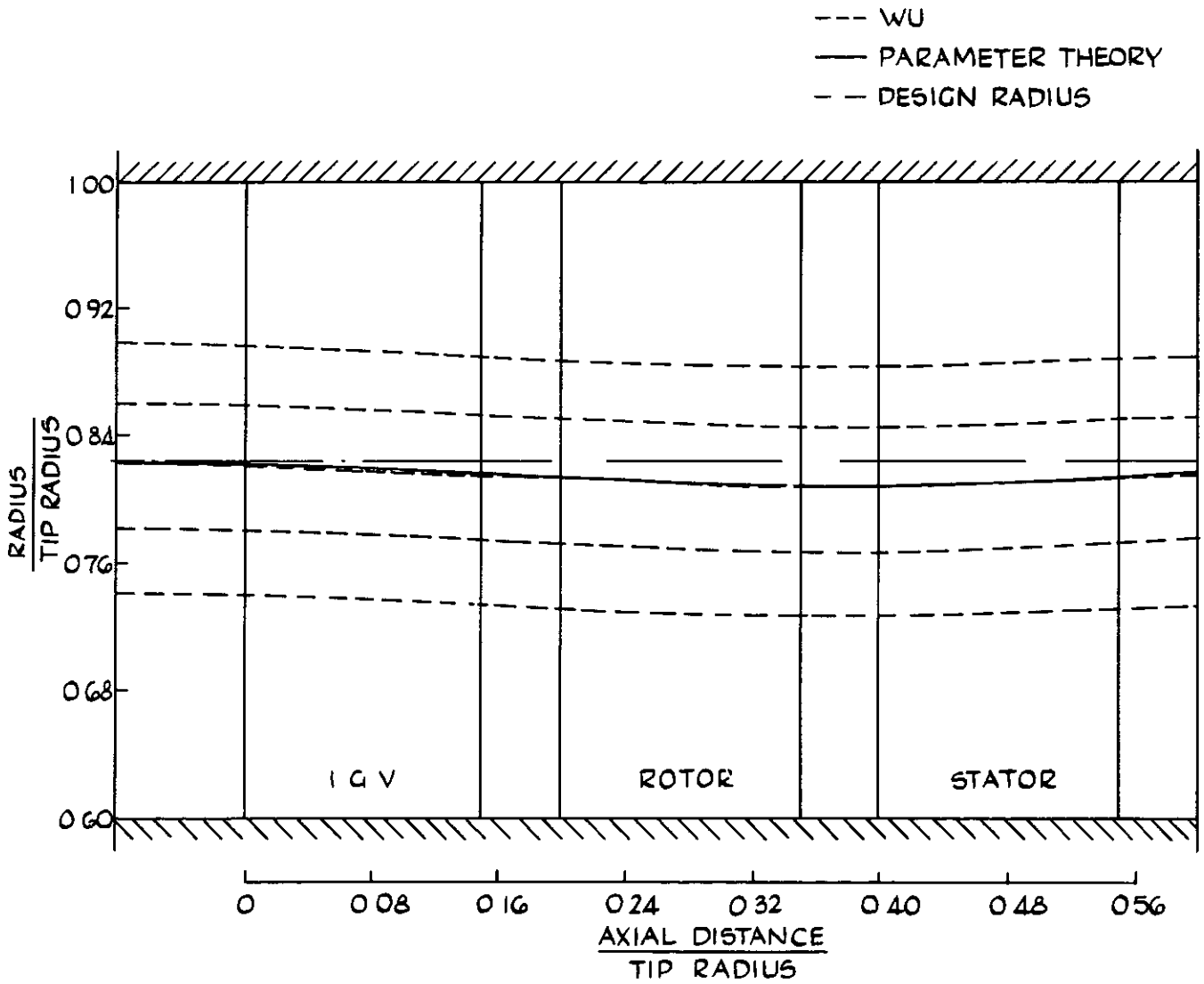

FIG 7. WU SINGLE-STAGE COMPRESSOR - DISPLACEMENT OF DESIGN-RADIUS STREAMLINE

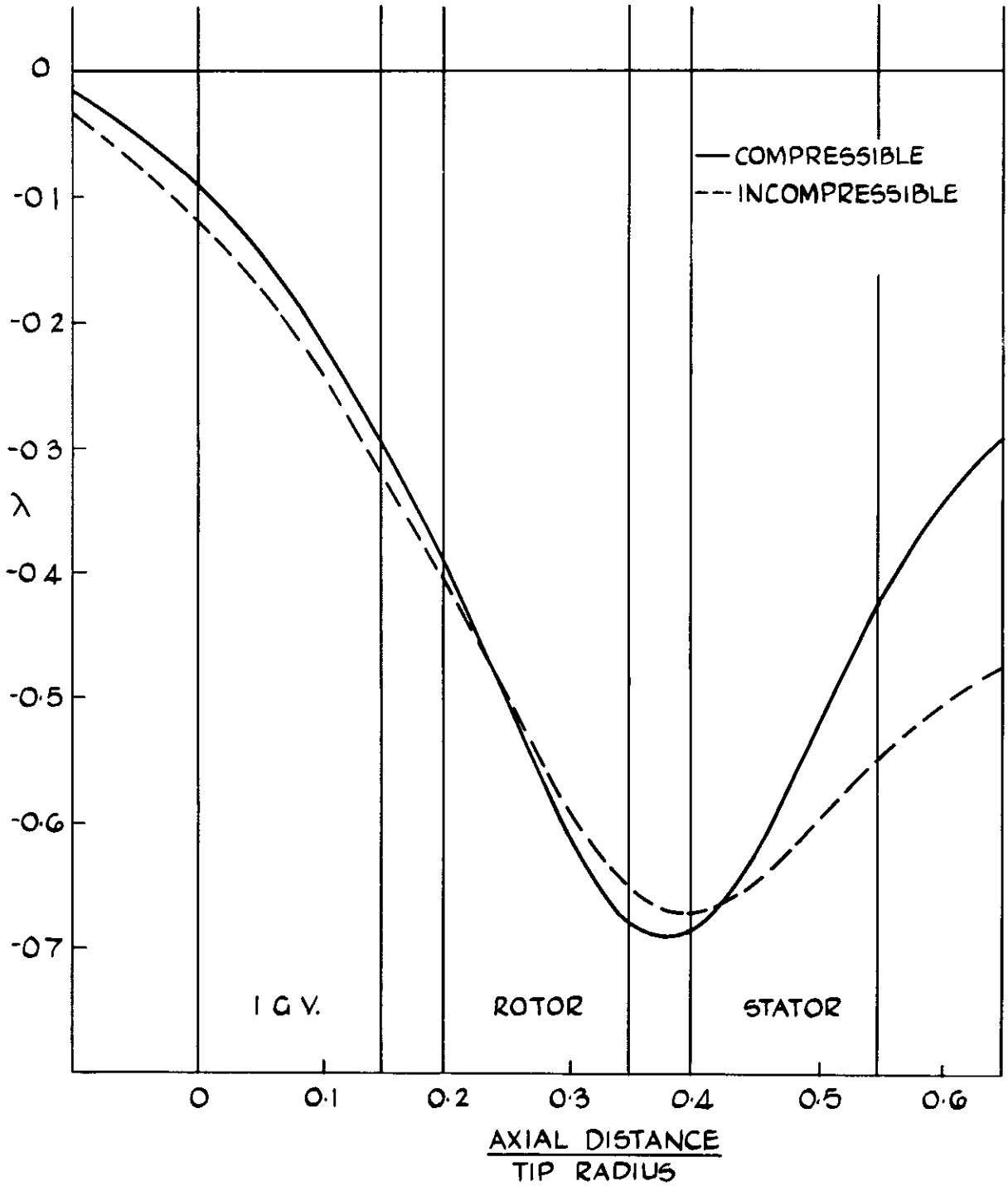

FIG. 8. WU SINGLE-STAGE COMPRESSOR - VARIATION OF λ

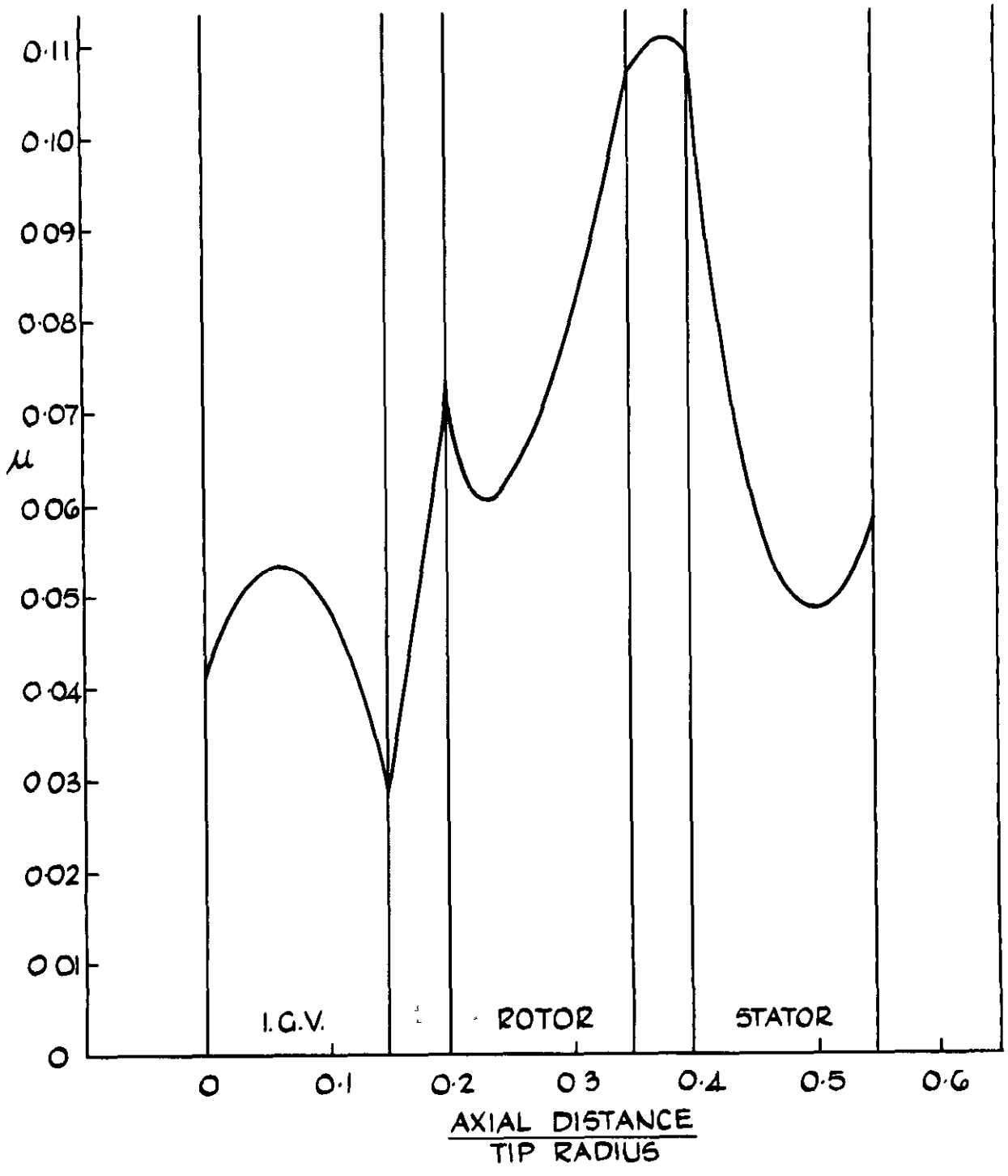

FIG. 9. WU SINGLE-STAGE COMPRESSOR - VARIATION OF μ

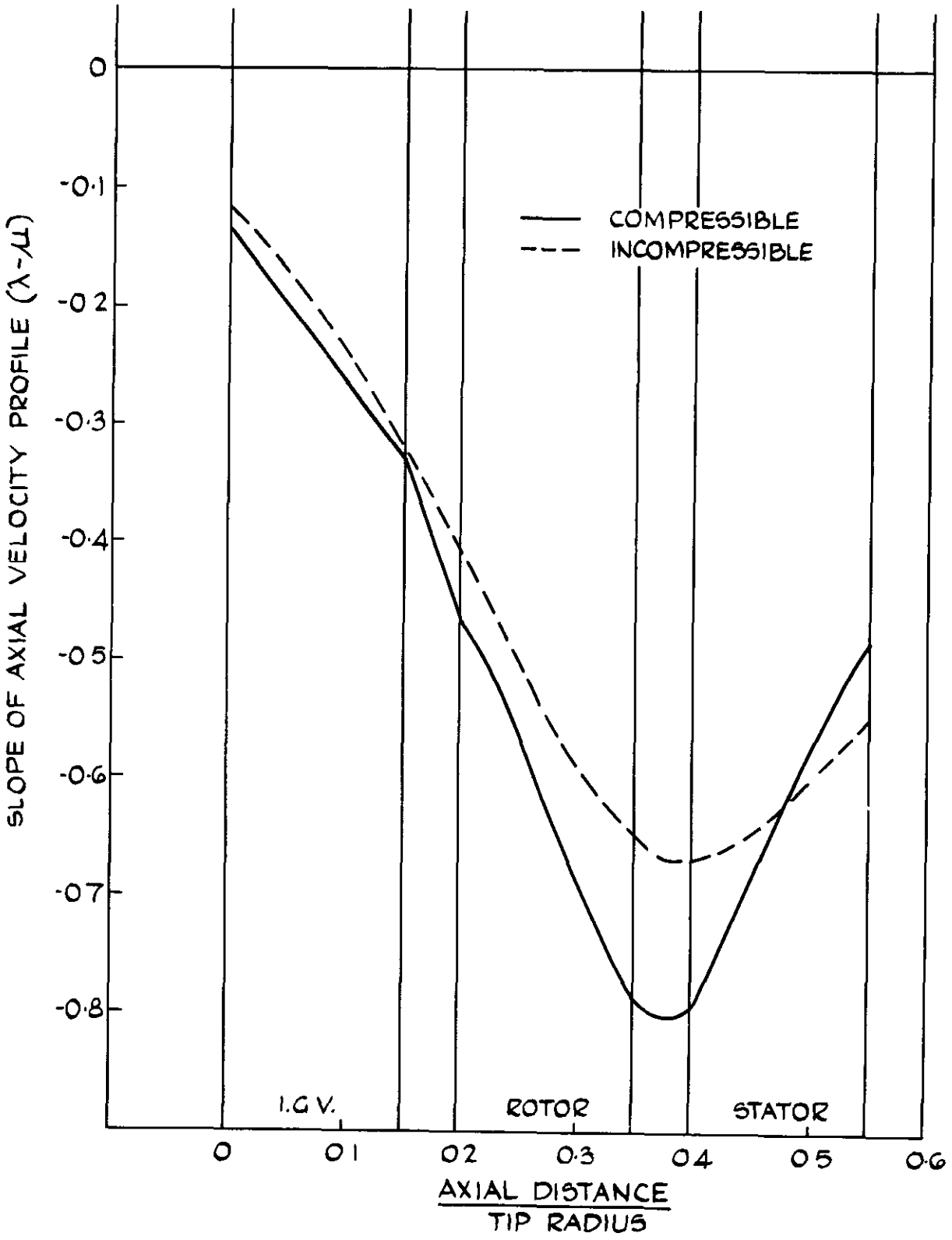

FIG 10. WU SINGLE-STAGE COMPRESSOR VARIATION OF SLOPE OF AXIAL-VELOCITY PROFILE (λ-μ)

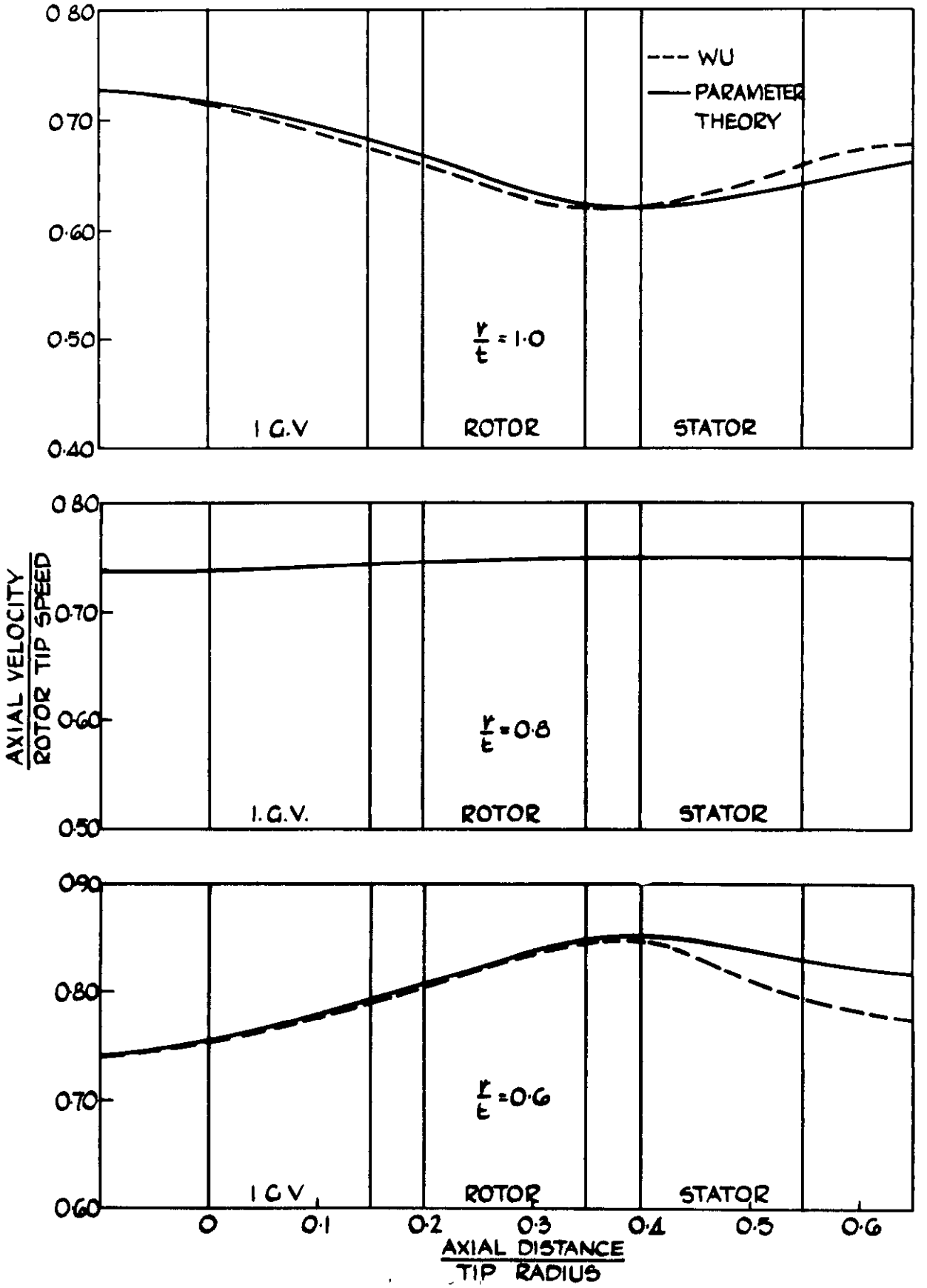

FIG 11. WU SINGLE-STAGE COMPRESSOR AXIAL VELOCITIES IN INCOMPRESSIBLE FLOW

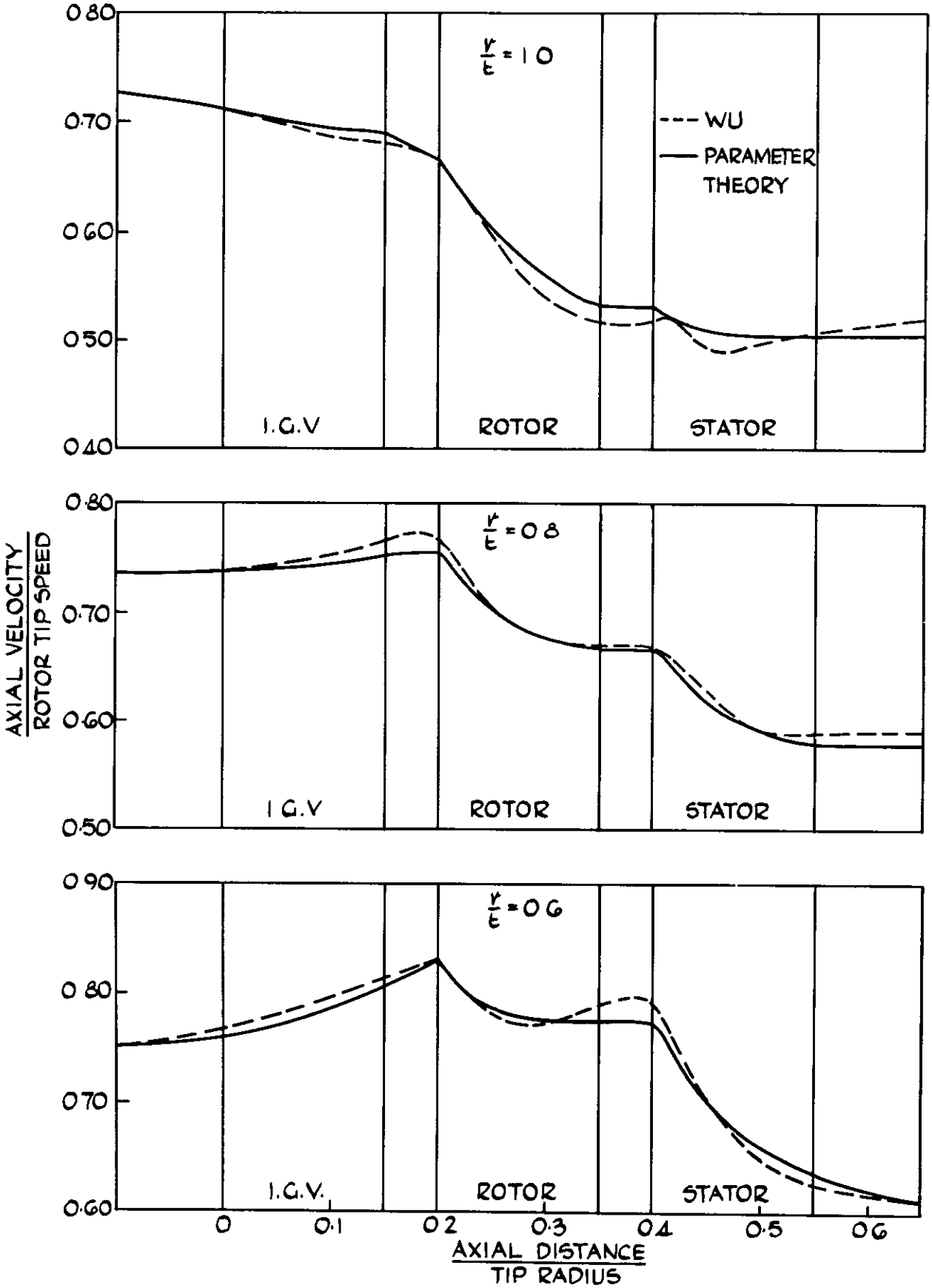

FIG 12 WU SINGLE-STAGE COMPRESSOR AXIAL VELOCITIES IN COMPRESSIBLE FLOW

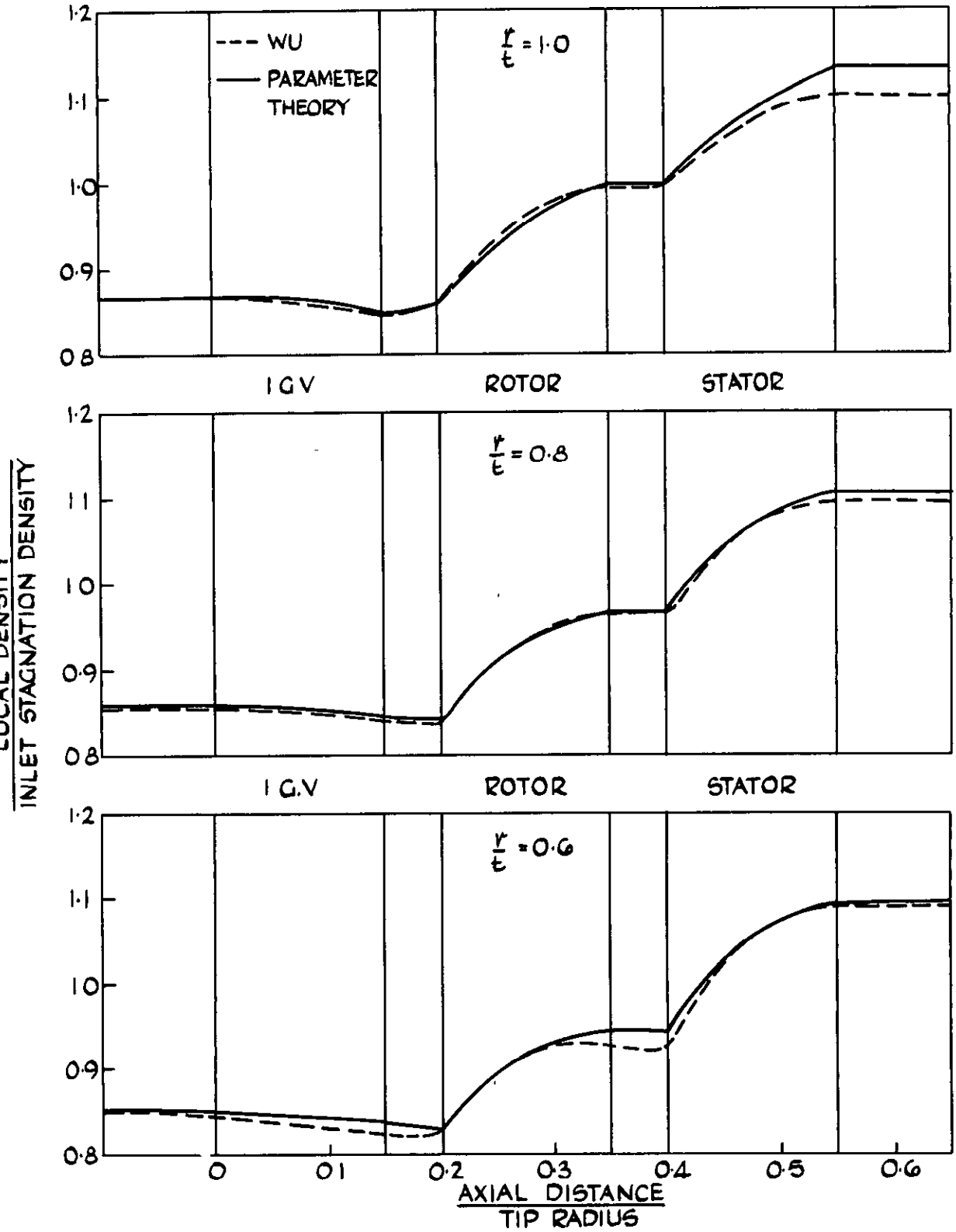

FIG. 13. WU SINGLE-STAGE COMPRESSOR - DENSITY VARIATIONS IN COMPRESSIBLE FLOW

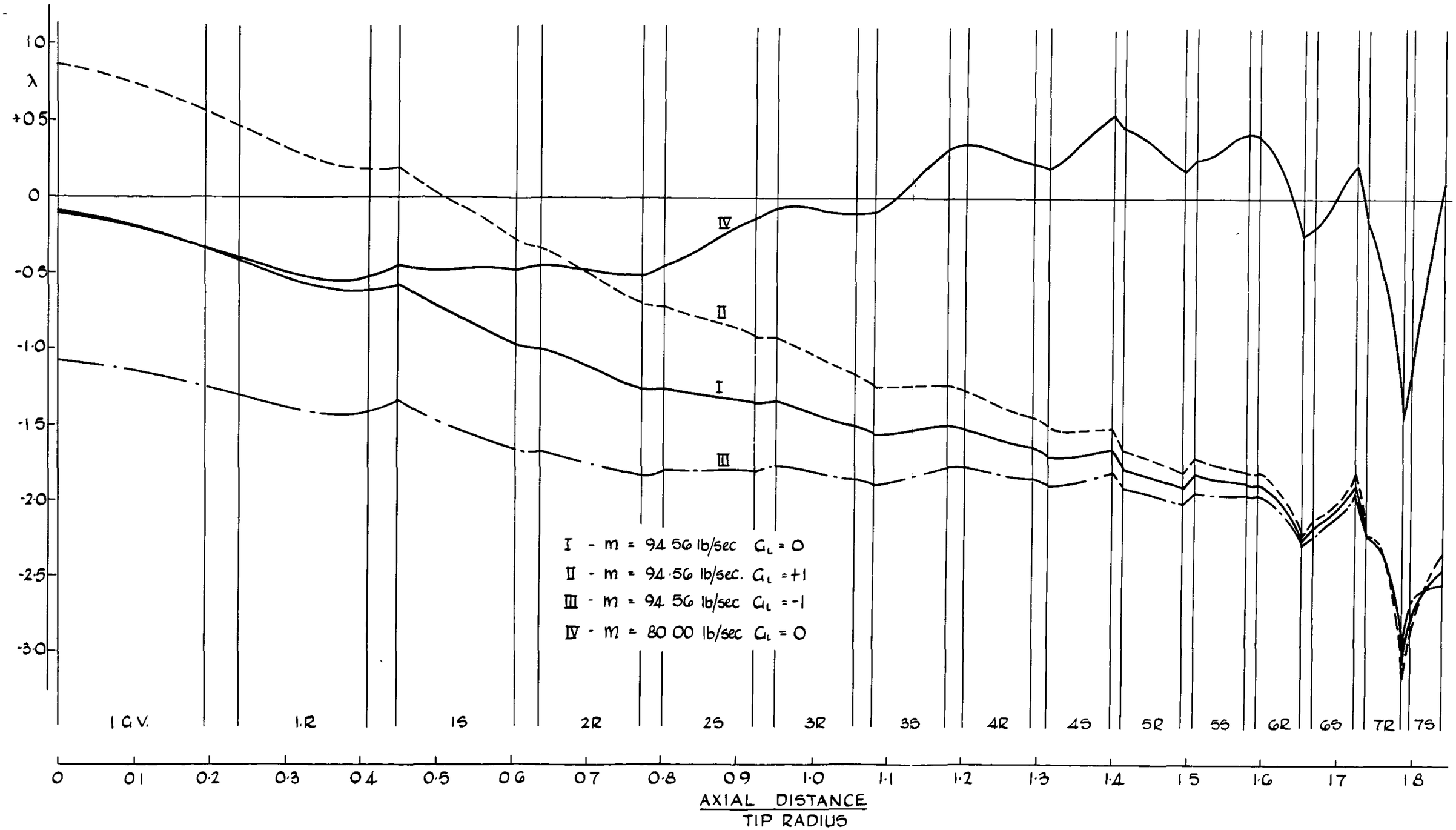

FIG 15. WU SEVEN-STAGE COMPRESSOR - VARIATION OF λ FOR VARIOUS MASS-FLOW RATES

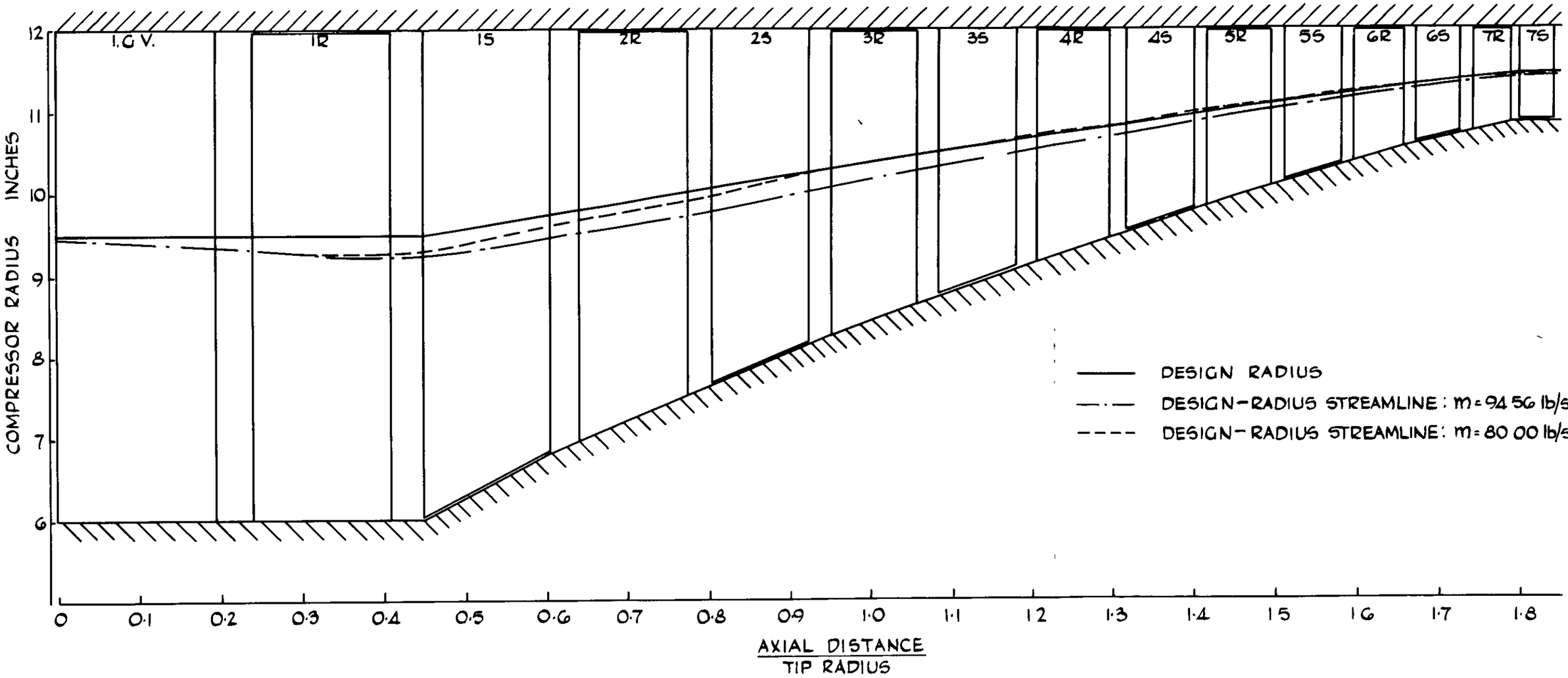

FIG. 14 WU SEVEN-STAGE COMPRESSOR - DISPLACEMENT OF DESIGN-RADIUS STREAMLINE

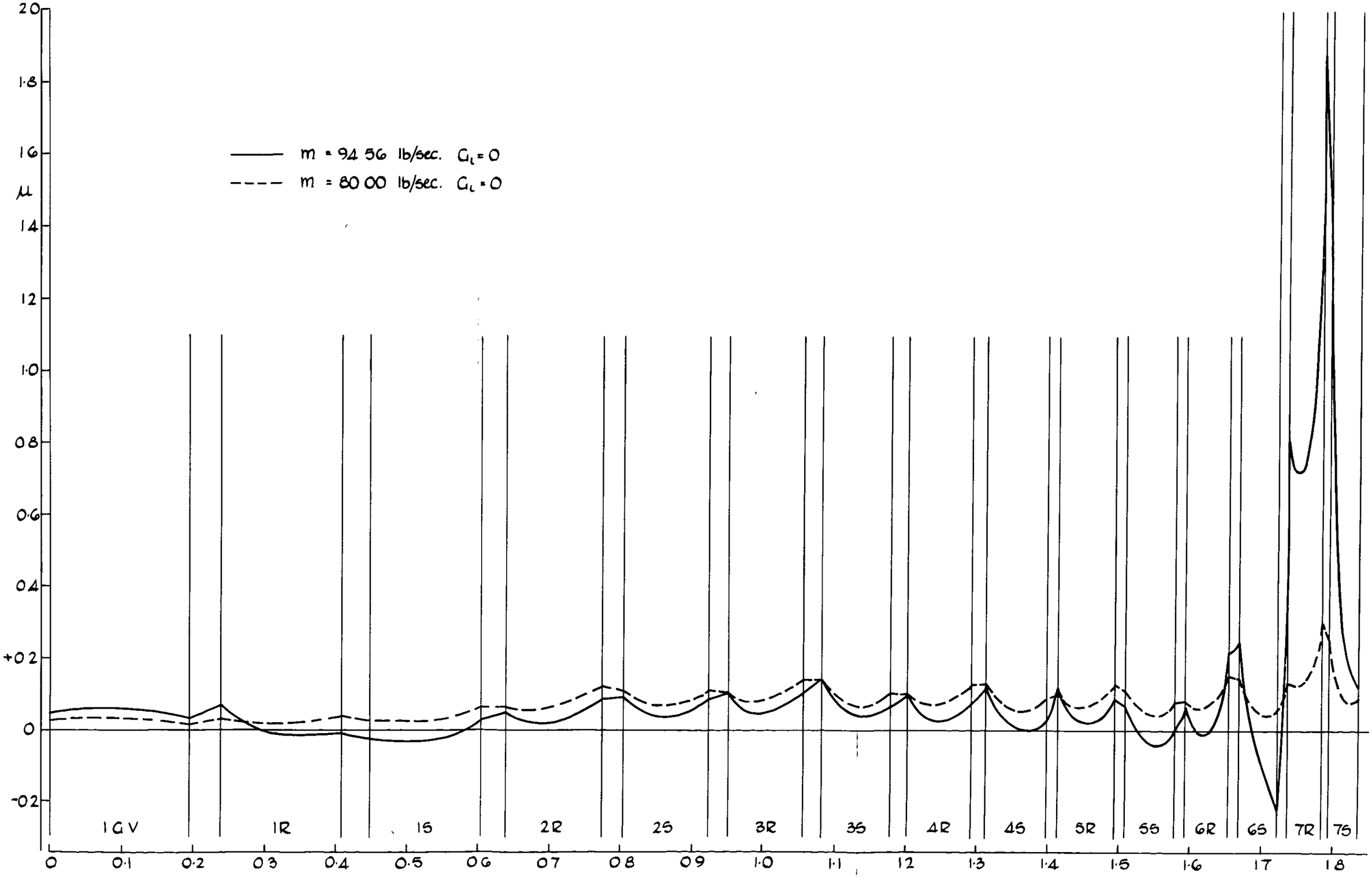

FIG. 16. WU SEVEN-STAGE COMPRESSOR - VARIATION OF μ

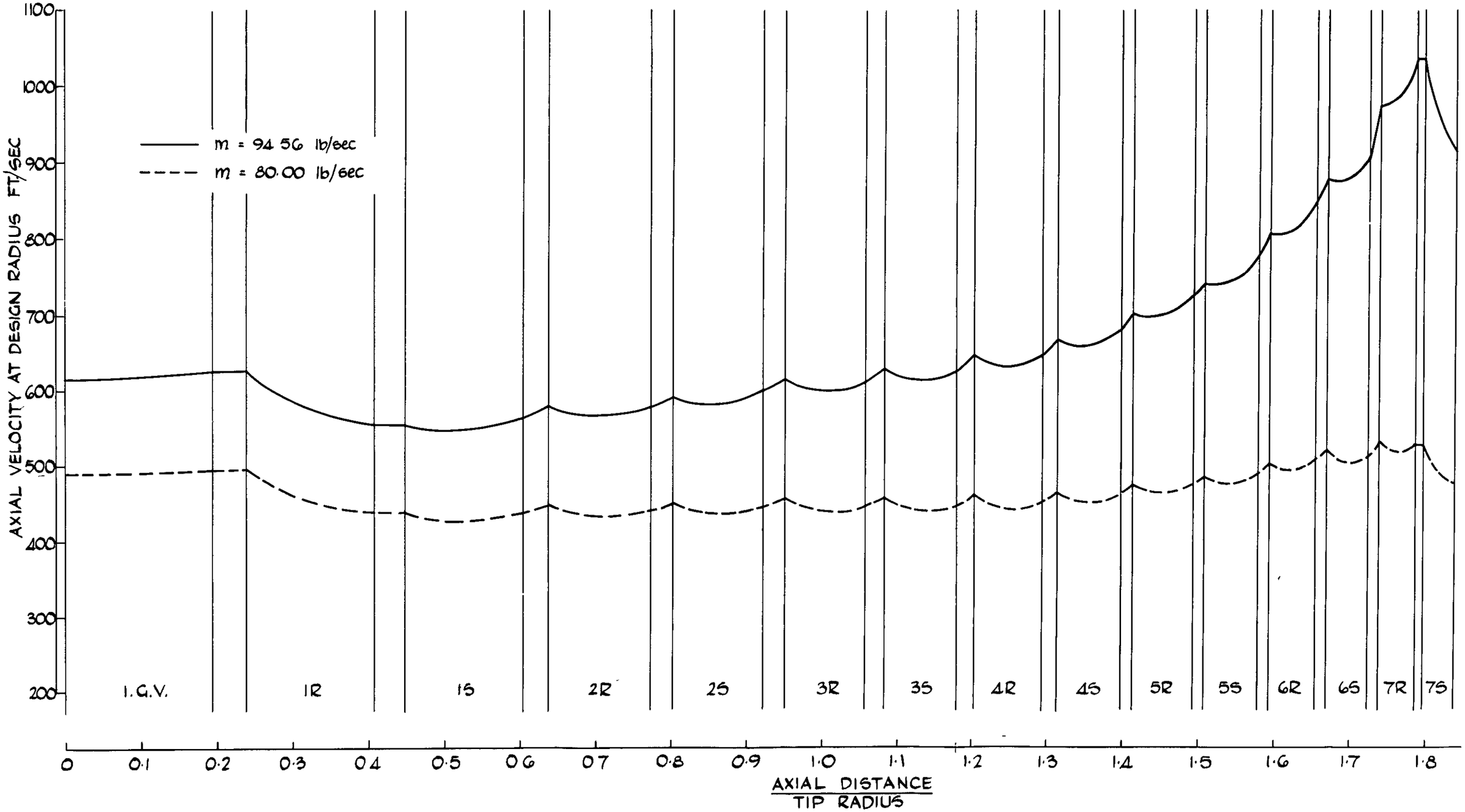

FIG .17. WU SEVEN-STAGE COMPRESSOR - VARIATION OF AXIAL VELOCITY AT THE DESIGN RADIUS

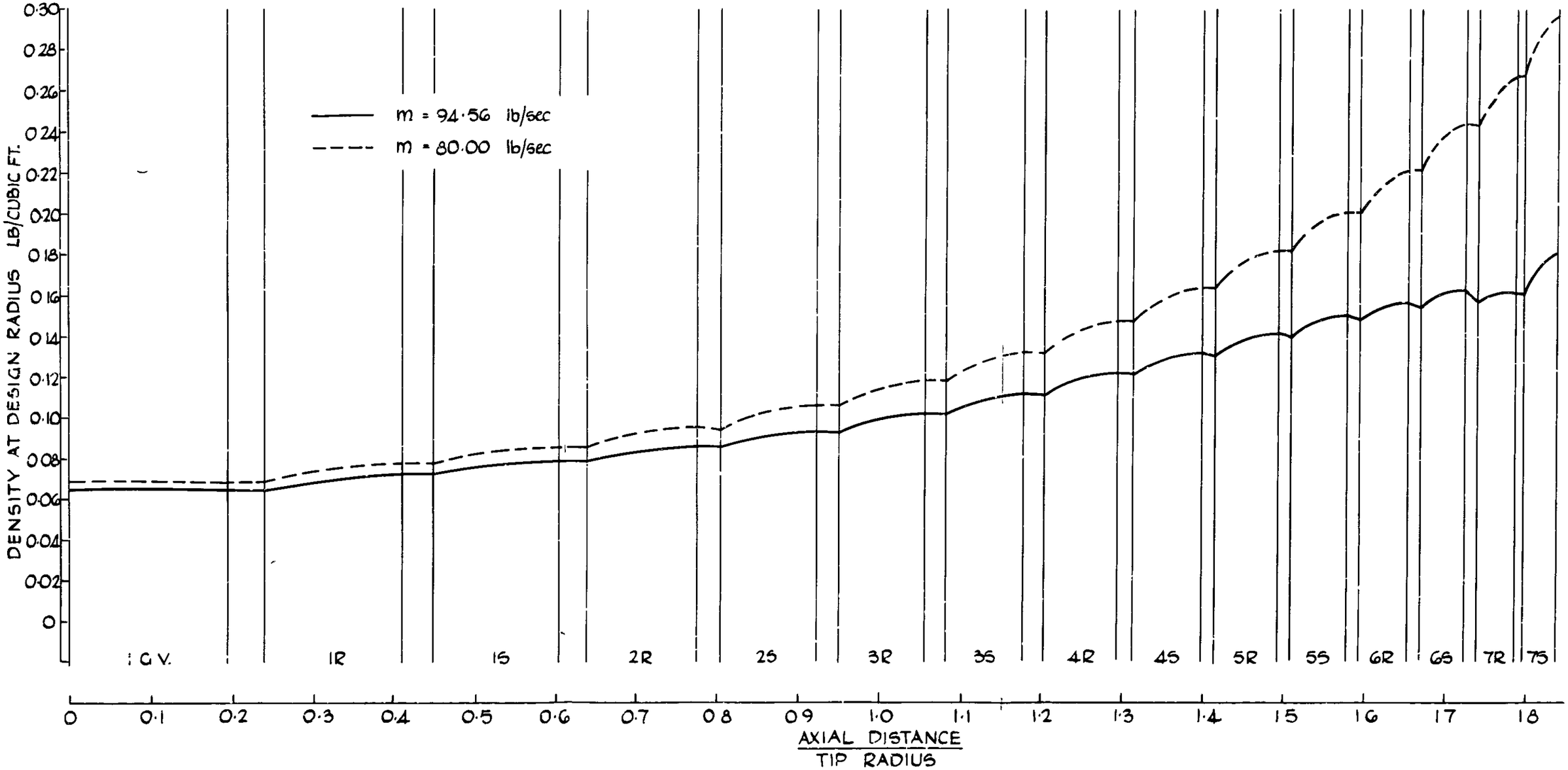

FIG. 18 WU SEVEN-STAGE COMPRESSOR - VARIATION IN DENSITY AT THE DESIGN RADIUS

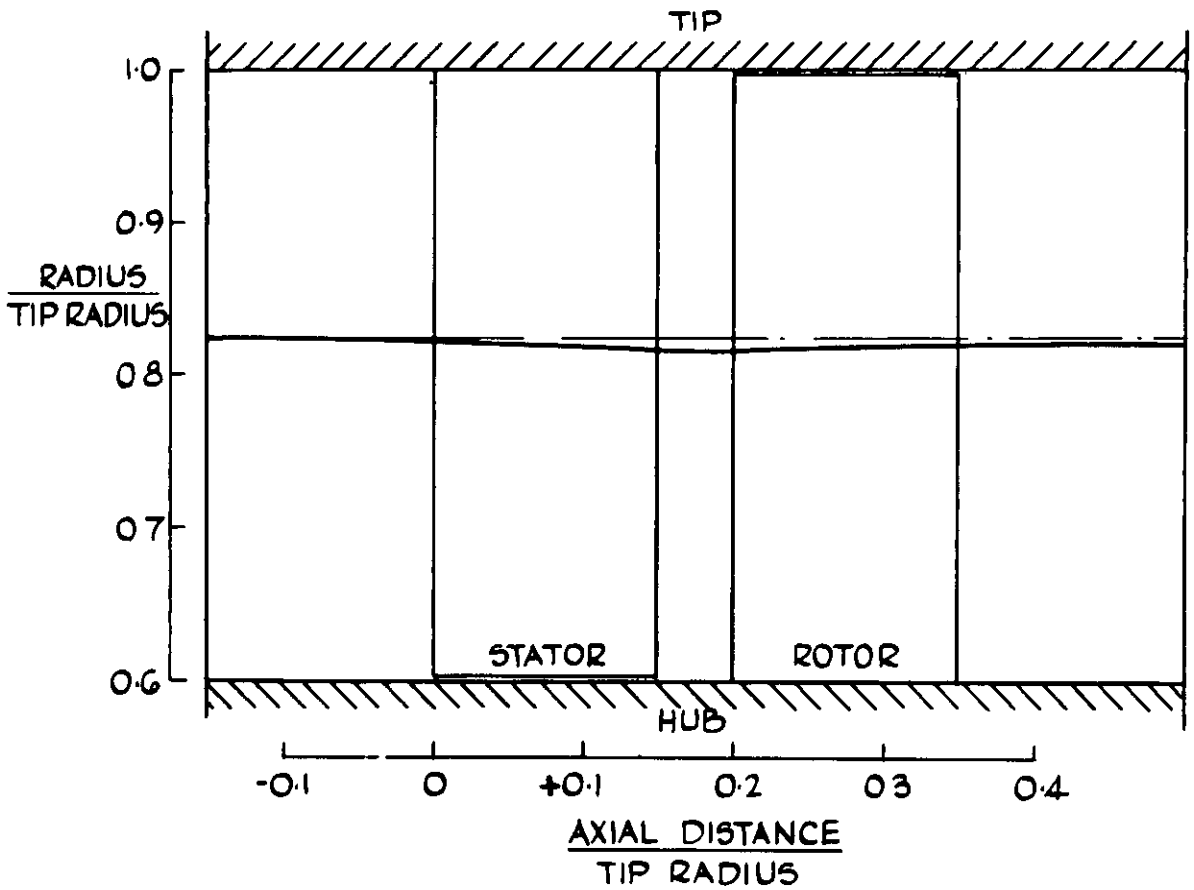

FIG.19. WU SINGLE-STAGE TURBINE - DISPLACEMENT OF DESIGN-RADIUS STREAMLINE IN INCOMPRESSIBLE FLOW

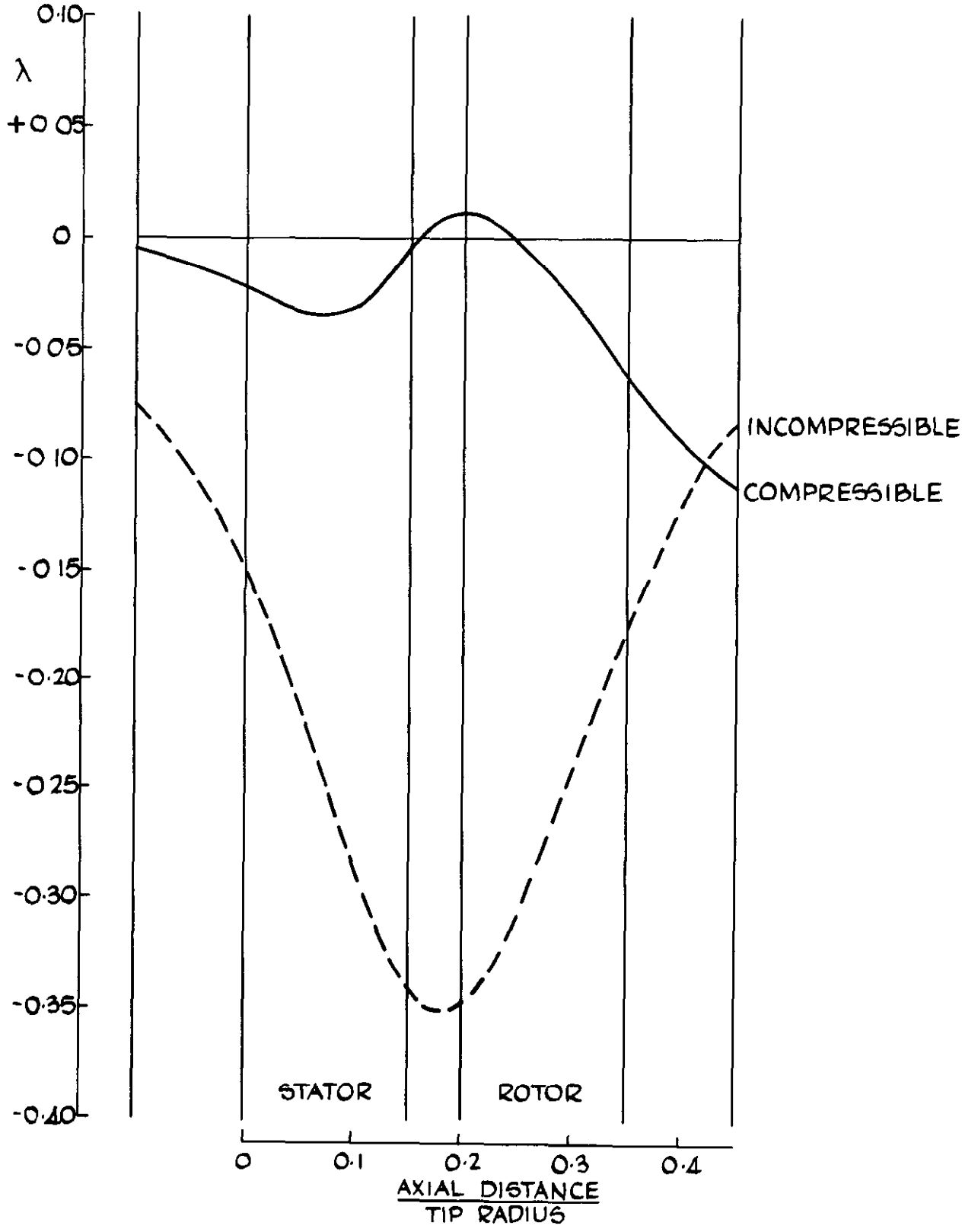

FIG. 20. WU SINGLE-STAGE TURBINE - VARIATION OF λ

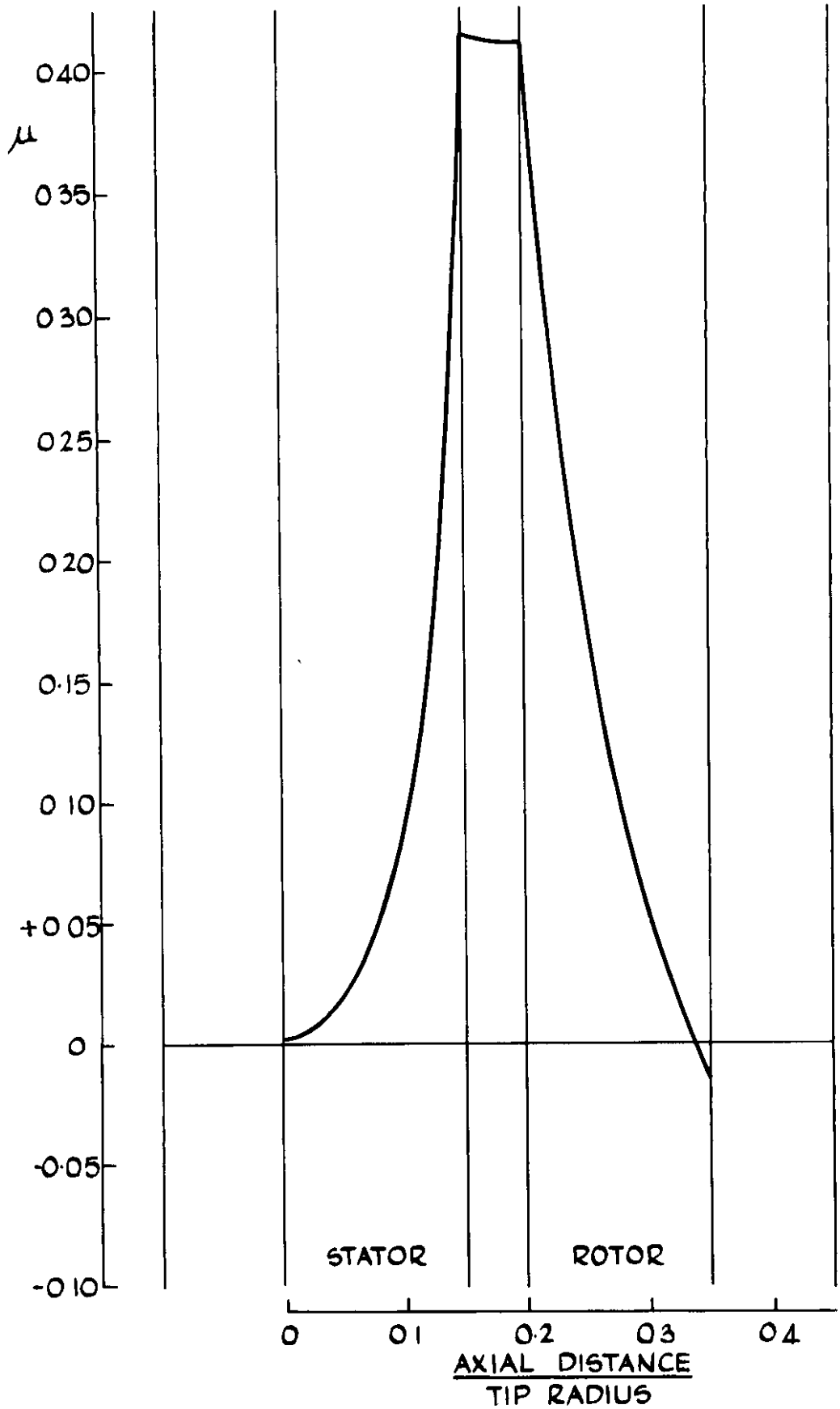

FIG. 21. WU SINGLE-STAGE TURBINE – VARIATION OF μ

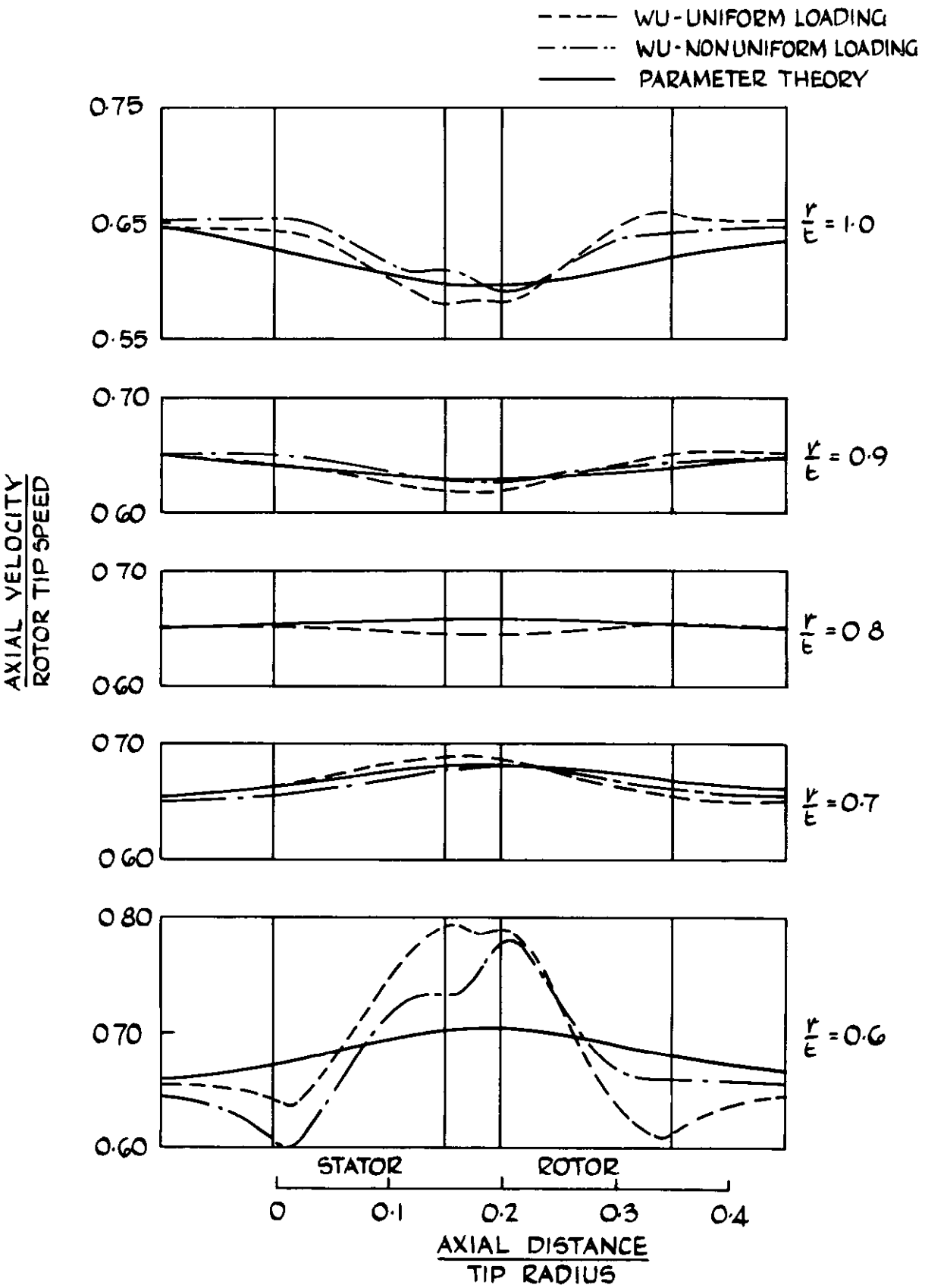

FIG 22 WU SINGLE-STAGE TURBINE AXIAL-VELOCITY VARIATIONS IN INCOMPRESSIBLE FLOW

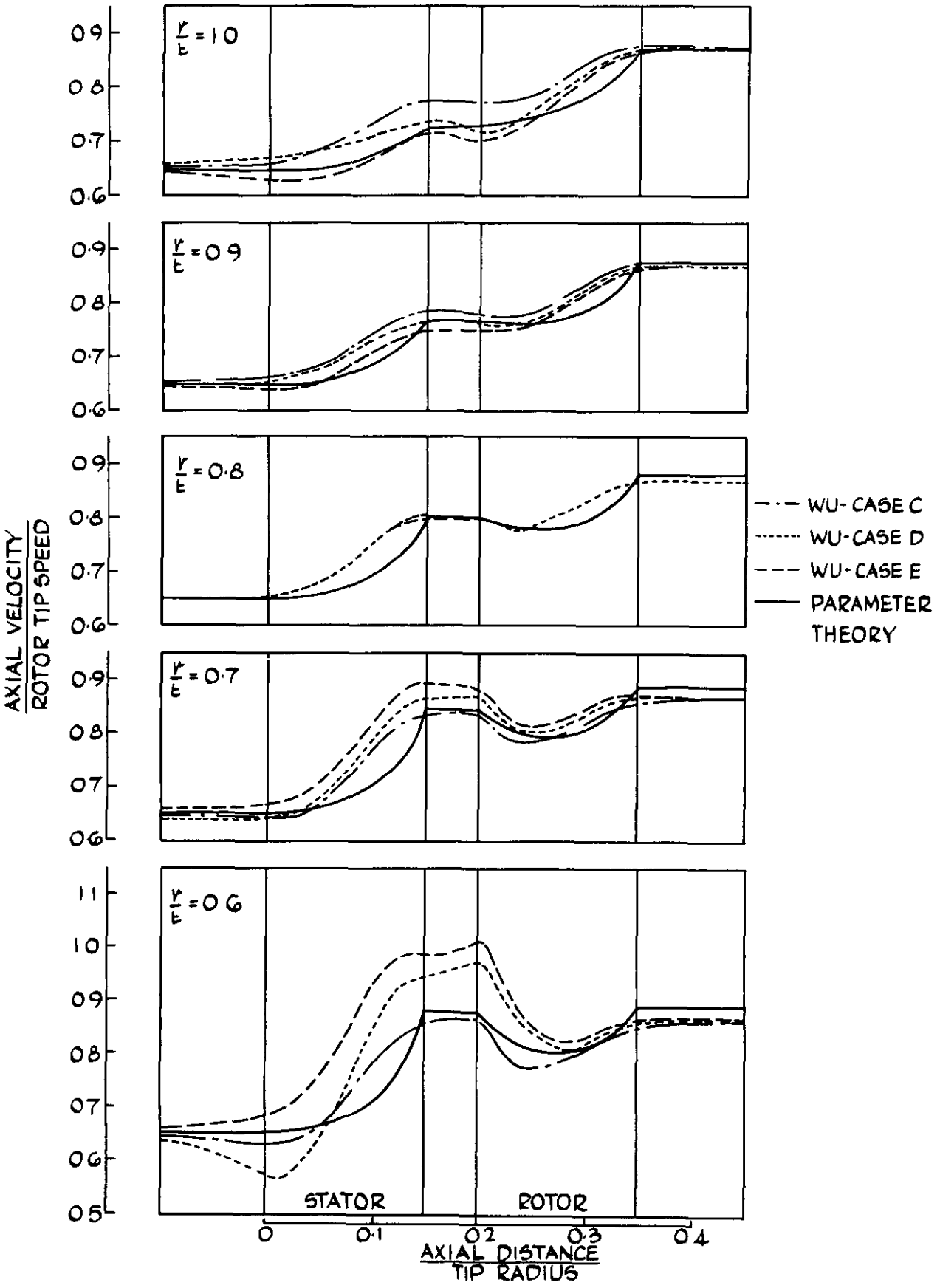

FIG 23. WU SINGLE-STAGE TURBINE AXIAL-VELOCITY VARIATIONS IN COMPRESSIBLE FLOW

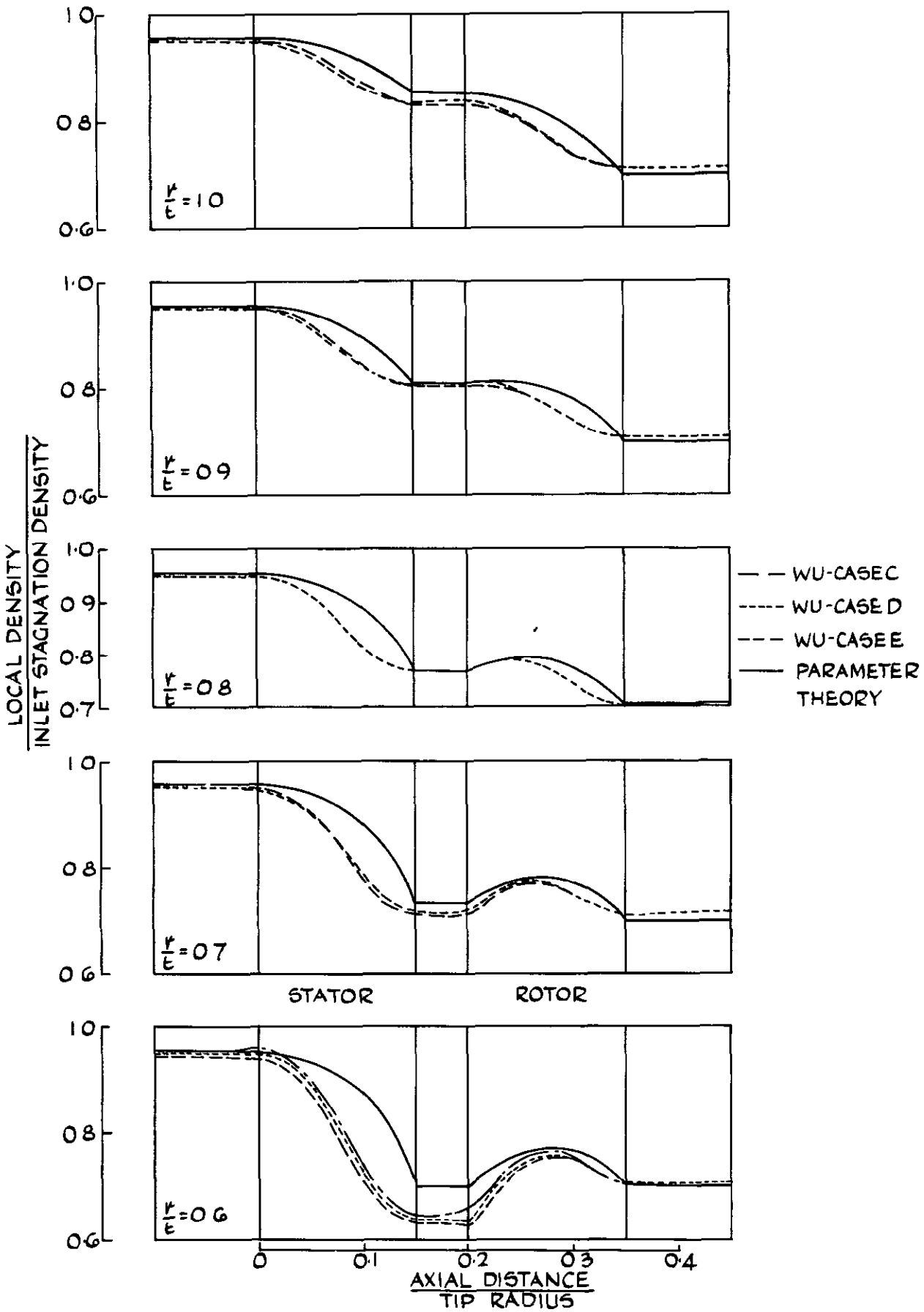

FIG.24 WU SINGLE-STAGE TURBINE - DENSITY VARIATIONS IN COMPRESSIBLE FLOW

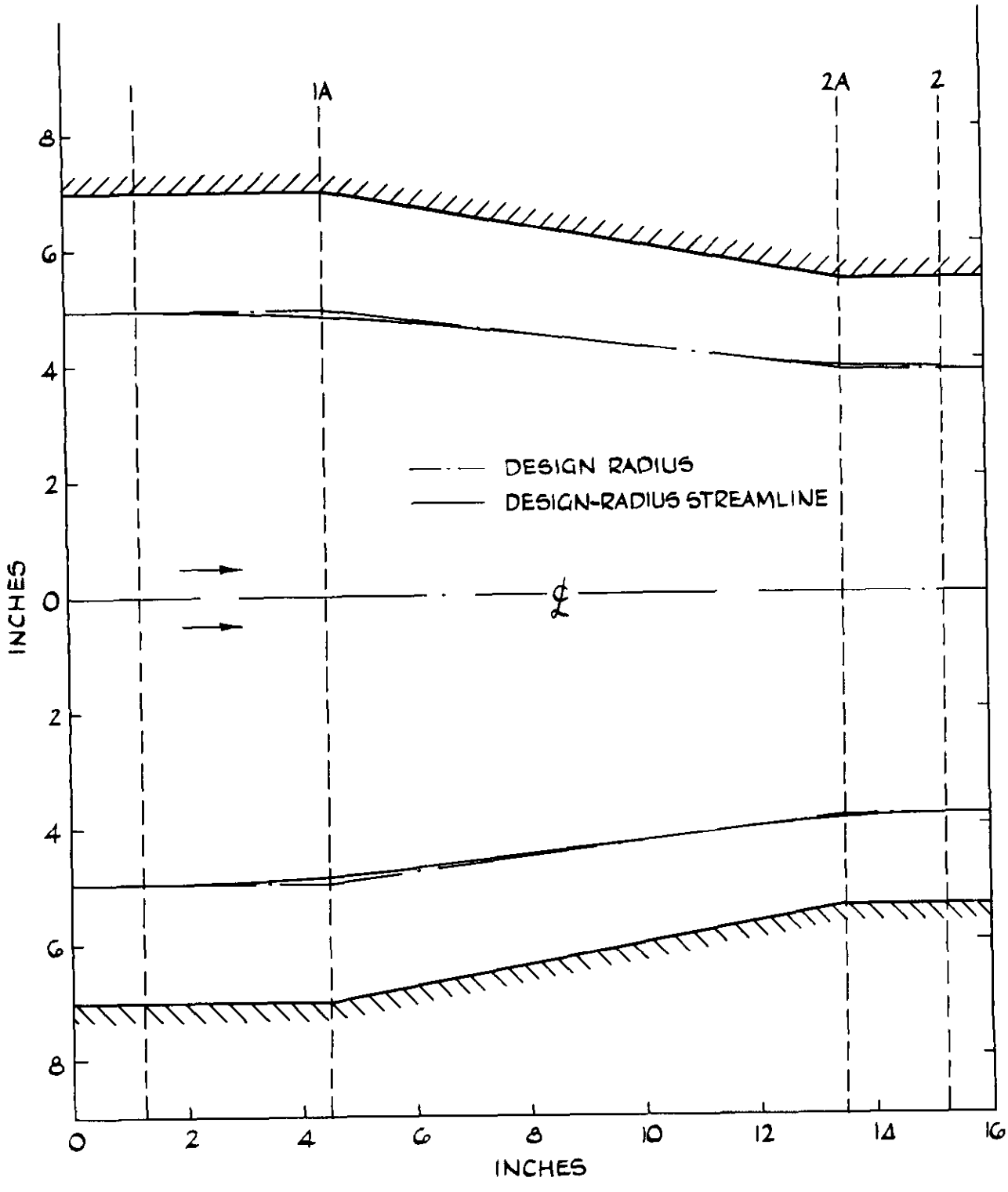

FIG 25 LEWIS FLOW IN CONICAL DUCTS

TEST No 1. DUCT CONFIGURATION

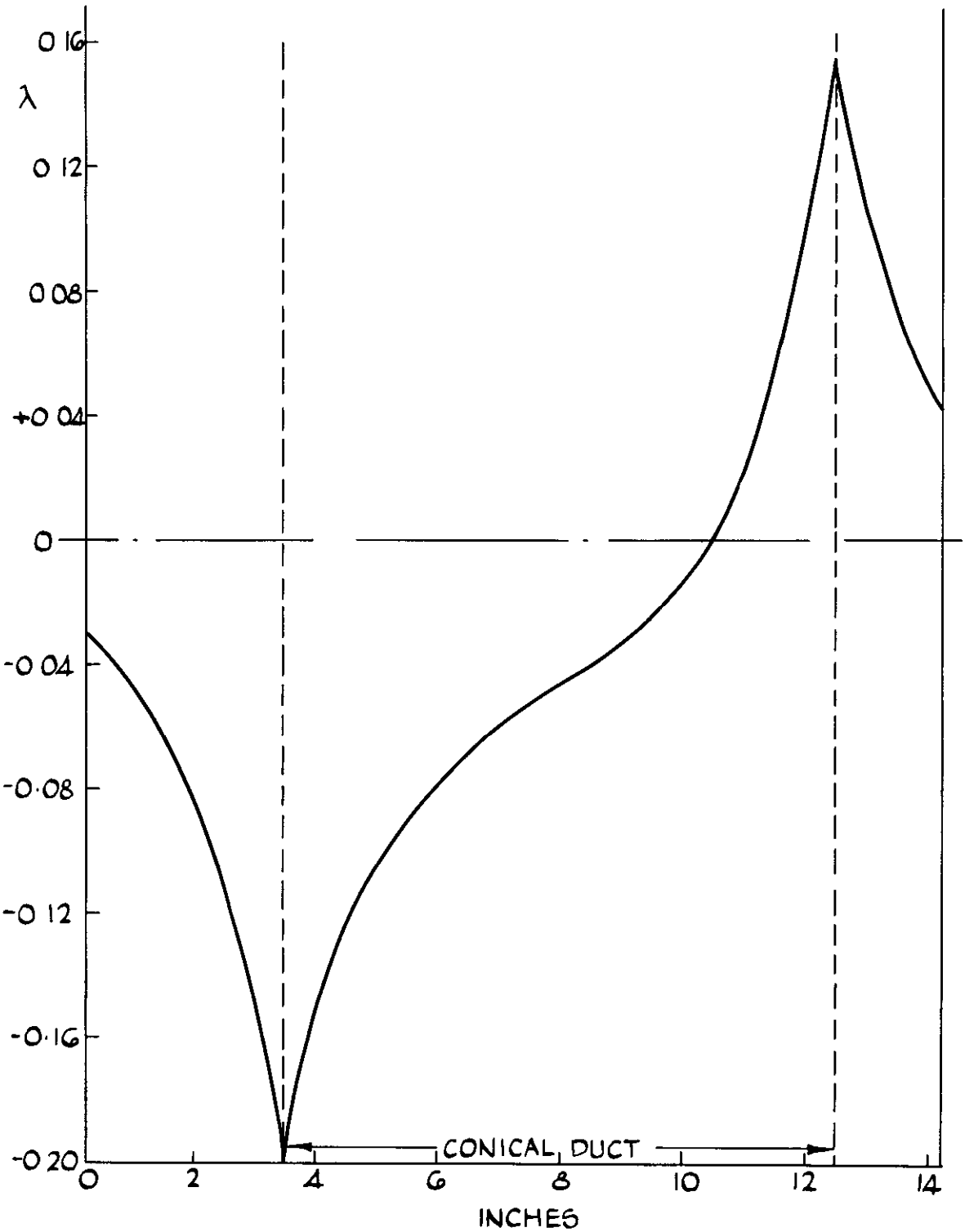

FIG. 26 LEWIS. FLOW IN CONICAL DUCTS
TEST No 1. VARIATION OF λ

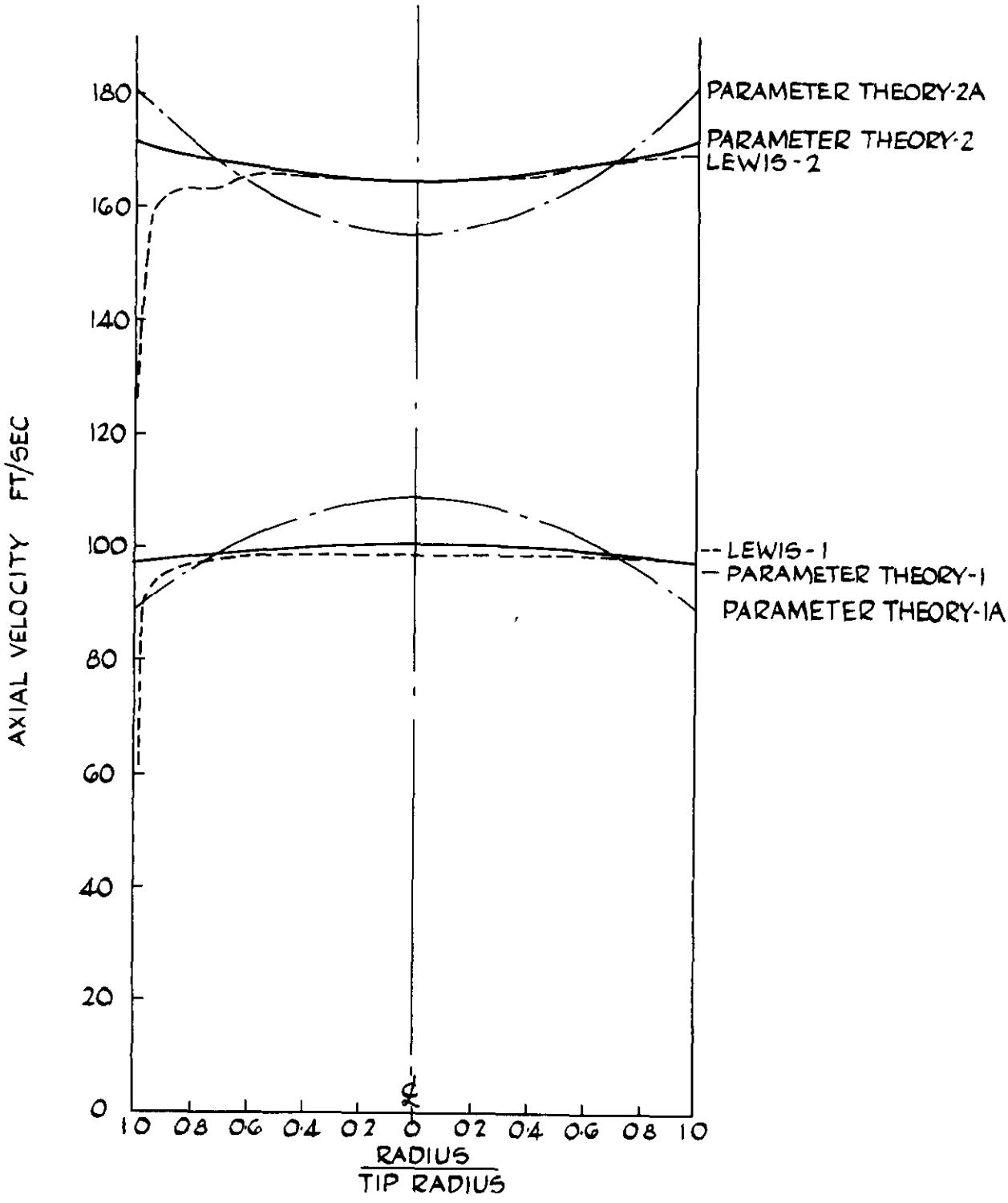

FIG 27. LEWIS. FLOW IN CONICAL DUCTS
TEST No 1 AXIAL-VELOCITY PROFILES

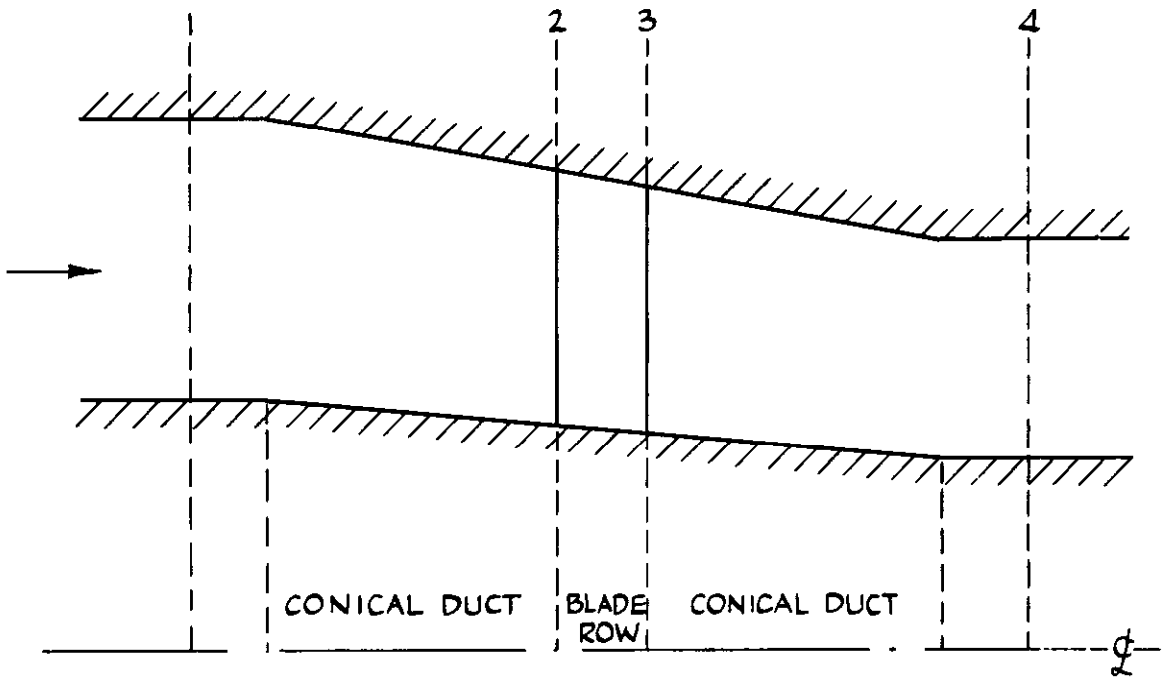

FIG 28 (a). CONVERGING DUCT TESTS 2 AND 3

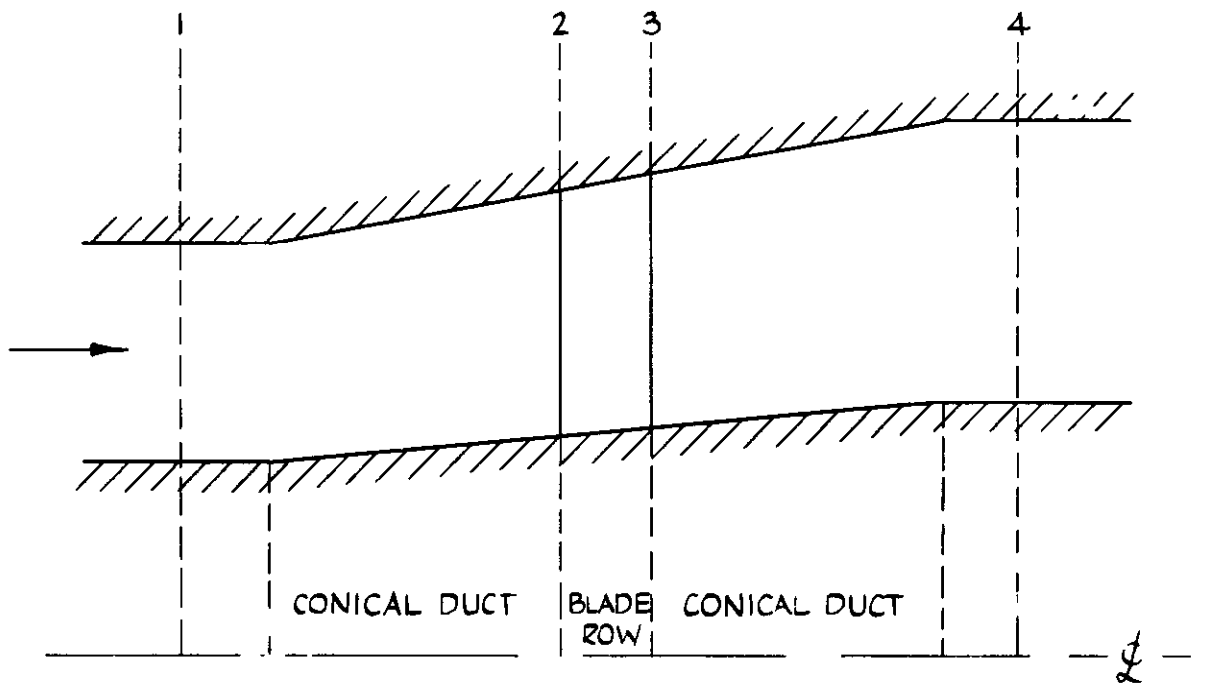

FIG 28 (b). DIVERG NG DUCT TESTS 4 AND 5

LEWIS FLOW N CON CAL DUCTS

DUCT CONFIGJRATIONS FOR TESTS 2, 3, 4 AND 5

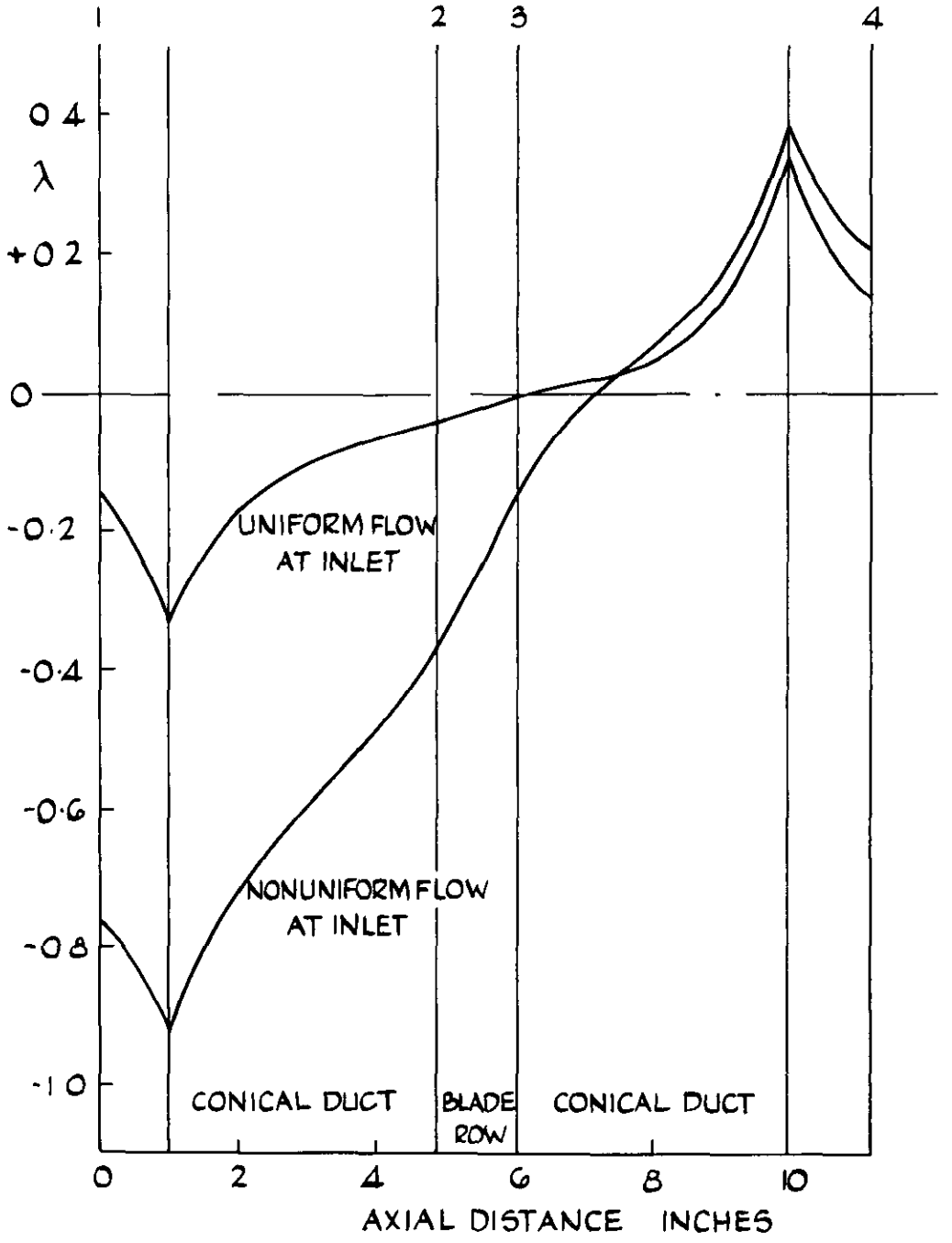

FIG. 29. LEWIS. FLOW IN A CONVERGING DUCT
VARIATION OF λ IN TEST Nos. 2 AND 3

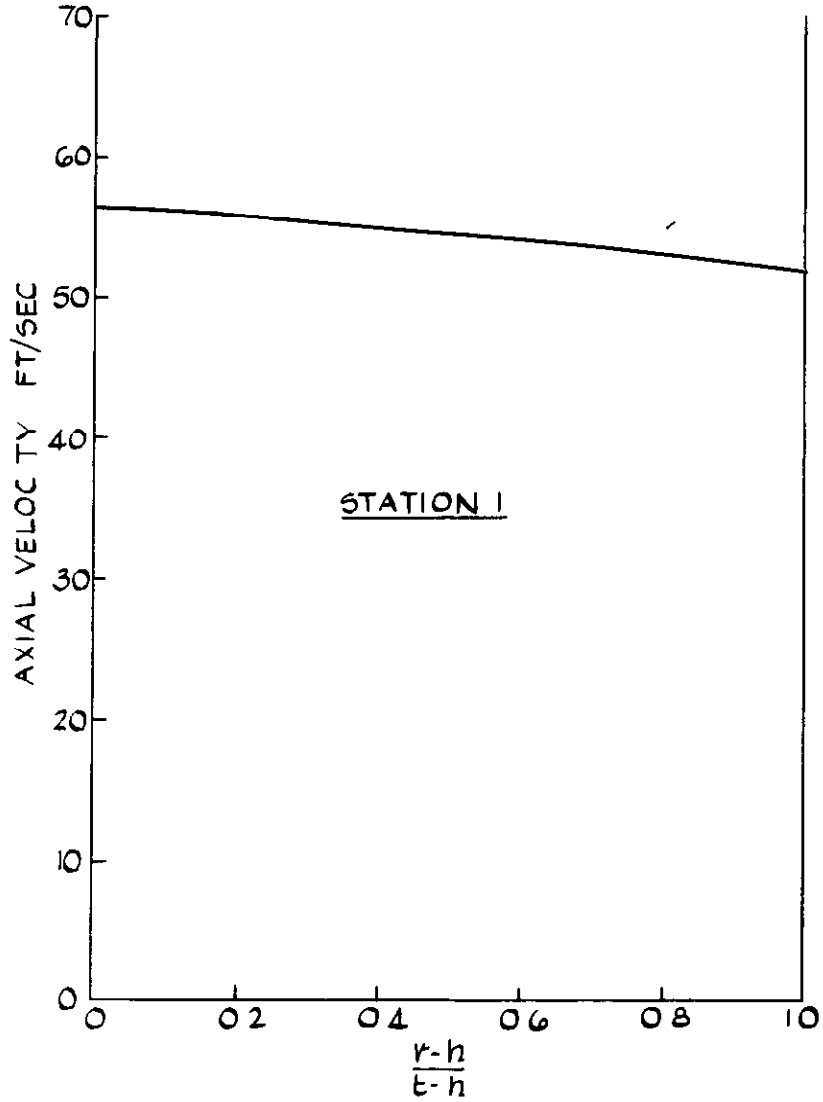

FIG 30

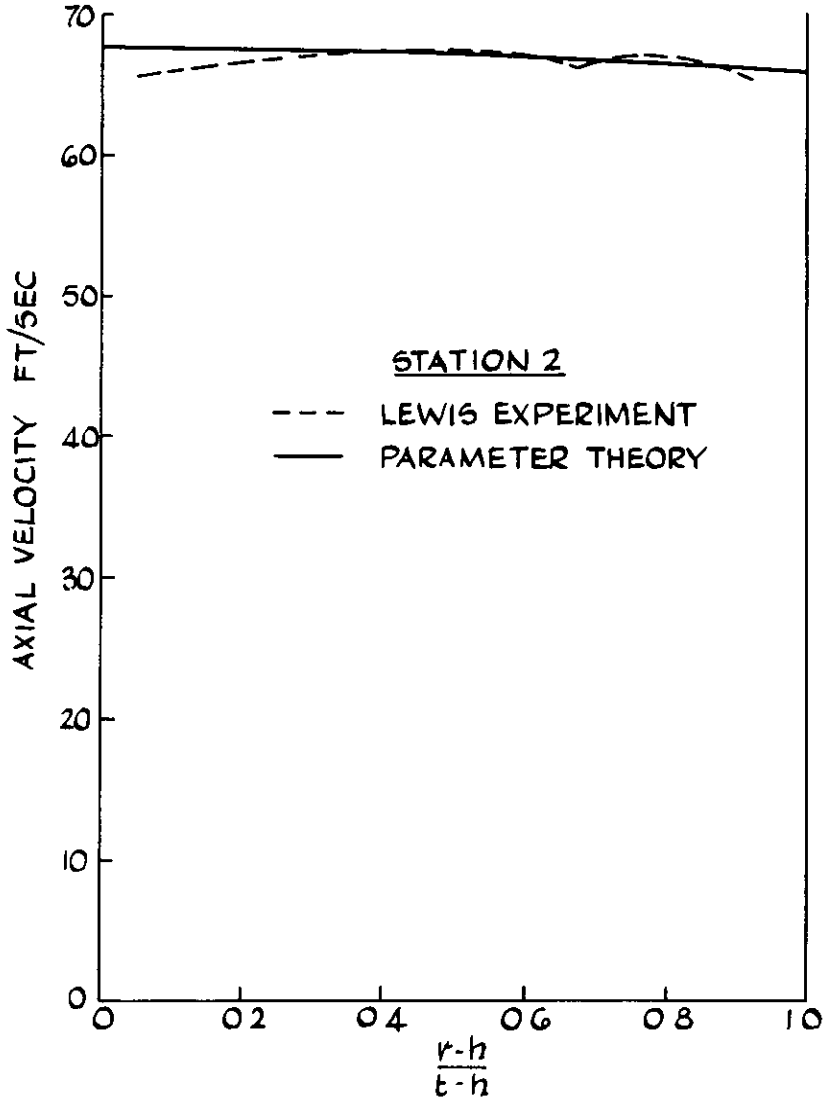

FIG 31

LEWIS FLOW IN A CONVERGING DUCT. AXIAL-VELOCITY PROFILES
TEST No 2 UNIFORM FLOW AT INLET

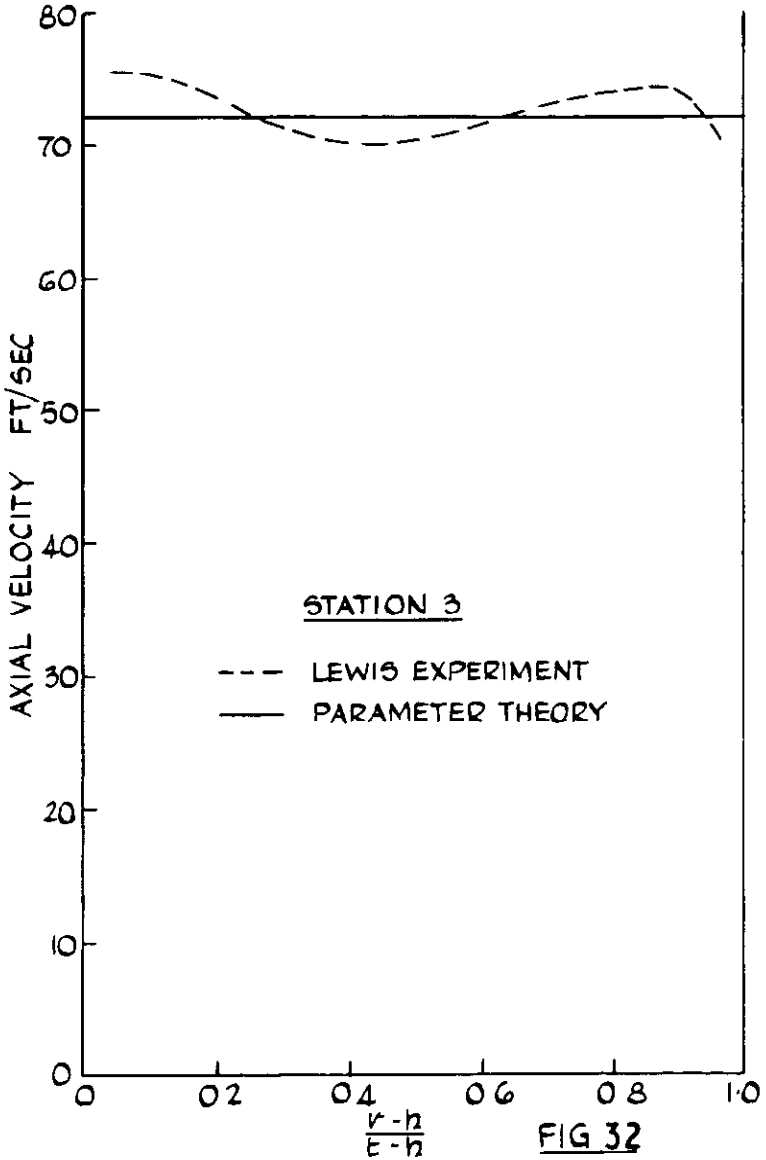

FIG 32

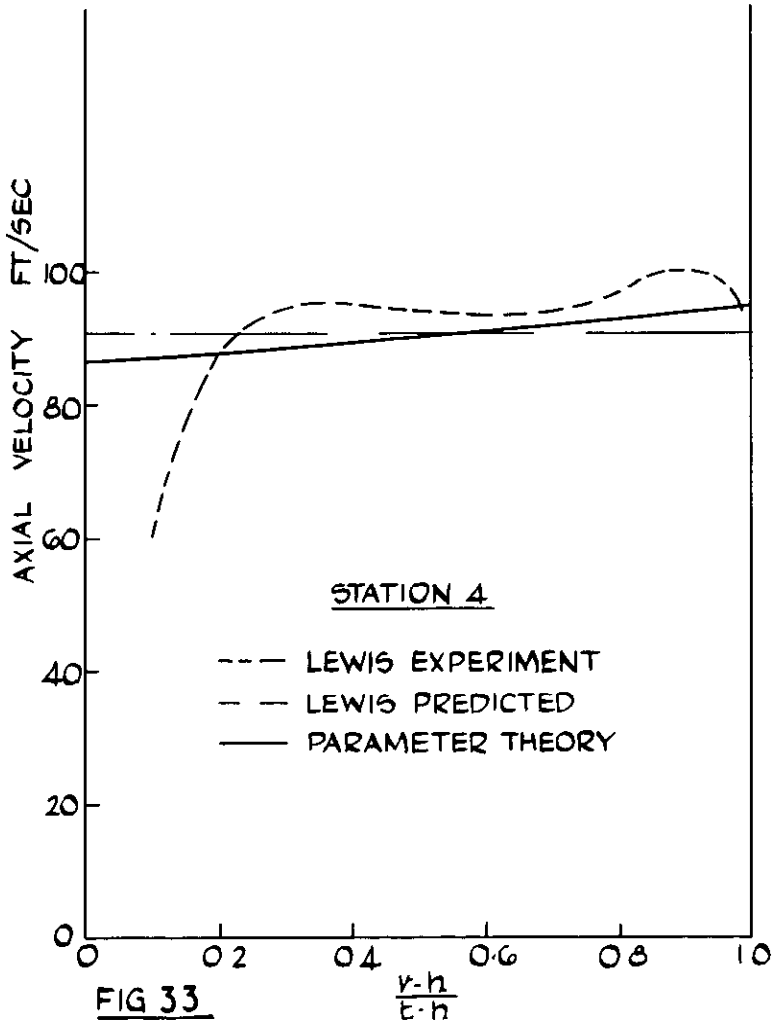

FIG 33

LEWIS FLOW IN A CONVERGING DUCT AXIAL-VELOCITY PROFILES
TEST No 2. UNIFORM FLOW AT INLET

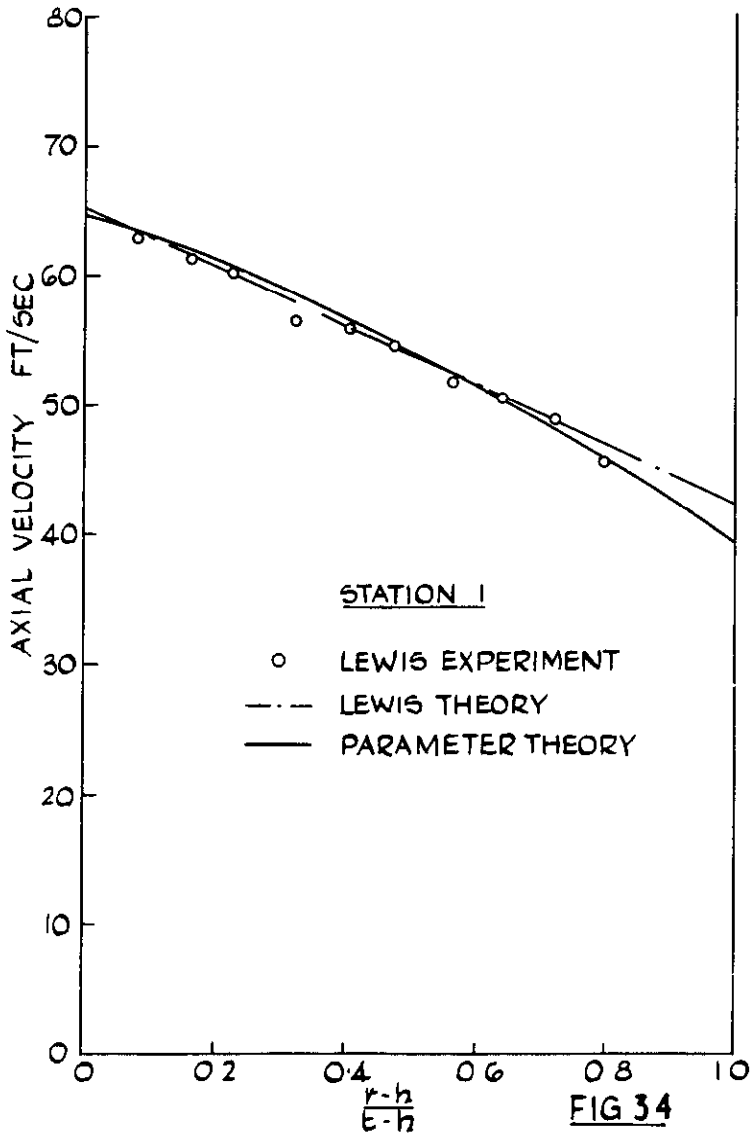

FIG 34

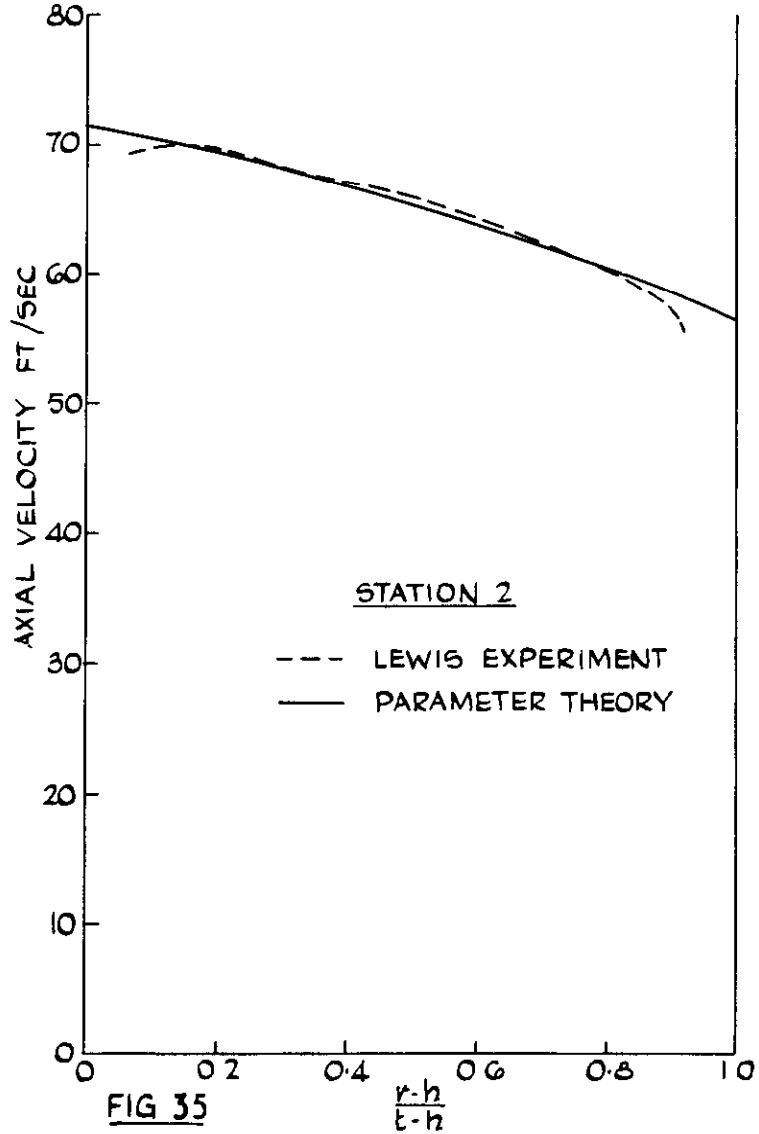

FIG 35

LEWIS FLOW IN A CONVERGING DUCT AXIAL-VELOCITY PROFILES

TEST No 3 NON-UNIFORM FLOW AT INLET

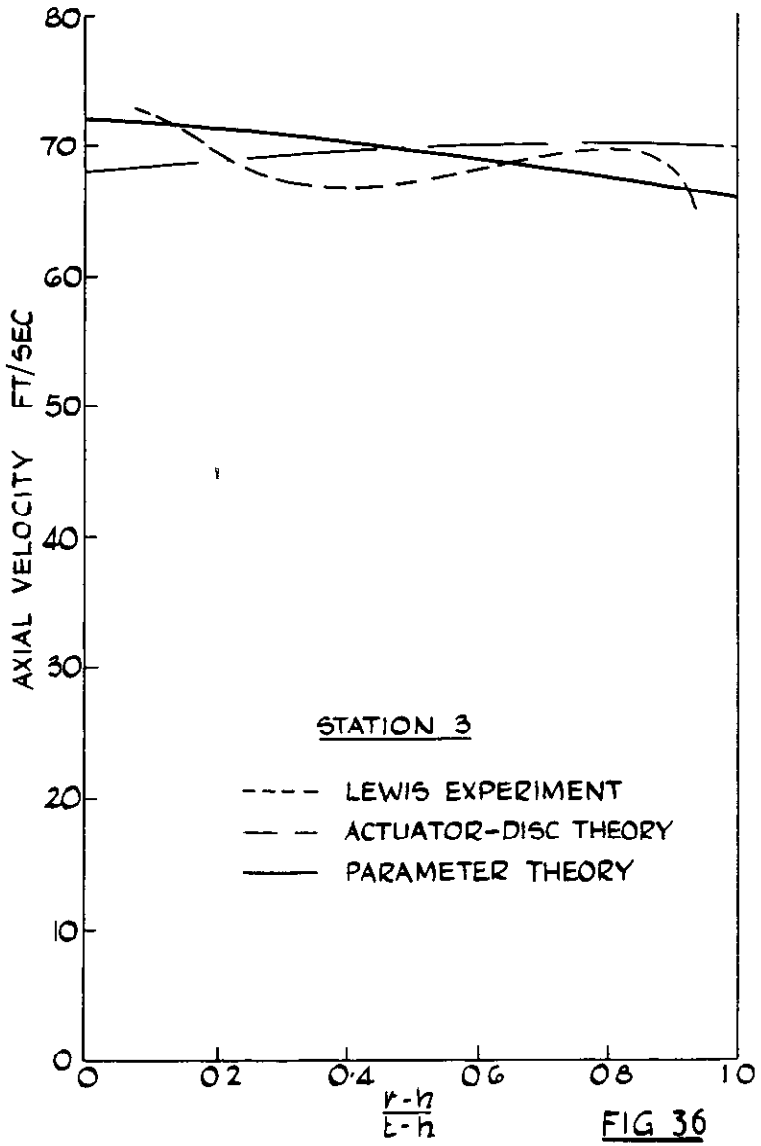

FIG 36

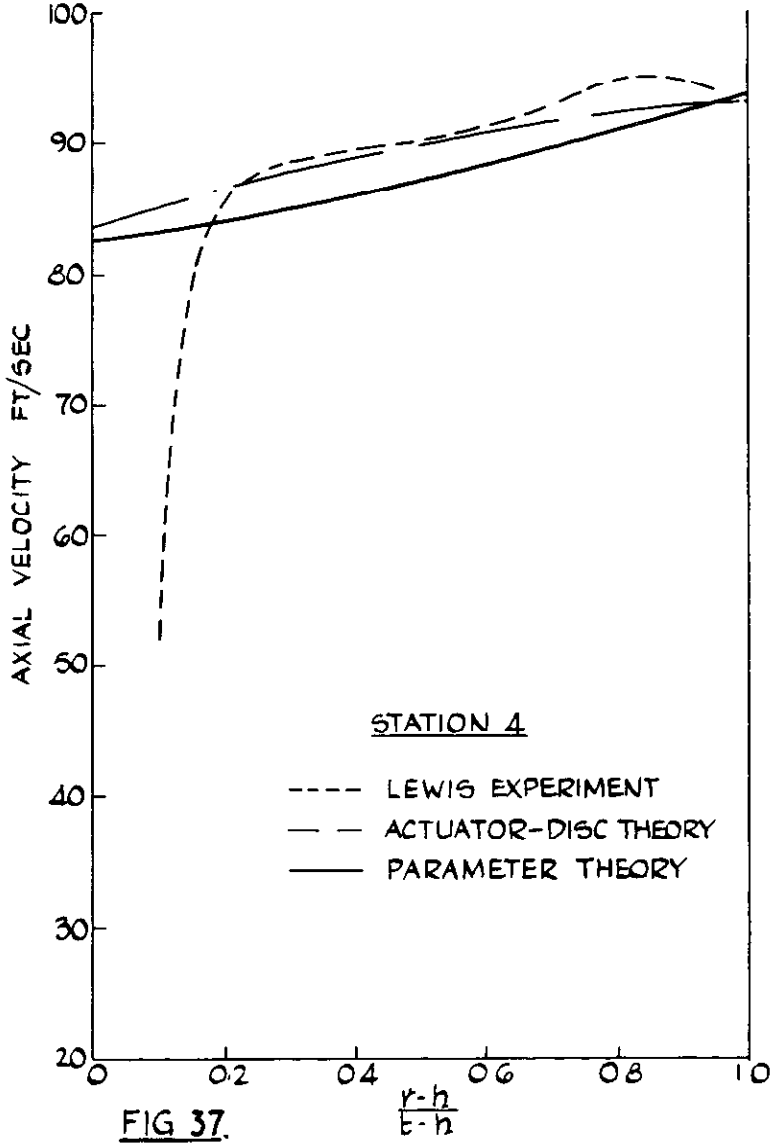

FIG 37.

LEWIS. FLOW IN A CONVERGING DUCT AXIAL-VELOCITY PROFILES

TEST No 3 NON-UNIFORM FLOW AT INLET

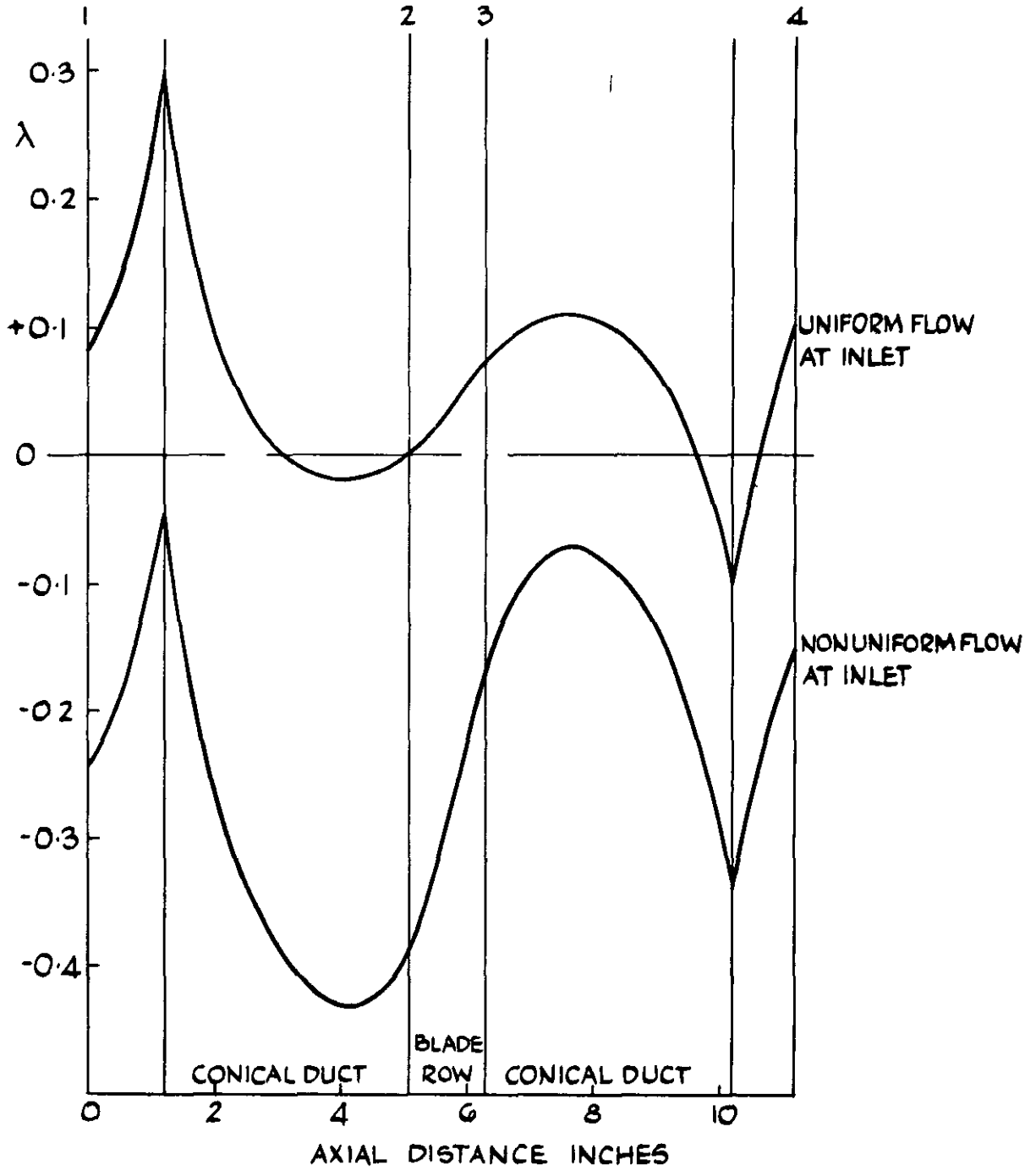

FIG. 38. LEWIS. FLOW IN A DIVERGING DUCT

VARIATION OF λ IN TEST Nos. 4 AND 5

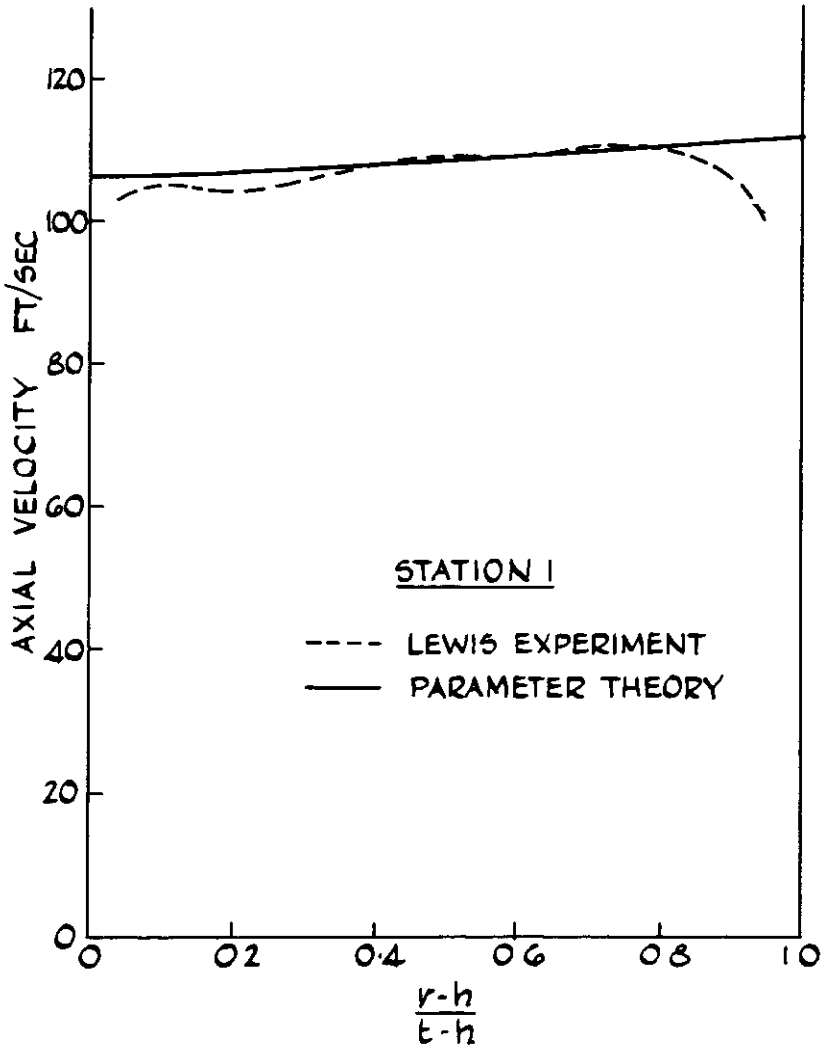

FIG 39

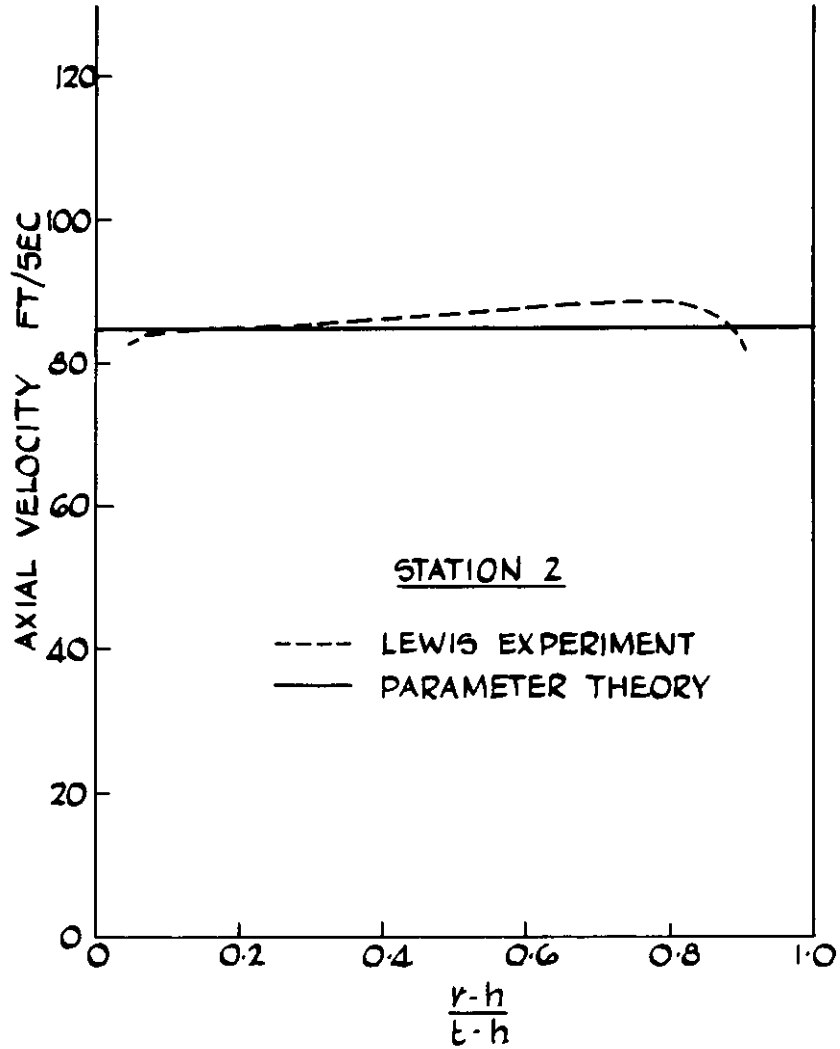

FIG.40.

LEWIS. FLOW IN A DIVERGING DUCT. AXIAL-VELOCITY PROFILES

TEST No.4. UNIFORM FLOW AT INLET

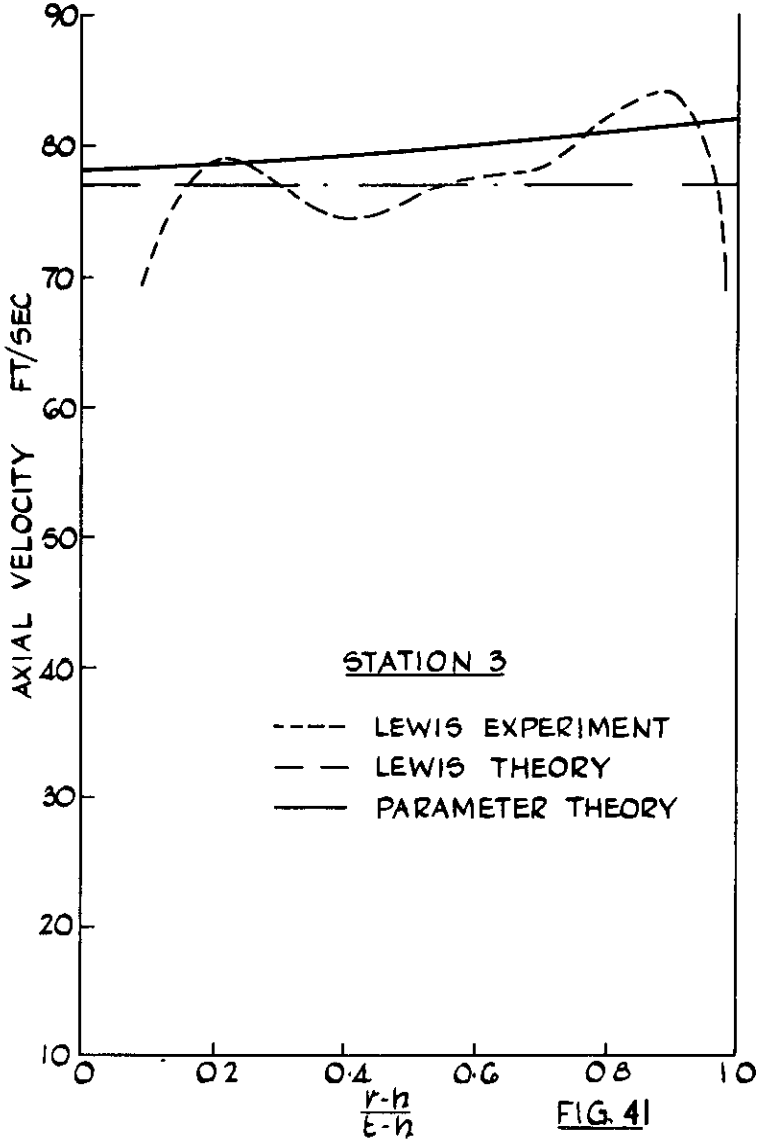

FIG. 41

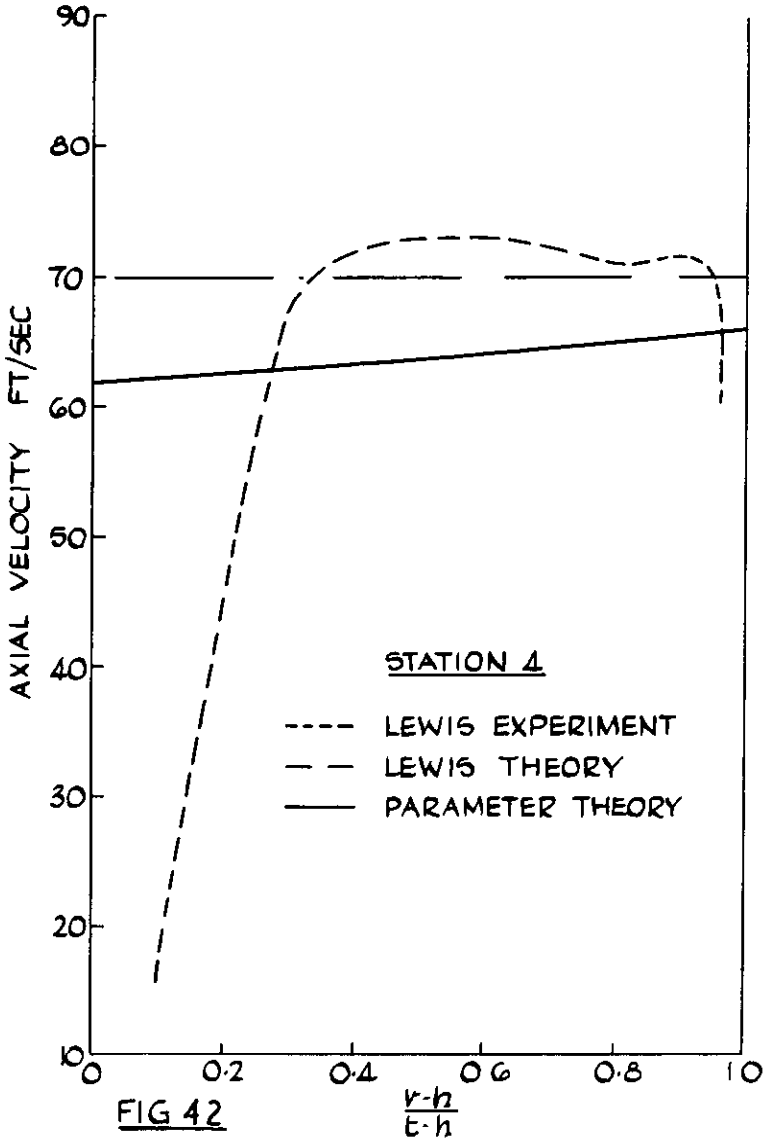

FIG 42

LEWIS. FLOW IN A DIVERGING DUCT AXIAL-VELOCITY PROFILES
TEST No 4 UNIFORM FLOW AT INLET

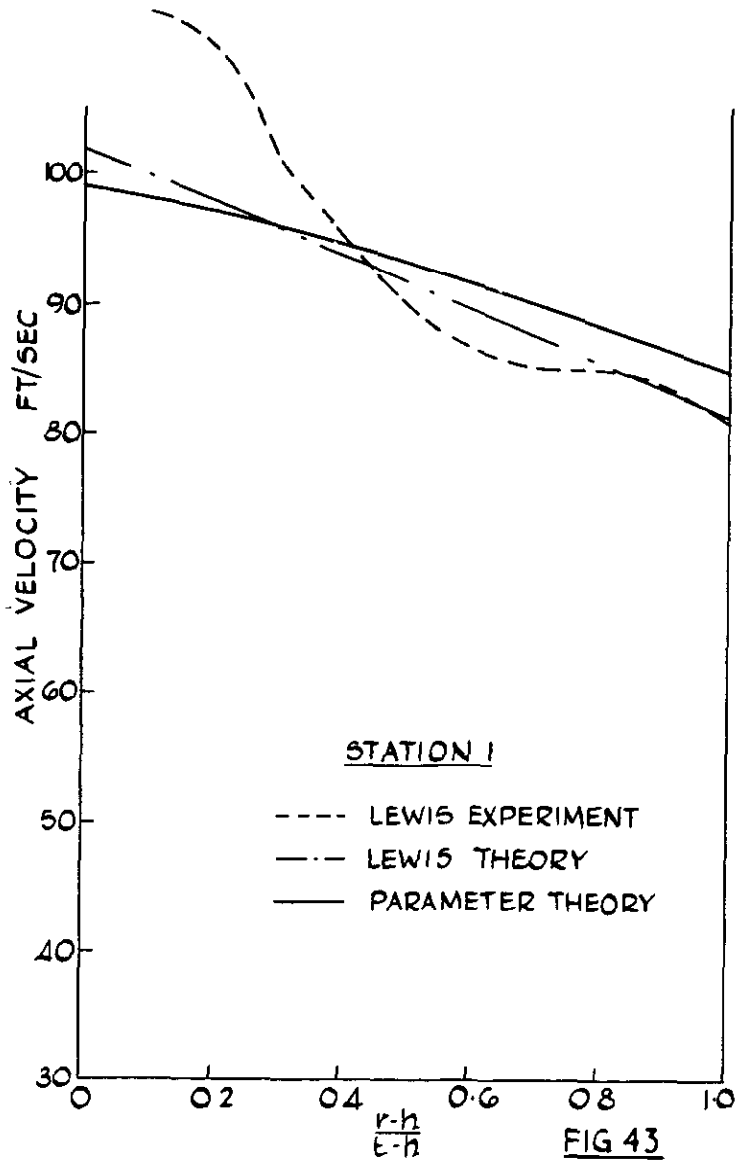

FIG 43

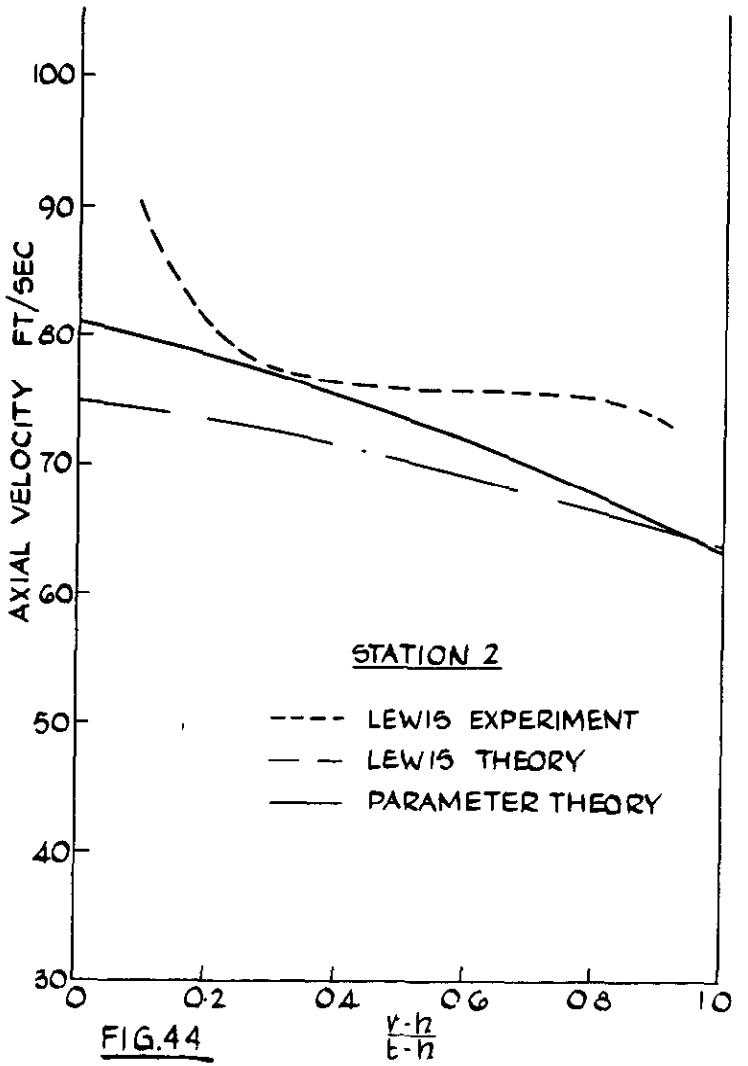

FIG.44

LEWIS FLOW IN A DIVERGING DUCT. AXIAL-VELOCITY PROFILES
TEST No 5 NON-UNIFORM FLOW AT INLET

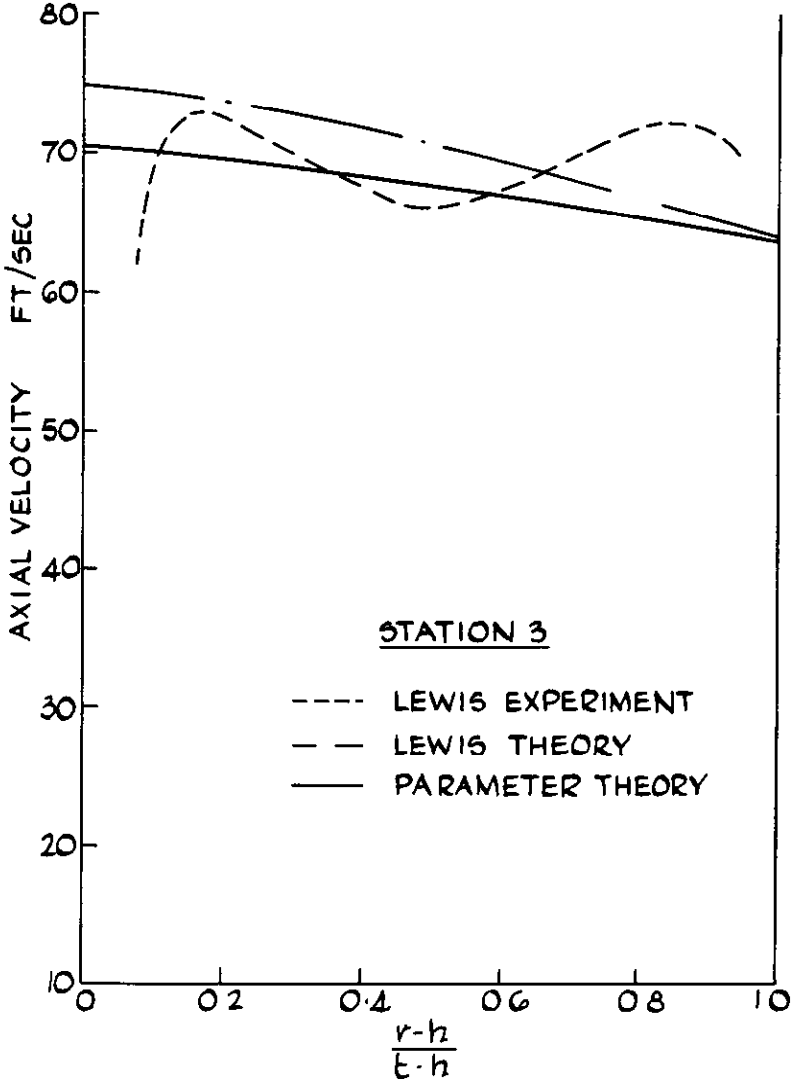

FIG 45

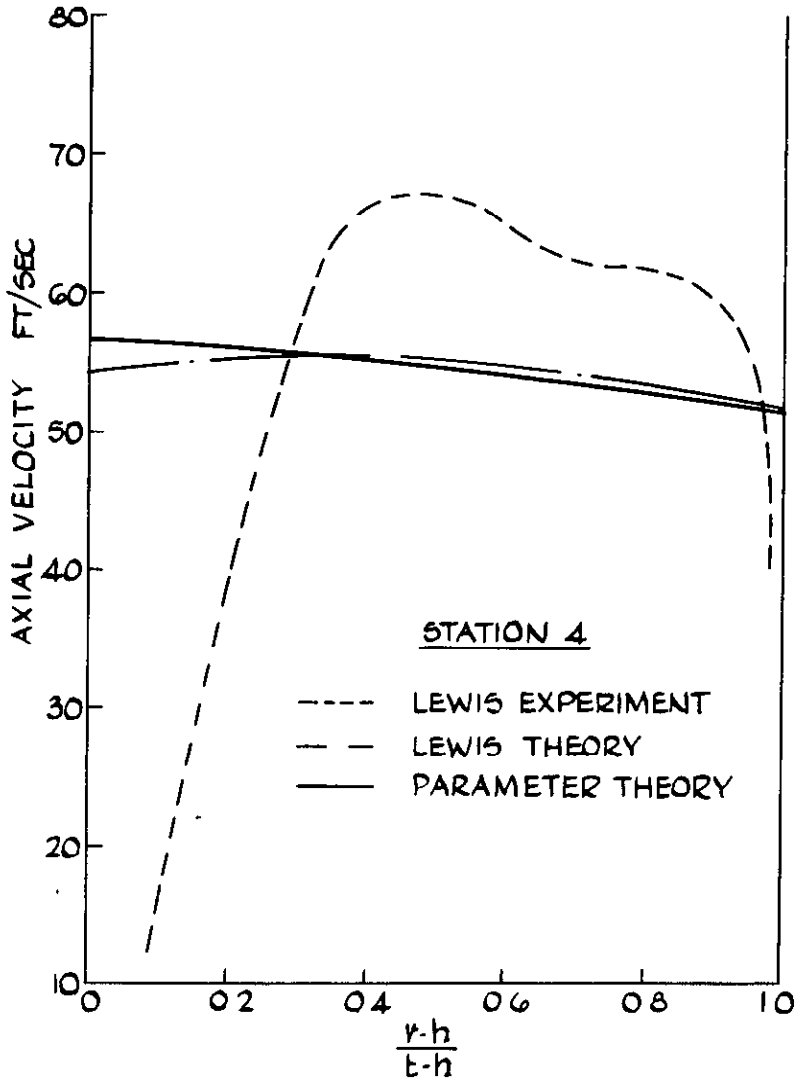

FIG. 46

LEWIS. FLOW IN A DIVERGING DUCT. AXIAL-VELOCITY PROFILES

TEST No 5. NON-UNIFORM FLOW AT INLET

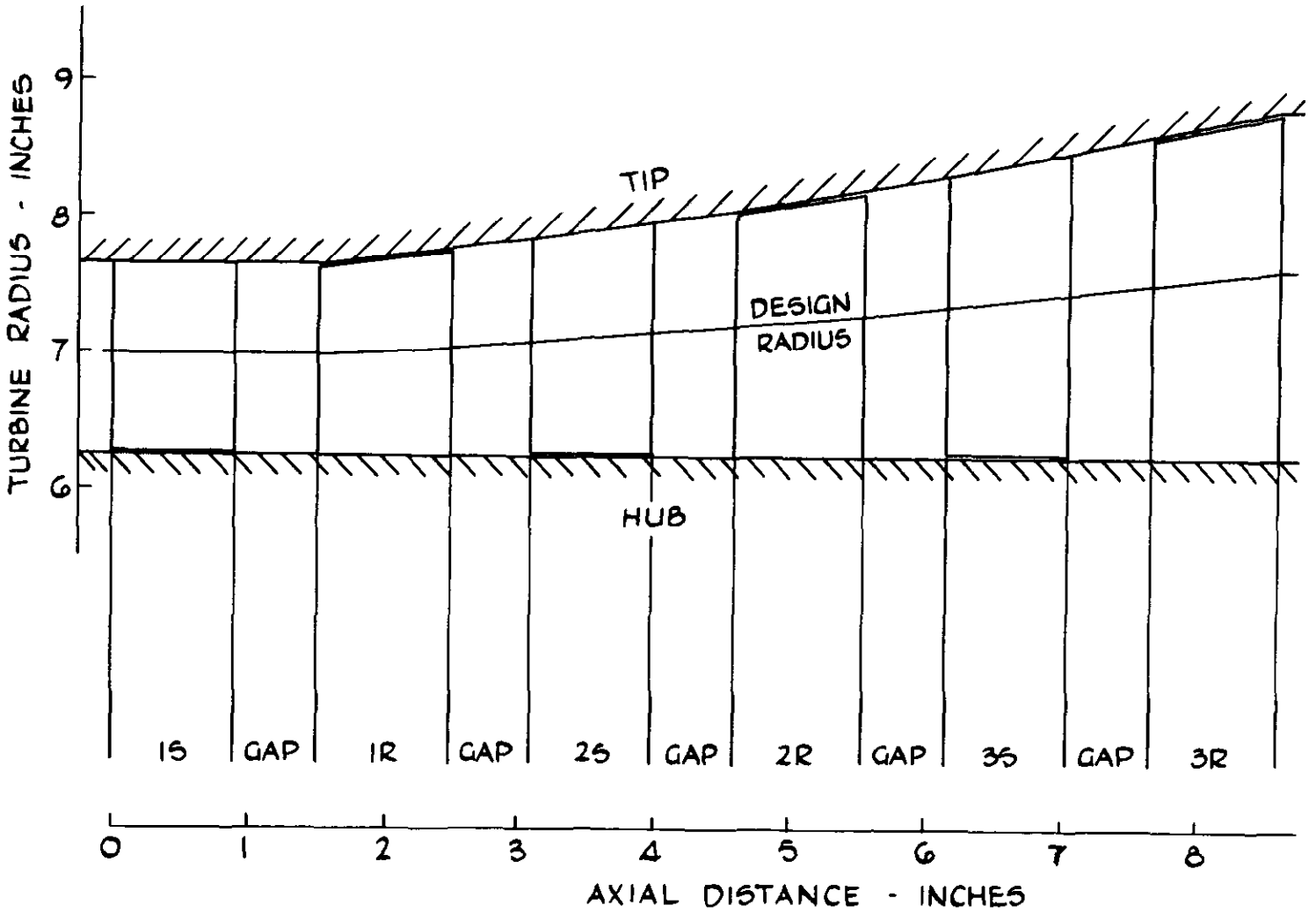

FIG.47 JOHNSTON AND SANSOME EXPERIMENTAL THREE-STAGE TURBINE TURBINE CONFIGURATION

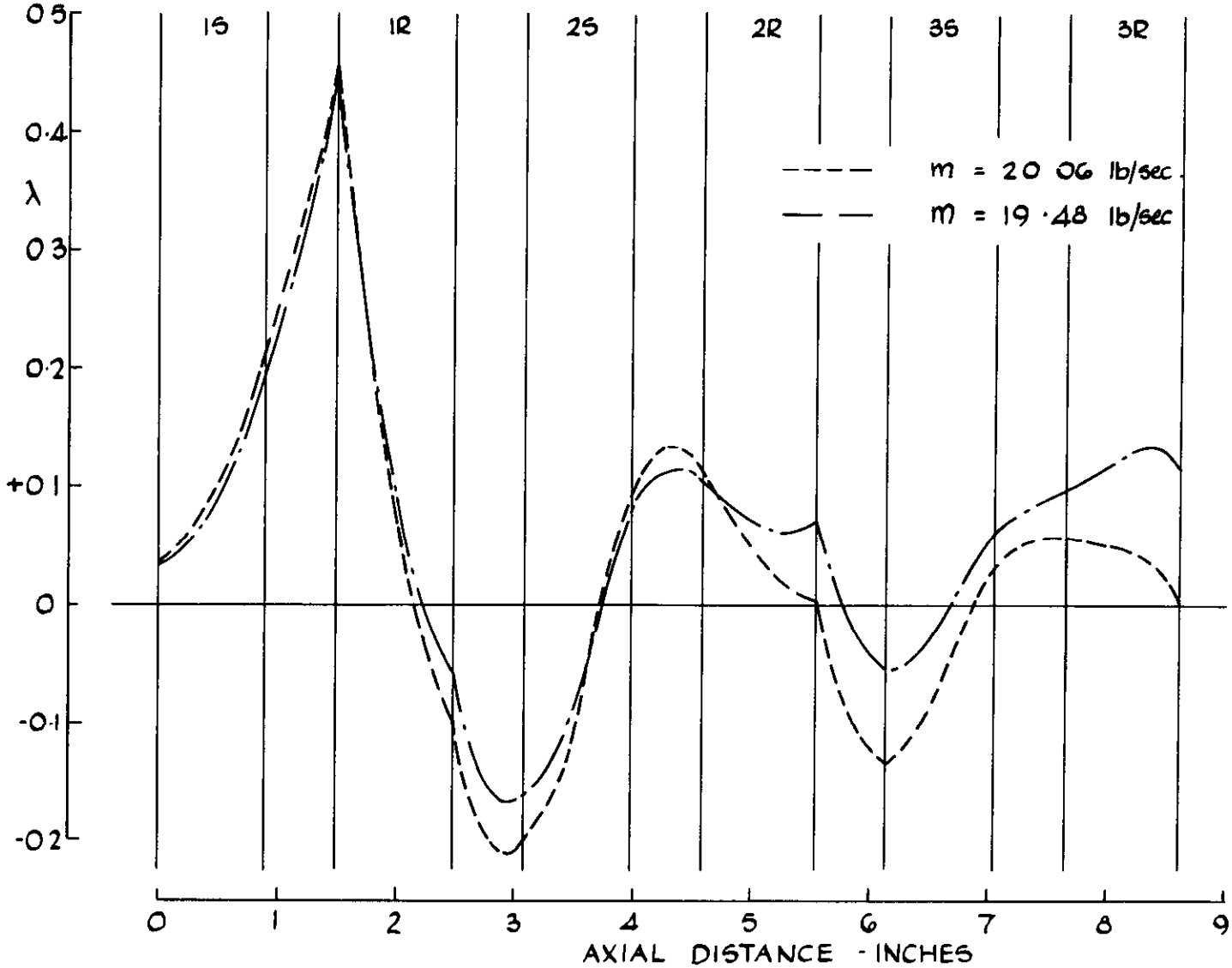

FIG 48 JOHNSTON AND SANSOME EXPERIMENTAL THREE-STAGE TURBINE

VARIATION OF λ

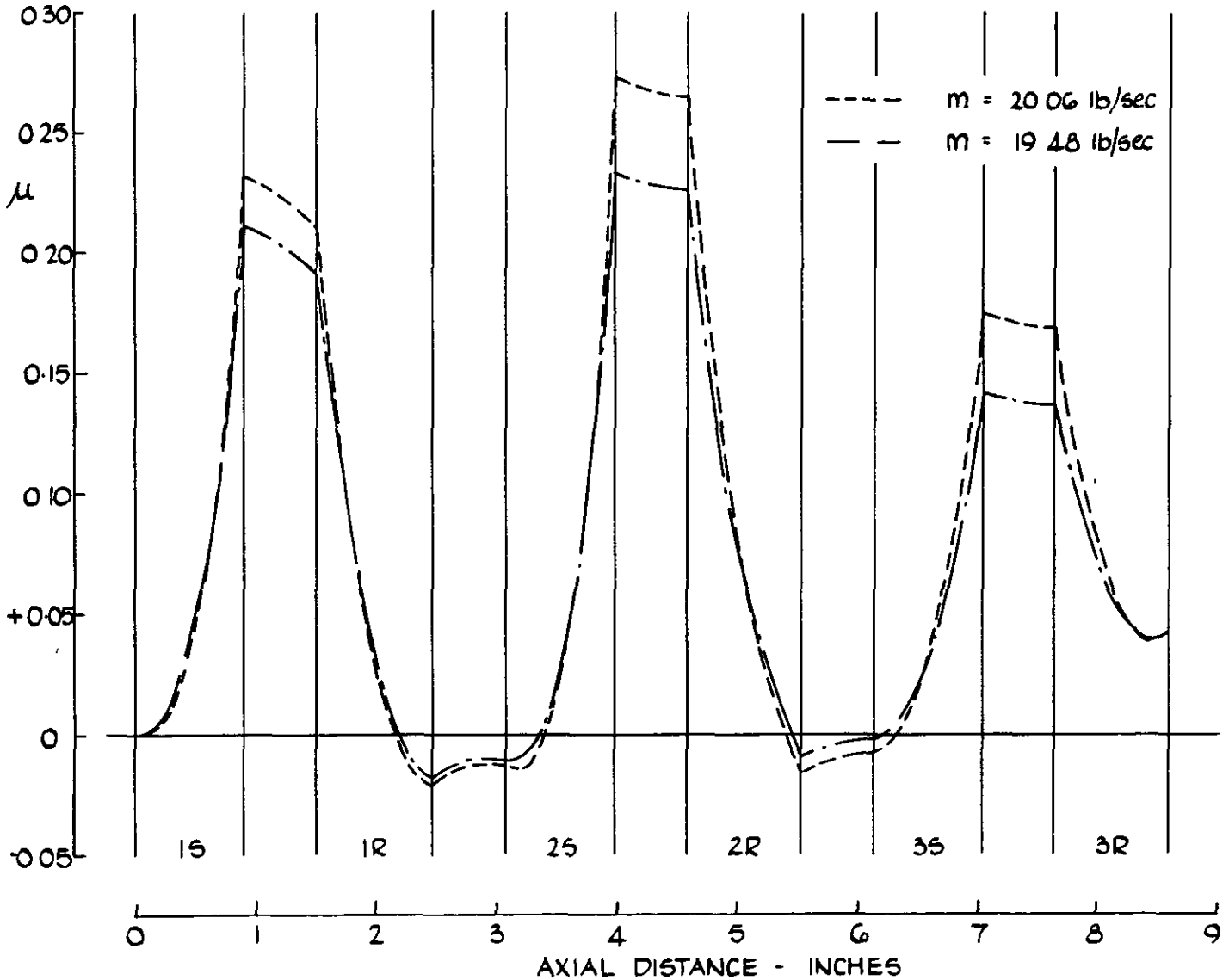

FIG. 49 JOHNSTON AND SANSOME EXPERIMENTAL THREE-STAGE TURBINE VARIATION OF μ

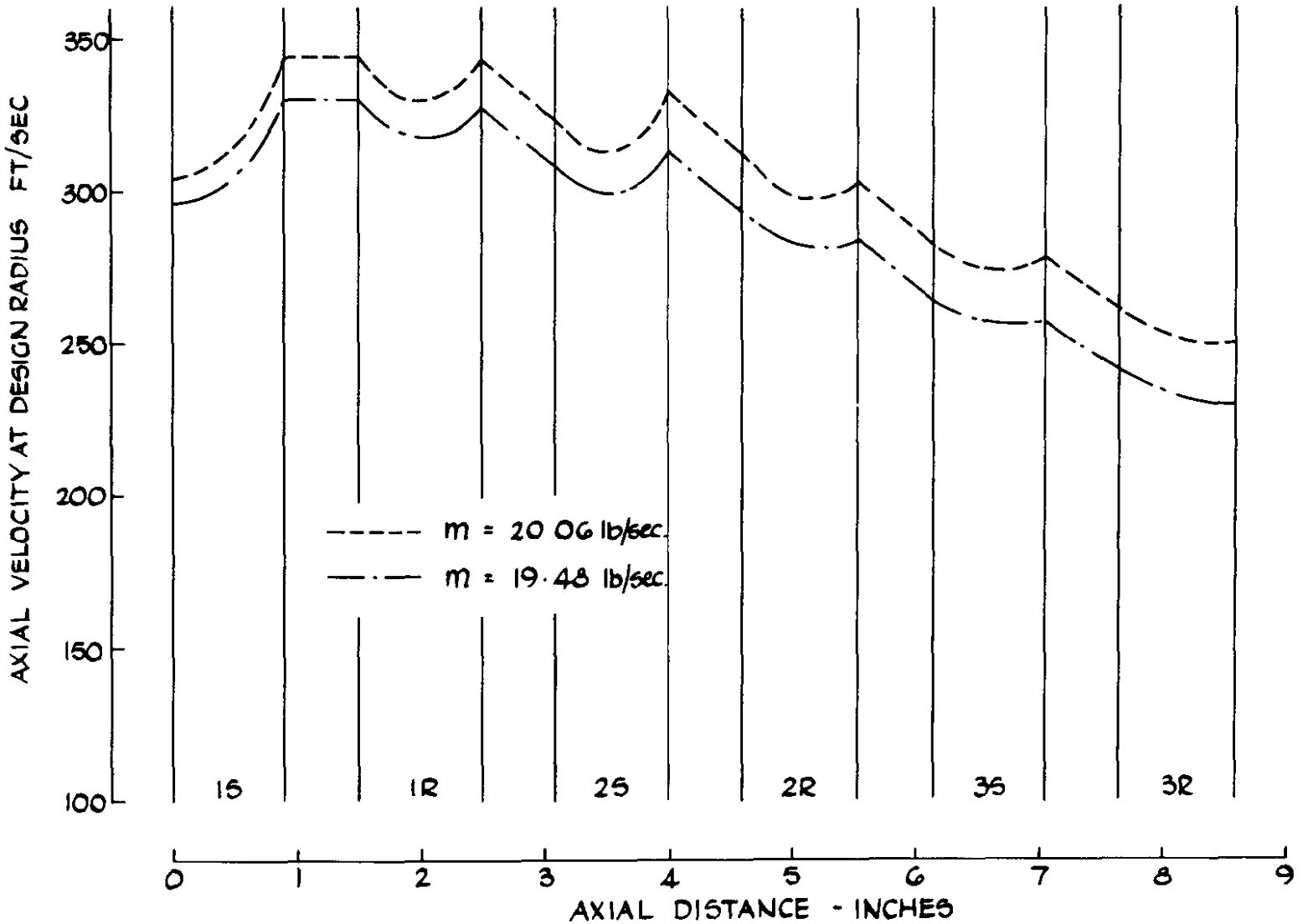

FIG. 50. JOHNSTON AND SANSOME EXPERIMENTAL THREE-STAGE TURBINE VARIATION OF AXIAL VELOCITY AT THE DESIGN RADIUS

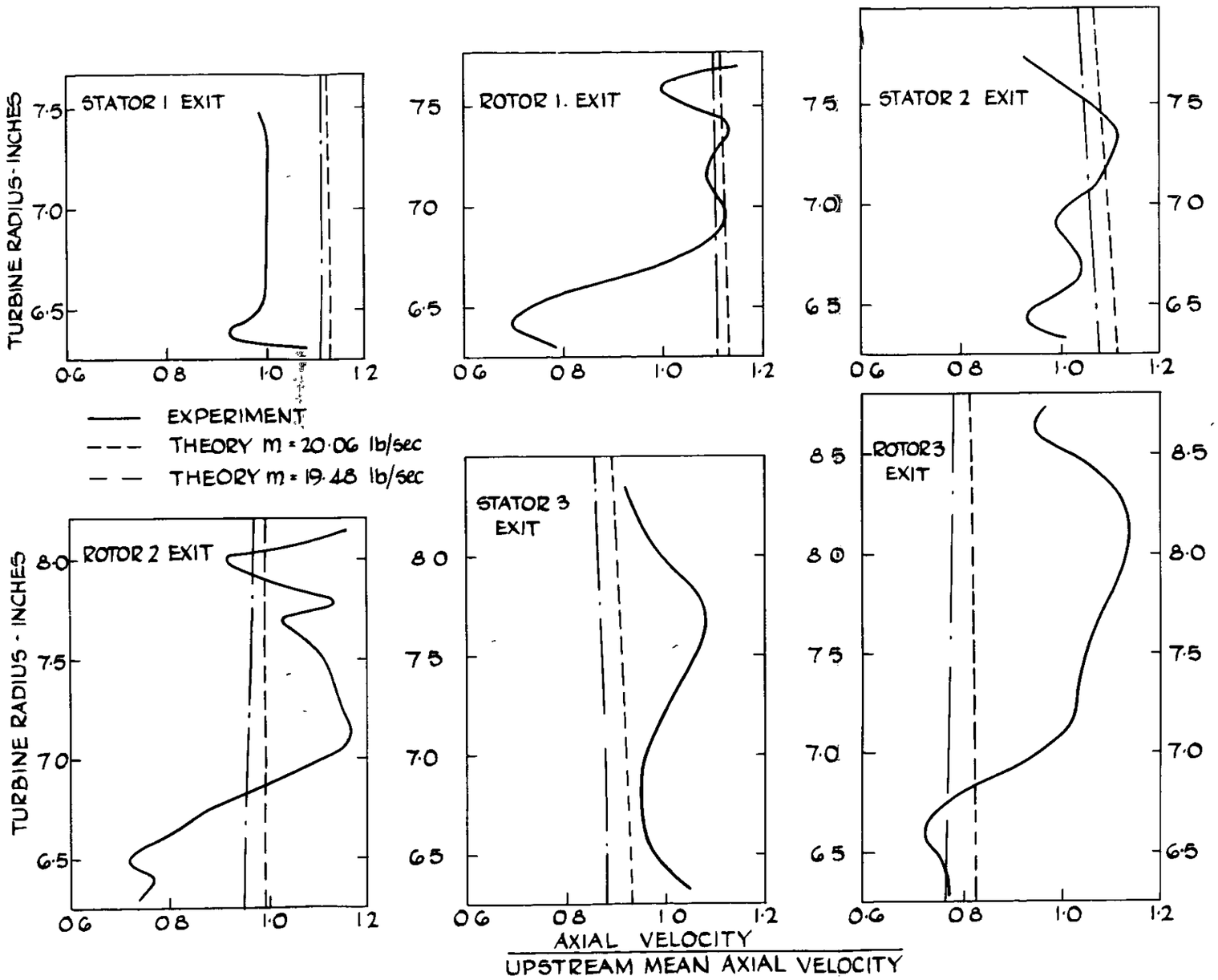

FIG. 51. JOHNSTON AND SANSOME EXPERIMENTAL THREE-STAGE TURBINE AXIAL-VELOCITY PROFILES

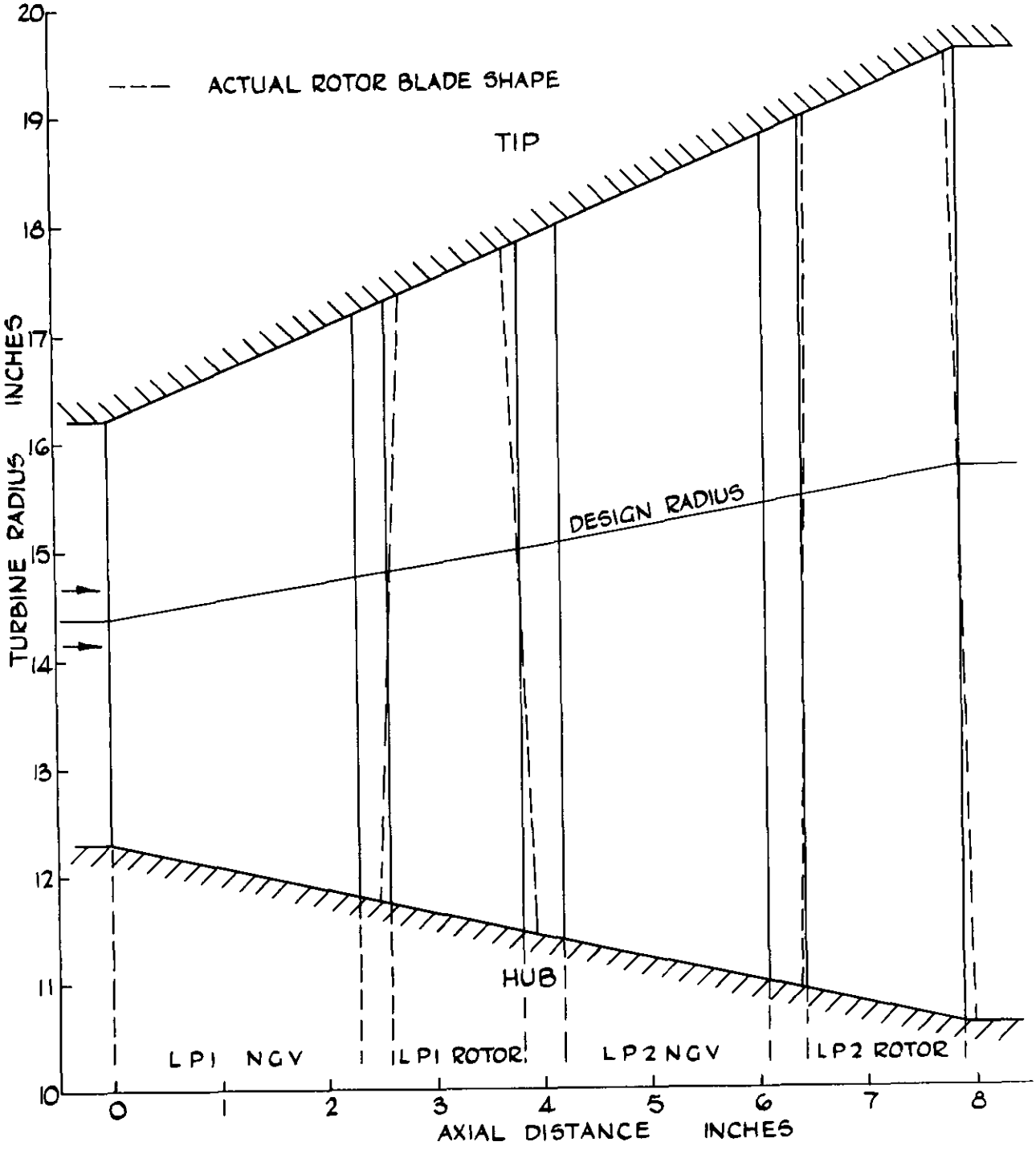

FIG.52. ROLLS-ROYCE TWO-STAGE TURBINE TURBINE CONFIGURATION

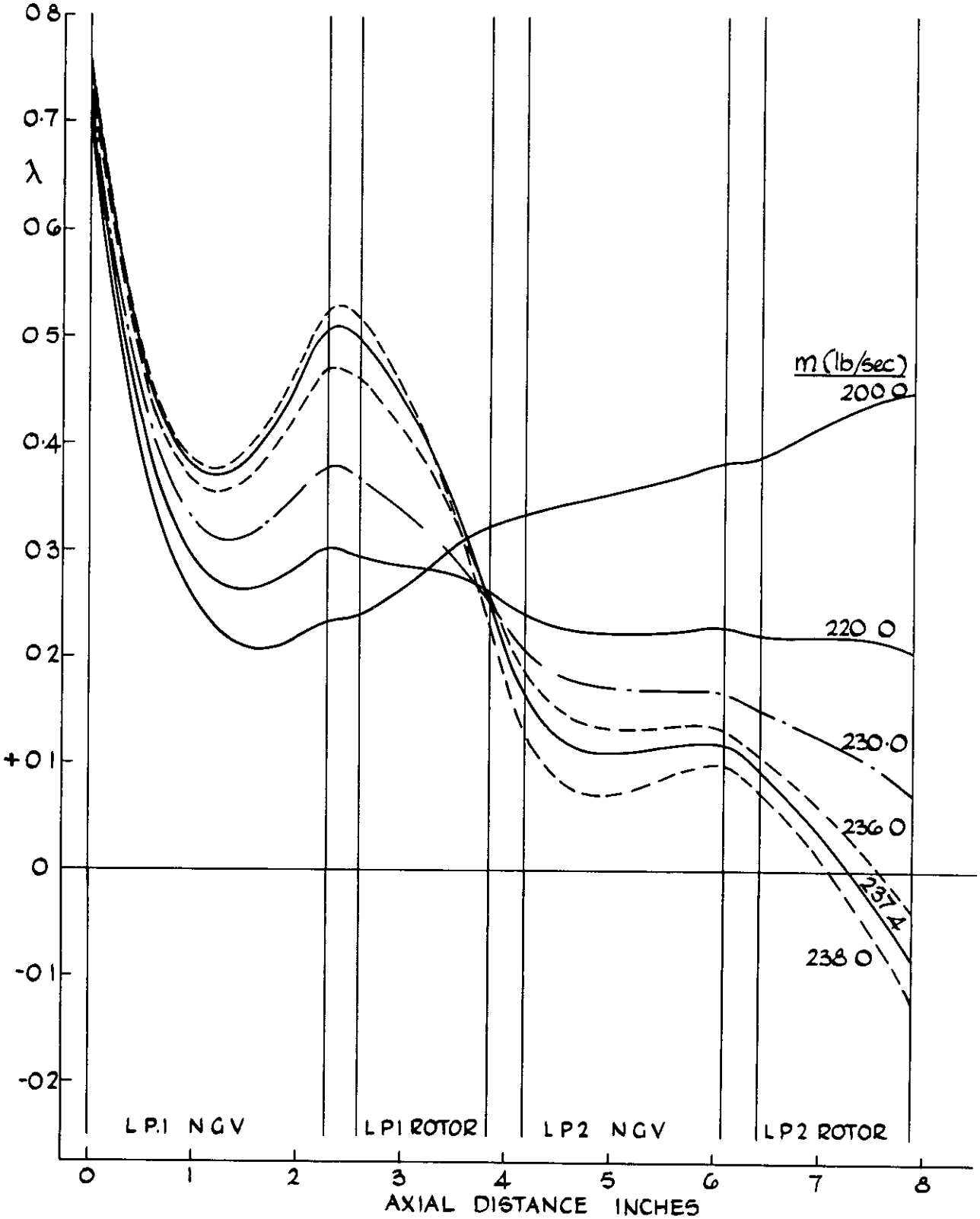

FIG.53. ROLLS-ROYCE TWO-STAGE TURBINE
VARIATION OF λ FOR VARIOUS MASS-FLOW RATES

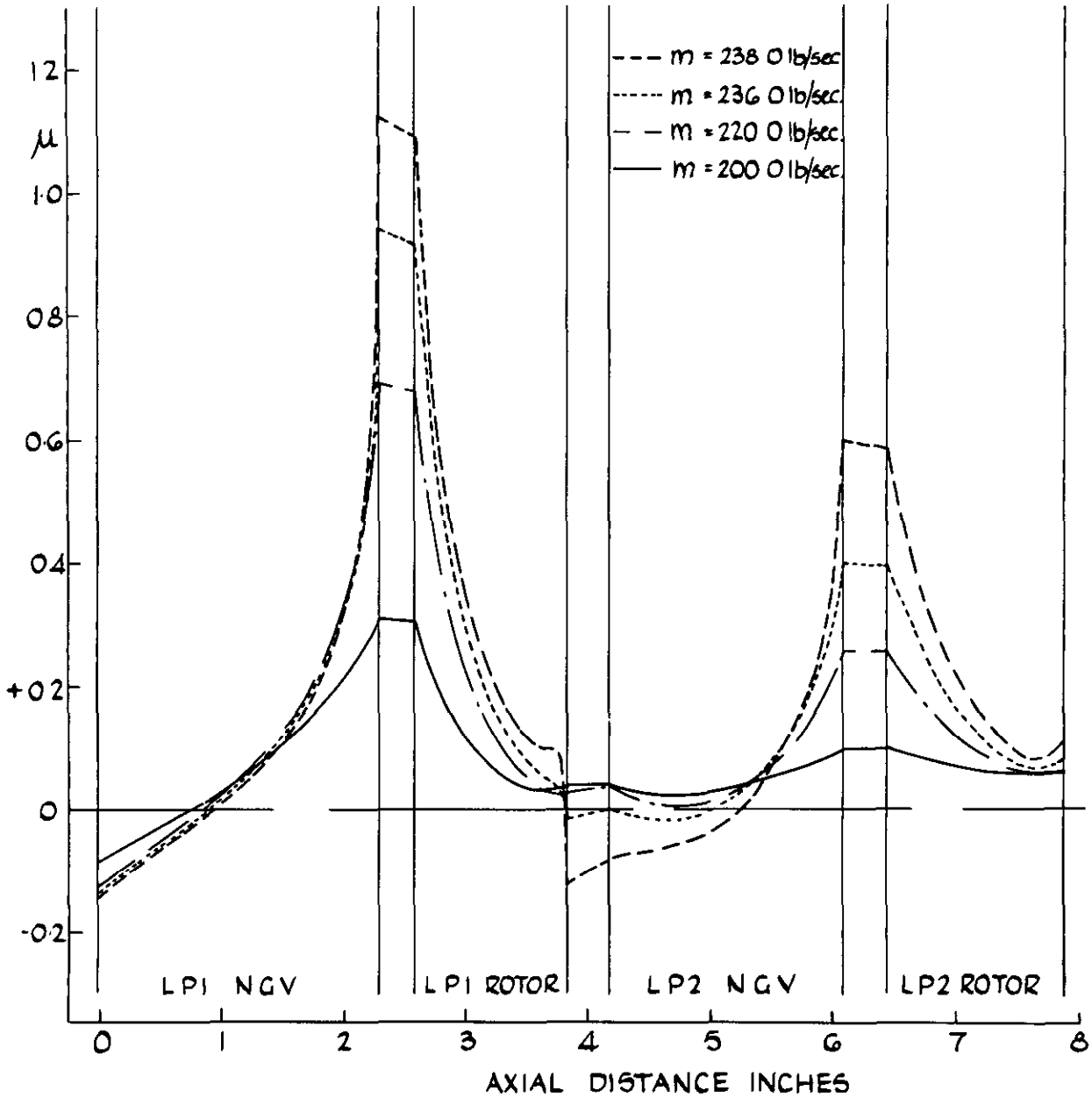

FIG.54. ROLLS-ROYCE TWO-STAGE TURBINE

VARIATION OF μ FOR VARIOUS MASS-FLOW RATES

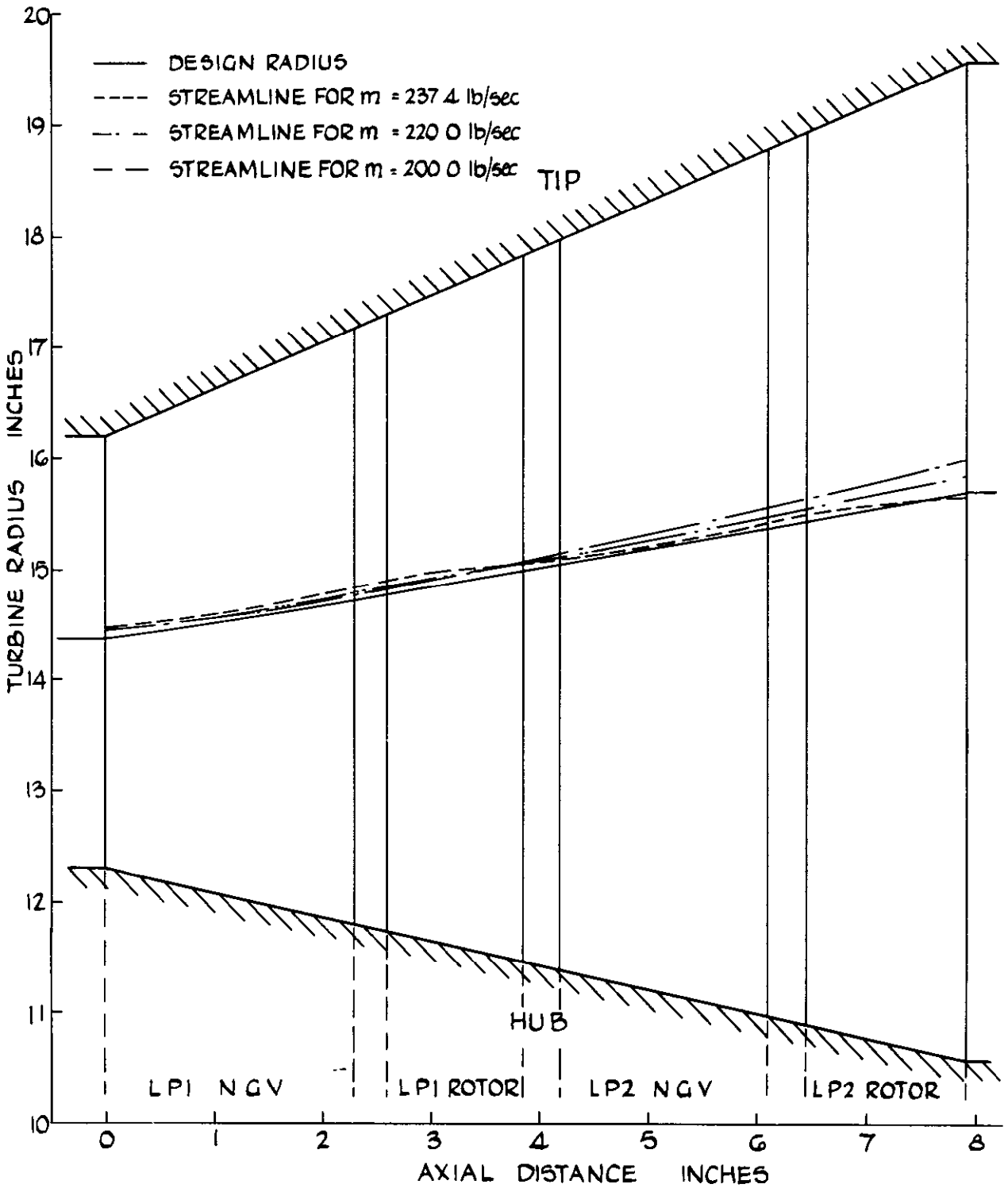

FIG 55 ROLLS-ROYCE TWO-STAGE TURBINE

DISPLACEMENT OF DESIGN-RADIUS STREAMLINE

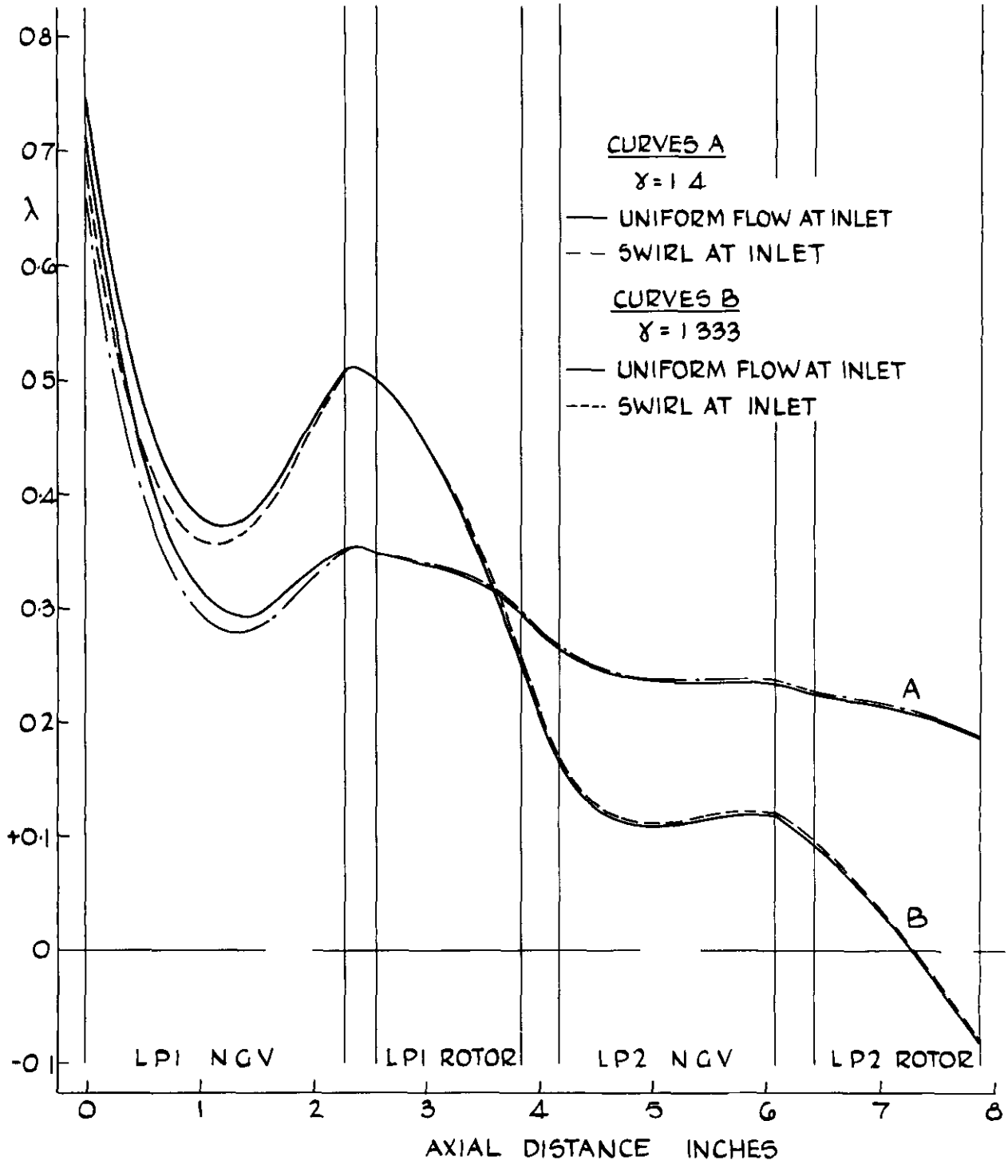

FIG 56 ROLLS-ROYCE TWO-STAGE TURBINE

VARIATION OF λ FOR VARIOUS FLOW CONDITIONS

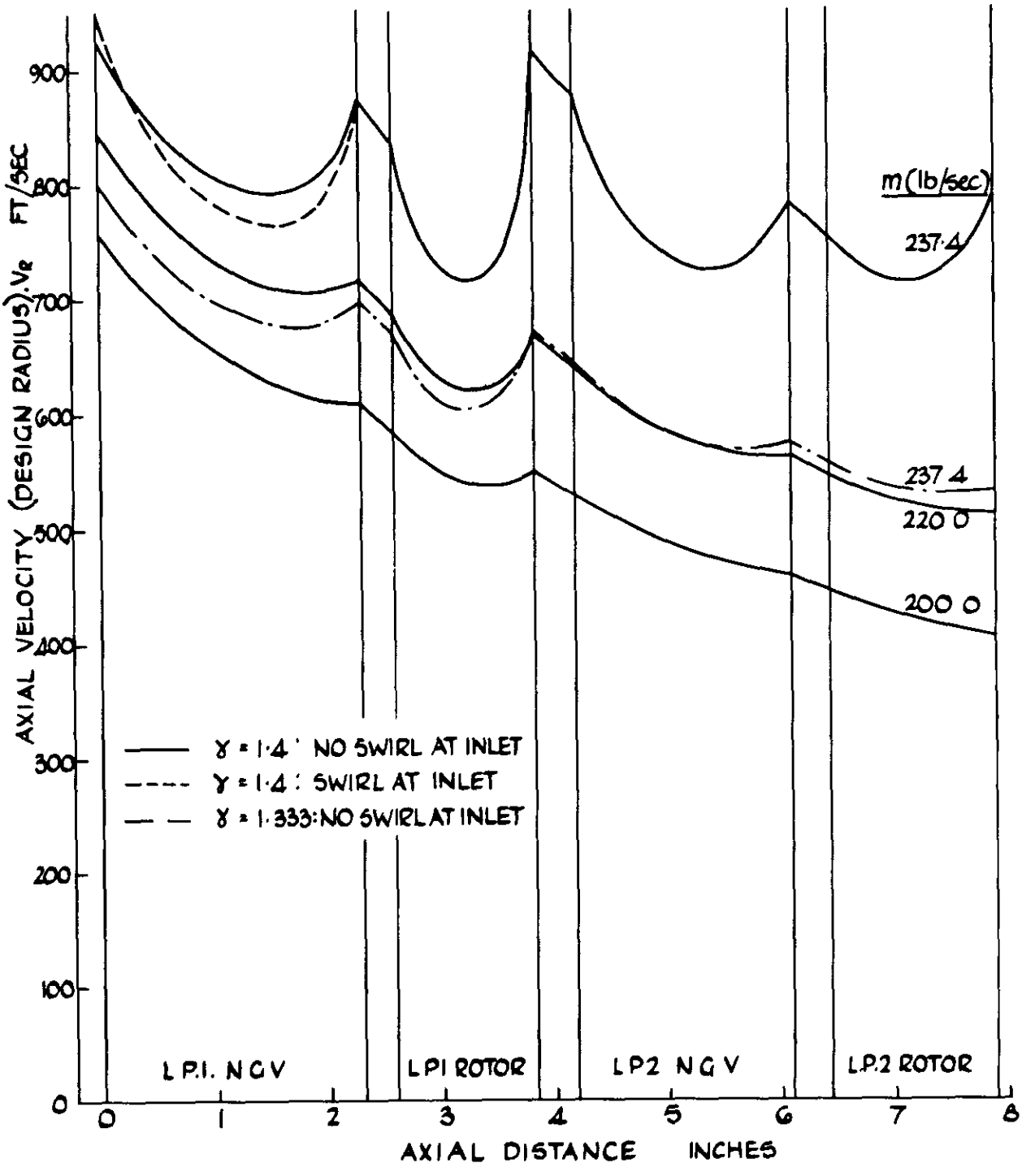

FIG 57. ROLLS-ROYCE TWO-STAGE TURBINE
AXIAL VELOCITY AT THE DESIGN RADIUS

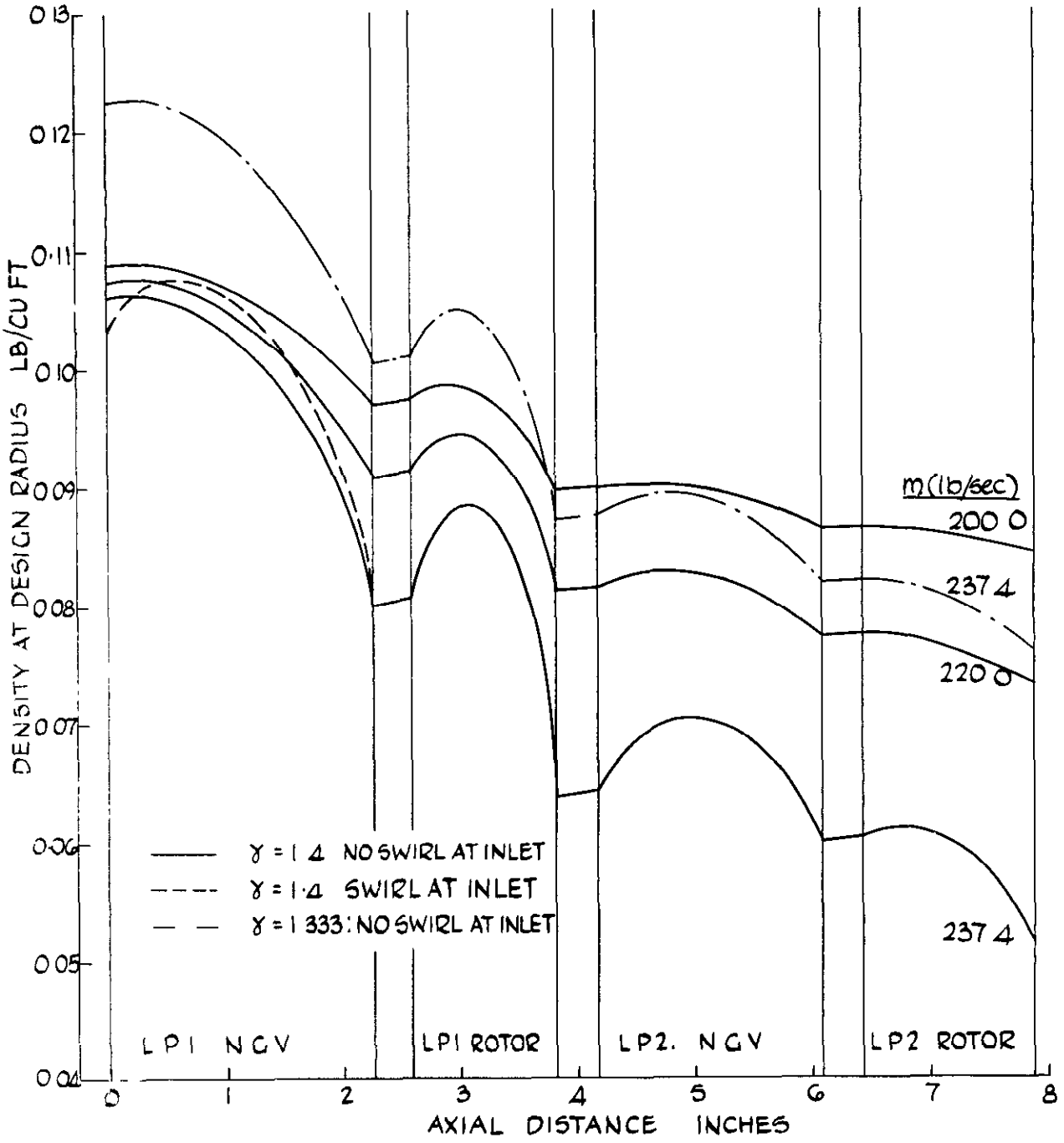

FIG 58. ROLLS-ROYCE TWO-STAGE TURBINE DENSITY AT THE DESIGN RADIUS

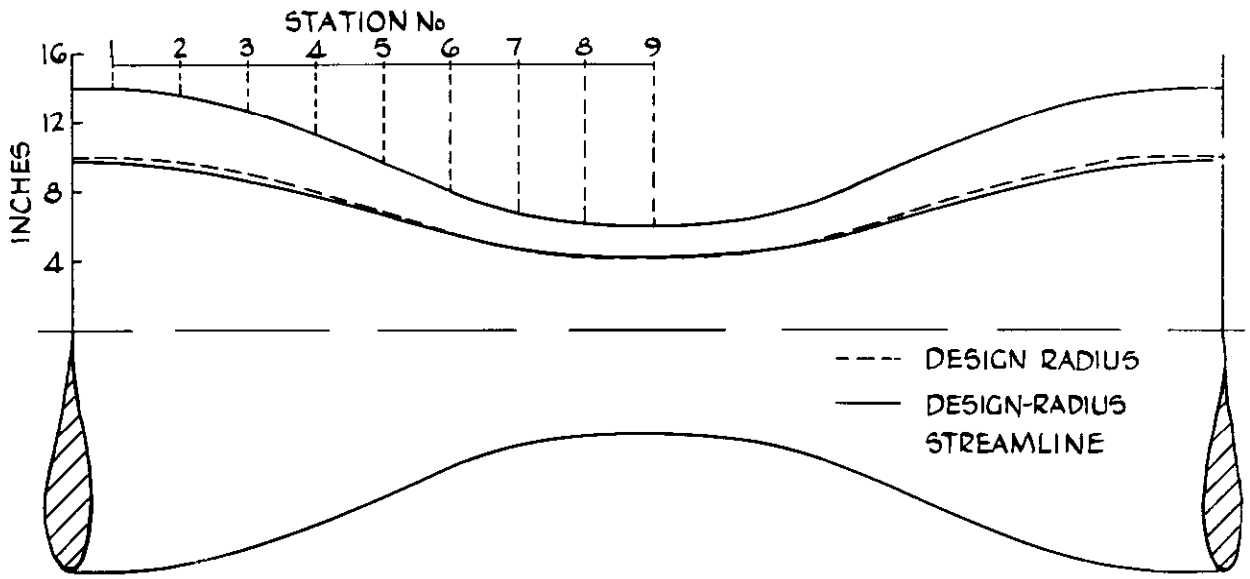

FIG. 59.(a) DISPLACEMENT OF DESIGN-RADIUS STREAMLINE

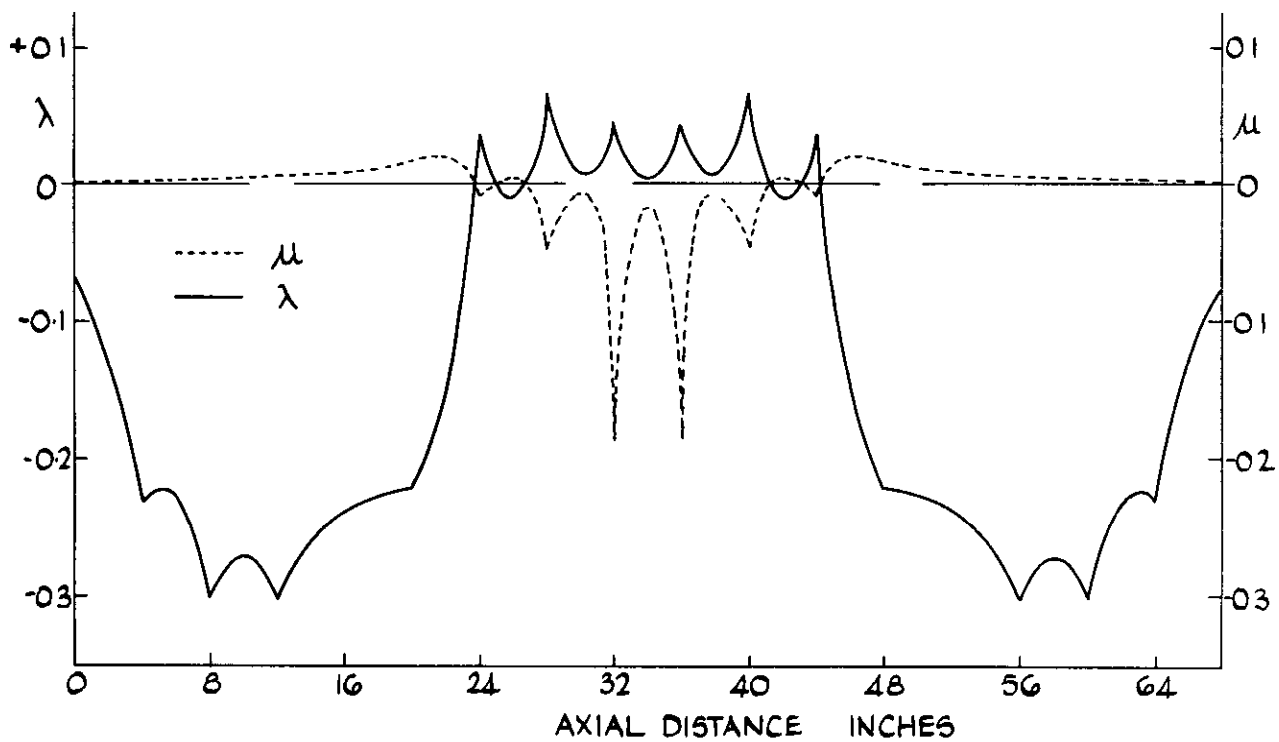

FIG. 59.(b) VARIATION OF λ AND μ

FLOW THROUGH A CONVERGING-DIVERGING NOZZLE

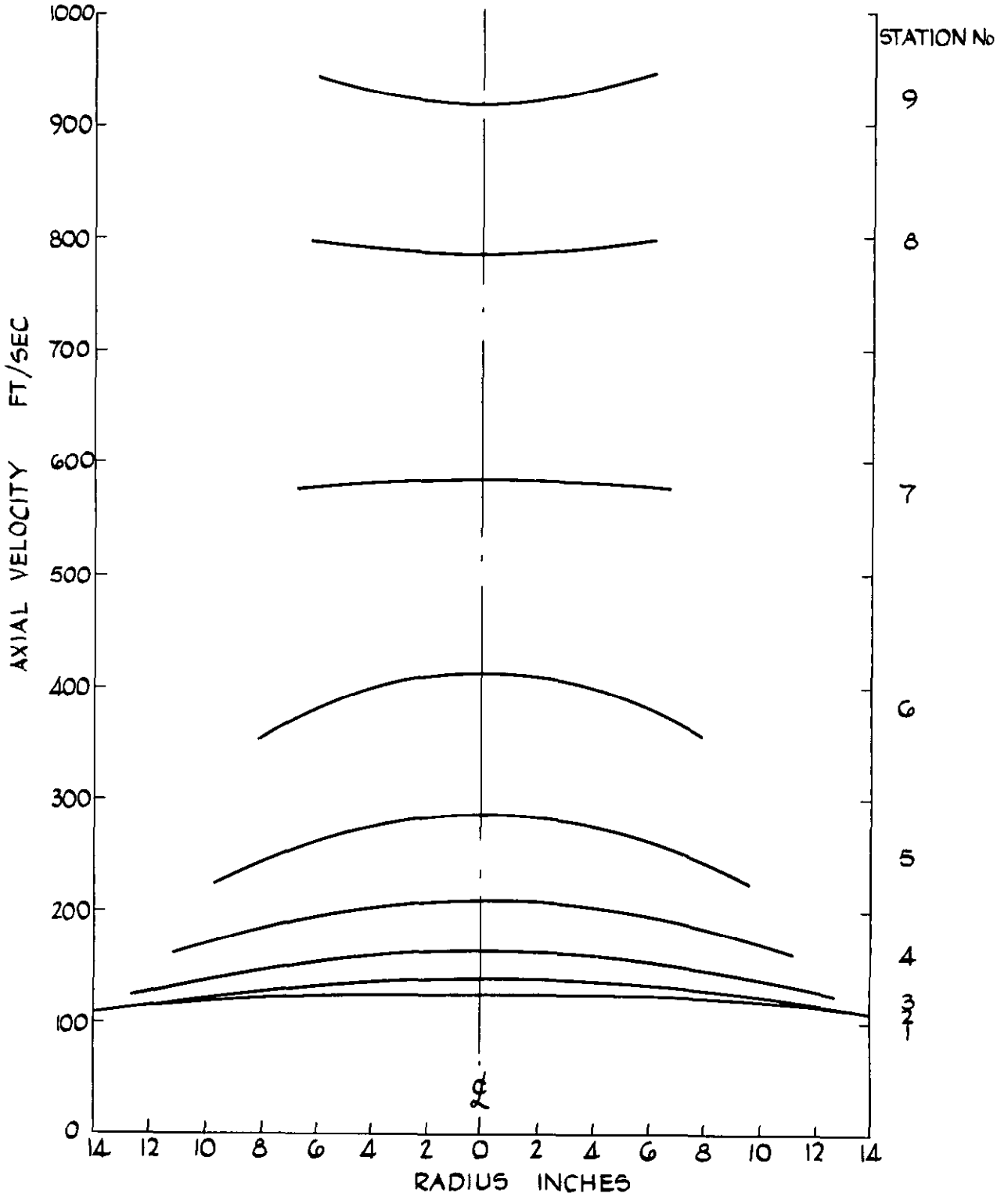

FIG.60. FLOW THROUGH A CONVERGING-DIVERGING NOZZLE

AXIAL-VELOCITY PROFILES

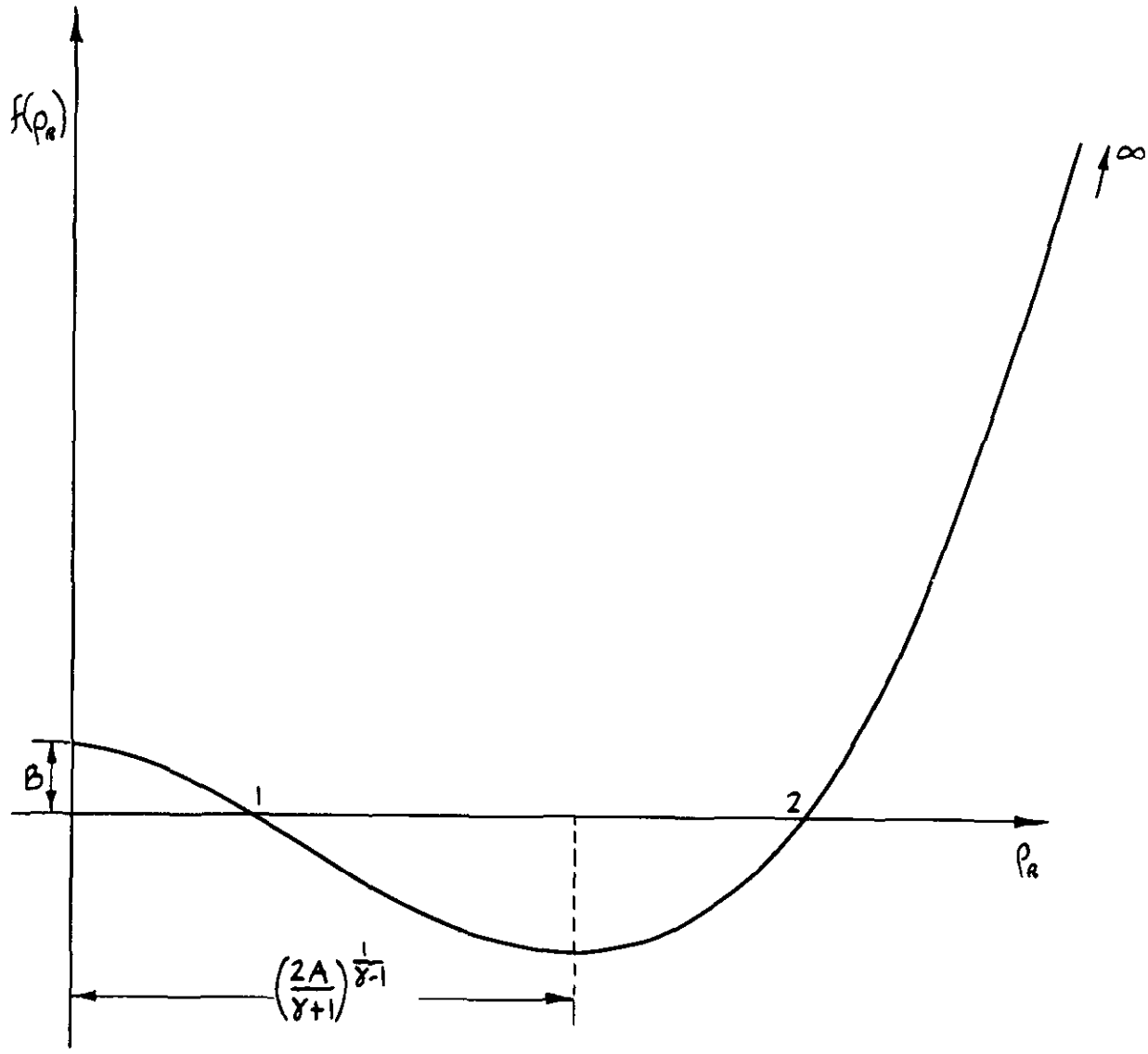

FIG 61. THE DENSITY EQUATION

A.R.C. C.P. No. 755
January, 1963

A PARAMETER THEORY FOR THE COMPRESSIBLE FLOW THROUGH VARIABLE-AREA TURBO-MACHINES

533.695.5:
533.6.011.34

Beavers, G.S.

The single-parameter theory proposed by Whitehead and Beavers (A.R.C. R&M 3335, 1961) for the analysis of incompressible flows through constant-area turbo-machines is extended to allow for the compressibility of the working fluid and for changes in the area of the turbo-machine. It is assumed that at any axial position, the density profile belongs to a fixed family of curves governed by a parameter μ, and the axial-velocity profile at the same point belongs to another family of profiles governed by μ and a second parameter λ. The problem can only be solved using an electronic computer, and a programme for the EDSAC2 computer of Cambridge University Mathematical Laboratory is described. Results from this programme have been compared with existing theoretical and experimental results and this comparison shows that the theory is sufficiently accurate for design and performance calculations.

A.R.C. C.P. No. 755
January, 1963

A PARAMETER THEORY FOR THE COMPRESSIBLE FLOW THROUGH VARIABLE-AREA TURBO-MACHINES

533.695.5:
533.6.011.34

Beavers, G.S.

The single-parameter theory proposed by Whitehead and Beavers (A.R.C. R&M 3335, 1961) for the analysis of incompressible flows through constant-area turbo-machines is extended to allow for the compressibility of the working fluid and for changes in the area of the turbo-machine. It is assumed that at any axial position, the density profile belongs to a fixed family of curves governed by a parameter μ, and the axial-velocity profile at the same point belongs to another family of profiles governed by μ and a second parameter λ. The problem can only be solved using an electronic computer, and a programme for the EDSAC2 computer of Cambridge University Mathematical Laboratory is described. Results from this programme have been compared with existing theoretical and experimental results, and this comparison shows that the theory is sufficiently accurate for design and performance calculations.

A.R.C. C.P. No. 755
January, 1963

A PARAMETER THEORY FOR THE COMPRESSIBLE FLOW THROUGH VARIABLE-AREA TURBO-MACHINES

533.695.5:
533.6.011.34

Beavers, G.S.

The single-parameter theory proposed by Whitehead and Beavers (A.R.C. R&M 3335, 1961) for the analysis of incompressible flows through constant-area turbo-machines is extended to allow for the compressibility of the working fluid and for changes in the area of the turbo-machine. It is assumed that at any axial position, the density profile belongs to a fixed family of curves governed by a parameter μ, and the axial-velocity profile at the same point belongs to another family of profiles governed by μ and a second parameter λ. The problem can only be solved using an electronic computer, and a programme for the EDSAC2 computer of Cambridge University Mathematical Laboratory is described. Results from this programme have been compared with existing theoretical and experimental results, and this comparison shows that the theory is sufficiently accurate for design and performance calculations.

Printed and published by
HER MAJESTY'S STATIONERY OFFICE

To be purchased from
York House, Kingsway, London W C 2
423 Oxford Street, London W 1
13A Castle Street, Edinburgh 2
109 St Mary Street, Cardiff
39 King Street, Manchester 2
50 Fairfax Street, Bristol 1
35 Smallbrook, Ringway, Birmingham 5
80 Chichester Street, Belfast 1
or through any bookseller

Printed in England

C.P. No. 755

S.O. Code No 23-9015-55